



HAL
open science

Deleting a Chromatin Remodeling Gene Increases the Diversity of Secondary Metabolites Produced by *Colletotrichum higginsianum*

Jean-Felix Dallery, Géraldine Le Goff, Emilie Adelin, Bogdan Iorga, Sandrine Pigné, Richard O'Connell, Jamal Ouazzani

► **To cite this version:**

Jean-Felix Dallery, Géraldine Le Goff, Emilie Adelin, Bogdan Iorga, Sandrine Pigné, et al.. Deleting a Chromatin Remodeling Gene Increases the Diversity of Secondary Metabolites Produced by *Colletotrichum higginsianum*. *Journal of Natural Products*, 2019, 82 (4), pp.813-822. 10.1021/acs.jnatprod.8b00796 . hal-02346243

HAL Id: hal-02346243

<https://hal.science/hal-02346243>

Submitted on 10 Mar 2021

HAL is a multi-disciplinary open access archive for the deposit and dissemination of scientific research documents, whether they are published or not. The documents may come from teaching and research institutions in France or abroad, or from public or private research centers.

L'archive ouverte pluridisciplinaire **HAL**, est destinée au dépôt et à la diffusion de documents scientifiques de niveau recherche, publiés ou non, émanant des établissements d'enseignement et de recherche français ou étrangers, des laboratoires publics ou privés.

Deleting a Chromatin Remodeling Gene Increases the Diversity of Secondary Metabolites Produced by *Colletotrichum higginsianum*

Jean-Félix Dallery,[†] Géraldine Le Goff,[†] Emilie Adelin,[†] Bogdan I. Iorga,[†] Sandrine Pigné,[‡]
Richard J. O'Connell,[‡] Jamal Ouazzani^{†*}

[†] Centre National de la Recherche Scientifique, Institut de Chimie des Substances Naturelles ICSN,
Avenue de la Terrasse 91198, Gif-sur-Yvette, cedex, France.

[‡] UMR BIOGER, INRA, AgroParisTech, Université Paris-Saclay, Avenue Lucien Brétignières,
78850, Thiverval-Grignon, France.

Colletotrichum higginsianum is the causal agent of crucifer anthracnose disease, responsible for important economic losses in Brassica crops. A mutant lacking the CclA subunit of the COMPASS complex was expected to undergo chromatin decondensation and the activation of cryptic secondary metabolite biosynthetic gene clusters. Liquid-state fermentation of the $\Delta cclA$ mutant coupled with *in situ* solid-phase extraction (LSF-SPE) led to the production of three families of compounds, namely colletorin and colletochlorin derivatives with two new representatives colletorin D (**1**) and colletorin D acid (**2**), the diterpenoid α -pyrone higginsianin family with two new analogs higginsianin C (**3**) and 13-*epi*-higginsianin C (**4**) and sclerosporide (**5**) coupling a sclerosporin moiety with dimethoxy inositol.

The ascomycete fungus *Colletotrichum higginsianum*, causal agent of crucifer anthracnose disease, is responsible for important economic losses on cultivated members of the Brassicaceae in tropical and sub-tropical regions but also infects the model plant *Arabidopsis thaliana*.^{1,2} Recently, the genome of this fungus was re-sequenced using long-read sequencing technology (PacBio SMRT) producing a gapless assembly of the 12 chromosomes.³ This new version of the genome has facilitated a more accurate annotation of secondary metabolism (SM) genes, which revealed that the *C. higginsianum* SM gene repertoire is one of the largest described to date,⁴ comprising 89 predicted SM Key Genes (SMKG) and 77 clusters.³ Transcriptome sequencing showed that of the 23 SM gene clusters expressed under any of the four tested conditions, the majority (21) were only induced during plant infection and the patterns of expression were highly stage-specific.³

Deleting genes coding chromatin-remodeling proteins has proven to be a successful approach to unlock cryptic secondary metabolism pathways in several genera of filamentous fungi.⁵⁻⁸

The COMPASS (COMplex of Proteins ASSociated with Set1) is conserved from yeast to multicellular eukaryotes and consists of eight proteins that collectively mediate the mono-, di- and trimethylation of lysine 4 in histone H3.⁹ In two Aspergilli (*A. nidulans* and *A. fumigatus*), the deletion of the gene encoding one COMPASS subunit called CclA resulted in the overproduction of at least 12 secondary metabolites, of which nine were identified and linked to corresponding SM gene clusters.^{5,10} Deletion of a *cclA* homolog in *Pestalotiopsis fici* led to the discovery of pestaloficiols T to V and ficipyrene C.⁸

In an effort to activate cryptic SM biosynthetic pathways in *C. higginsianum*, we deleted an orthologue of the *cclA* gene in this fungus. Phenotypic characterization of the resulting mutant and complemented strain is reported elsewhere (Dallery et al., submitted). A key finding from comparative metabolite profiling with HPLC-MS was that several compounds are over-produced by the $\Delta cclA$ mutant relative to the wild-type strain. While some of these were already reported from *C. nicotianae*¹¹⁻¹³ and more recently *C. higginsianum*,^{14,15} an additional five new compounds were also detected. Here, we report the characterization of these new molecules that belong to three

different families: two new colletorin and colletochlorin derivatives, namely colletorin D (**1**) and colletorin D acid (**2**), two new representatives of the higginsianin family, namely higginsianin C (**3**) and 13-*epi*-higginsianin C (**4**), and sclerosporide (**5**), a novel conjugate of the sesquiterpene sclerosporin and dimethoxy inositol.

The *C. higginsianum* mutant $\Delta cclA$ mutant was obtained by targeted gene deletion. The mutant and the wild type (*C. higginsianum* IMI 349063) were grown identically in potato dextrose broth (PDB) with *in-situ* solid-phase extraction (SPE) on Amberlite XAD-16 resin beads.^{16,17} After five days of growth at 25 °C and 150 rpm, the medium was removed by filtration. The recovered resin was washed extensively with H₂O and the trapped compounds desorbed with EtoAc, purified by a combination of flash chromatography and preparative HPLC and identified by 1D, 2D-NMR and mass spectrometry.

The comparison of the HPLC-ELSD chromatograms of the $\Delta cclA$ and the wild type extracts shows that the mutant over produces compounds that were either not detectable or produced in only small amounts by the wild type (Figure 1).

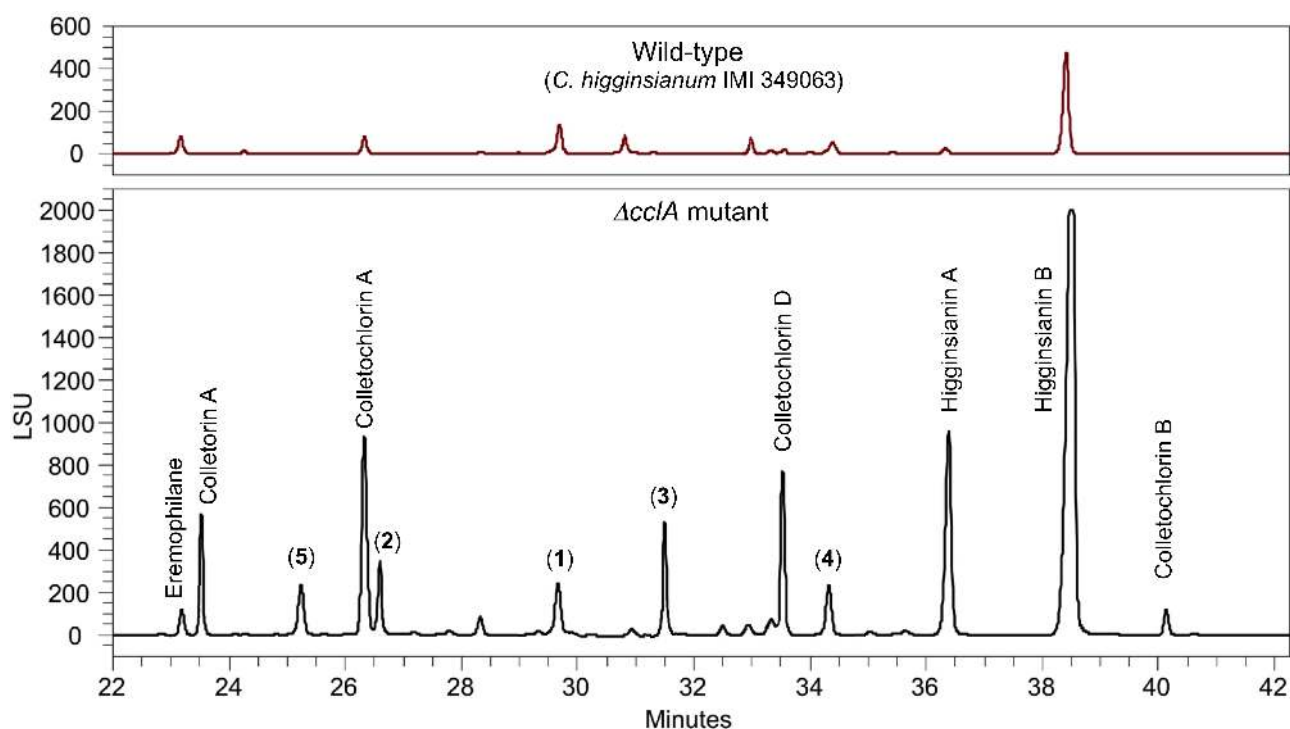


Figure 1. HPLC-ELSD comparison of the raw extracts obtained from the wild-type strain (*C. higginsianum* IMI 349063) and $\Delta cclA$ mutant (LSU = light scattering units).

The first group of compounds belongs to the colletorin/colletochlorin family.^{11,12,15,18-20} Among the four sub-groups A-D, only the C sub-group was not detected in the $\Delta cclA$ mutant while only colletochlorin A (7) was detected in the wild type. Compounds **1** and **2** are reported here for the first time. Their ¹H and ¹³C NMR data are shown in Table 1.

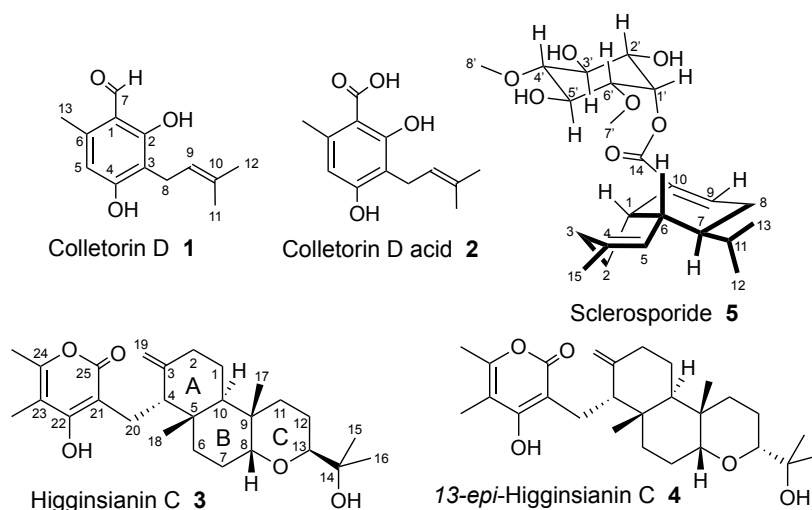


Table 1. NMR Data of Compounds **1** and **2** and Comparison with Colletochlorin D (**9**).

N ^o	Colletochlorin D 9 (500 MHz, CDCl ₃)		Compound 1 (500 MHz, CDCl ₃)		Compound 2 (500 MHz, CD ₃ OD)	
	δ_C , type	δ_H mult, (<i>J</i> in Hz)	δ_C , type	δ_H mult, (<i>J</i> in Hz)	δ_C , type	δ_H mult, (<i>J</i> in Hz)
1	113.5, C	-	113.1, C	-	104.1, C	-
2-OH		6.43, s		6.23, s		-
2	162.5, C	-	164.0, C	-	163.3, C	-
4-OH		12.69, s		12.69, s		-
3	114.8, C	-	111.5, C	-	112.6, C	-
4	156.6, C	-	162.7, C	-	159.6, C	-
5	114.7, C	-	110.8, CH	6.15, s	110.3, CH	6.15, s
6	137.9, C	-	142.4, C	-	140.8, C	-
7	193.6, CH	10.14, s	193.3, CH	10.10, s	170.9, C	-
8	22.2, CH ₂	3.40, d (7.2)	21.6, CH ₂	3.40, d (7.2)	21.4, CH ₂	3.22 d (7.2)
9	121.2, CH	5.25, t (6.9)	121.3, CH	5.27, t (7.2)	122.9, CH	5.17, t (7.2)
10	133.8, C	-	136.4, C	-	130.0, C	-
11	26.1, CH ₃	1.80, s	26.1, CH ₃	1.84, s	24.7, CH ₃	1.72, s
12	17.9, CH ₃	1.71, s	18.3, CH ₃	1.78, s	16.8, CH ₃	1.61, s
13	14.7, CH ₃	2.60, s	18.2, CH ₃	2.51, s	23.0, CH ₃	2.42, s

NMR data for **1** are similar to those of the colletochlorin D (**9**), except for the presence of a proton at position 5 in **1**. Based on the molecular formula deduced from the HRESIMS, **1** is the dechlorinated form of **9** and was named colletorin D. The main difference between **1** and **2** is the shift in C-7 from the aldehyde position at δ_C 193.3 to a carboxyl position at δ_C 170.9, which is supported by the molecular formula deduced from the HRESIMS. Compound **2** was named colletorin D acid.

Based on the structures of the known colletorin/colletochlorin compounds produced by *Colletotrichum* and the new metabolites highlighted in this study, a plausible pathway for the biosynthesis of all members of this family is presented in Figure 2. The precursors are orsellinic acid for 5-chloro derivatives and orcinol for 1-chloro derivatives through a chloroorcinol

intermediate. All of these compounds were previously reported as *Colletotrichum* metabolites.^{15,19,21} Except for colletochlorin H in which the tetrahydropyran ring closure seems unusual, all of the reactions reported in Figure 2 are very common in fungal secondary metabolite biosynthetic pathways and the genes encoding these enzymes are distributed in different *Colletotrichum* clusters.³

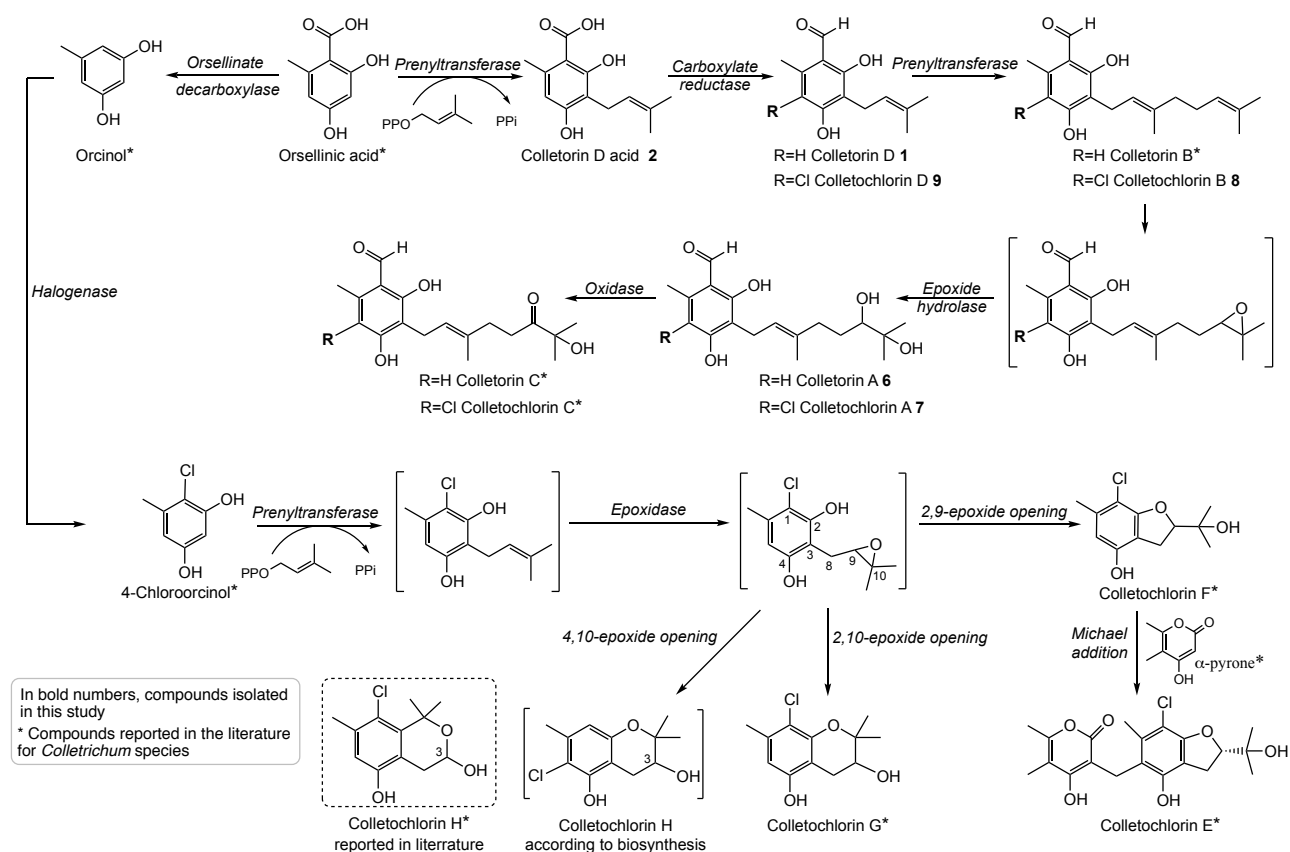


Figure 2. Proposed biosynthetic pathway of the colletorin/colletochlorin family (Although the colletochlorin H structure reported by Masi et al.²⁰ is supported by specific NMR data (shift of proton 3-H), the fact remains that this structure does not fit with the biosynthetic scheme and may perhaps require re-examination).

Besides the colletorin/colletochlorin family, related compounds carrying the 5-chloro-2,4-dihydroxy-6-methylbenzaldehyde moiety were previously isolated from other fungal strains e.g. ascochlorin,²²⁻²⁴ cylindrols,²⁵ ascofuranone,²⁶ and illicolins.²⁷

The second group of metabolites produced by the $\Delta cclA$ mutant consisted of two new higginsianins **3** and **4** isolated together with higginsianin A (**10**). These compounds are not detected in the wild type extract. Compound **3** was obtained as a white powder. Its molecular formula, $C_{27}H_{40}O_5$, was

deduced by HRESIMS with m/z 445.2974 $[M+H]^+$. This formula was corroborated by the ^{13}C NMR spectrum and revealed eight degrees of unsaturation. Based on the following spectroscopic data, these degrees of unsaturation were attributed to the α -pyrone moiety, the methyldiene group and three six-membered rings. The ^{13}C NMR spectrum revealed the presence of 27 carbons, attributed by ^1H - ^{13}C EDT-HSQC to six methyl carbons (δ_{C} 10.5, 17.4, 21.6, 22.7, 25.8 and 25.8), seven methylene groups (δ_{C} 19.8, 22.7, 24.7, 25.8, 30.8, 33.3 and 39.6), one methyldiene group (δ_{C} 110.4), four methine groups including two oxygen-bond methines at δ_{C} 75.5 (C-8) and 83.2 (C-13), and nine non-protonated carbons including the α -pyrone carbonyl at δ_{C} 168.2 (C-25), two double bonds of the pyrone moiety [δ_{C} 104.1 (C-21) and δ_{C} 168.4 (C-22), δ_{C} 109.2(C-23) and δ_{C} 156.8 (C-24)] and a non-protonated carbon linked to the methyldiene group [δ_{C} 150.8 (C-3)]. The $^n\text{J}_{\text{H-}^{13}\text{C}}$ connectivities provided by HMBC NMR experiment are listed in Table 2.

Table 2. NMR Spectroscopic Data of Compounds **3** and **4** and Comparison with Higginsianin A (**10**)

N°	Compound 3 (500MHz, CD ₃ OD)			Compound 4 (500MHz, CD ₃ OD)			Higginsianin A (500 MHz, CD ₃ OD)	
	δ_{C} , type	δ_{H} ,mult, J in Hz	HMBC	δ_{C} , type	δ_{H} ,mult, J in Hz	HMBC	δ_{C} , type	δ_{H} ,mult, J in Hz
1	24.7, CH ₂	1.38, m; 1.56, m	-	23.5, CH ₂	1.31, m; 1.56, m	-	25.8, CH ₂	1.40, td (4.2, 13.0); 1.57, m
2	33.3, CH ₂	2.09, m; 2.47, td (5.4, 13.6)	1, 3, 19	33.0, CH ₂	2.09, m; 2.51, td (5.4, 13.6)	1, 3, 19	33.2, CH ₂	2.11, m; 2.47 td (5.2, 13.5)
3	150.8, C	-	-	150.7, C	-	-	150.1, C	-
4	56.1, CH	2.17, m	-	57.2, CH	2.09, m	-	55.9, CH	2.18, m
5	38.5, C	-	-	38.7, C	-	-	38.7, C	-
6	30.8, CH ₂	1.02, td, (3.2, 12.9); 2.16, m	5, 8, 10	30.6, CH ₂	0.93, td, (3.2, 12.9); 2.39, m	8, 10	30.5, CH ₂	1.00, m; 2.05, m
7	25.8, CH ₂	1.77, m; 1.93, m	-	25.6, CH ₂	1.69, m; 1.98, m	-	23.7, CH ₂	1.84, m; 1.86, m
8	75.5, CH	3.56, bs	6, 7, 13	83.1, CH	3.22, bs	6, 7	84.4, CH	3.72, br t (2.5)
9	37.5, C	-	-	35.8, C	-	-	45.1, C	-
10	45.0, CH	1.91, m	-	35.2, CH	2.33, bd (12.9)	-	39.9, CH	1.81, m
11	39.6, CH ₂	1.38, m; 1.66, m	-	37.4, CH ₂	1.06, td (4.0, 13.6); 2.03, br t (13.6)	-	49.8, CH ₂	1.27, dd (9.5, 12.5); 2.26, dd (6.5, 12.5)
12	19.8, CH ₂	1.53, m; 1.73, m	-	22.9, CH ₂	1.42, m; 1.67, m	-	74.7, CH	4.91, m
13	83.2, CH	3.53, dd (2.2, 11.5)	8, 12	85.5, CH	3.16, dd (2.2, 11.5)	8, 11, 14, 16	128.4, CH	5.23, td (1.3, 8.7)
14	74.8, C	-	-	73.4, C	-	-	136.6, C	-
15	25.8, CH ₃	1.19, s	13, 14, 16	25.3, CH ₃	1.19, s	13, 14, 16	26.1, CH ₃	1.72, s
16	25.8, CH ₃	1.17, s	13, 14, 15	25.7, CH ₃	1.26, s	13, 14, 15	18.2, CH ₃	1.71, s
17	21.6, CH ₃	0.83, s	8, 9, 10, 11	23.5, CH ₃	0.83, s	8, 9, 10, 11	21.1, CH ₃	0.98, s
18	22.7, CH ₃	0.94, s	4, 5, 6, 10	24.1, CH ₃	0.99, s	4, 5, 6, 10	22.2, CH ₃	0.96, s
19	110.4, CH ₂	4.20, bs; 4.48, bs	2, 4	110.0, CH ₂	4.21, bs; 4.48, bs	2, 3, 4	110.7, CH ₂	4.20, dd 1.6, 2.5); 4.50, dd (2.0, 2.5)
20	22.7, CH ₂	2.60, dd (4.4, 13.1); 2.81, bdd (13.1)	3, 4, 21, 25	22.7, CH ₂	2.65, dd (4.4, 13.1); 2.85, bdd (13.1)	3, 4, 21, 25	22.6, CH ₂	2.59, dd (4.7, 13.1); 2.78, dd (12.1, 13.1)
21	104.1, C	-	-	104.5, C	-	-	103.9, C	-
22	168.4, C	-	-	167.7, C	-	-	168.2, C	-
23	109.2, C	-	-	108.6, C	-	-	108.9, C	-
24	156.8, C	-	-	156.8, C	-	-	156.8, C	-
25	168.2, C	-	-	168.2, C	-	-	167.8, C	-
26	10.5, CH ₃	1.92, s	22, 23, 24	10.4, CH ₃	1.93, s	22, 23, 24	10.5, CH ₃	1.91, s
27	17.4, CH ₃	2.19, s	23, 24	17.3, CH ₃	2.20, s	23, 24	17.4, CH ₃	2.19, s

Interestingly, the ^1H and ^{13}C NMR spectra of **3** resemble those recorded for higginsianin A **10** (Table 2) and are consistent with a polycyclic diterpene ring system joined to a tetra-substituted α -pyrone ring. As in **10**, HMBC correlations in **3** from Me-27 to C-23 and C-24, Me-26 to C-22, C-23 and C-24 and C-20 to C-21 and C-25 allowed construction of the tetra-substituted α -pyrone ring. Ring A was built according to the COSY correlations between H-1, H-2 and H-19 and the HMBC connectivities from H-19 to C-4 and C-2, Me-18 to C-4, C-5 and C-10. Ring A was linked to the tetra-substituted α -pyrone ring through C-20 according to HMBC correlations from H-20 to C-3, C-4, C-21 and C-25. Ring B was built and connected to ring A based on COSY correlations between H-6, H-7 and H-8 and HMBC correlations from Me-18 to C-4, C-5, C-6 and C-10, H-6 to C-5, C-10 and C-8, Me-17 to C-8, C-9 and C-10 (Figure 3).

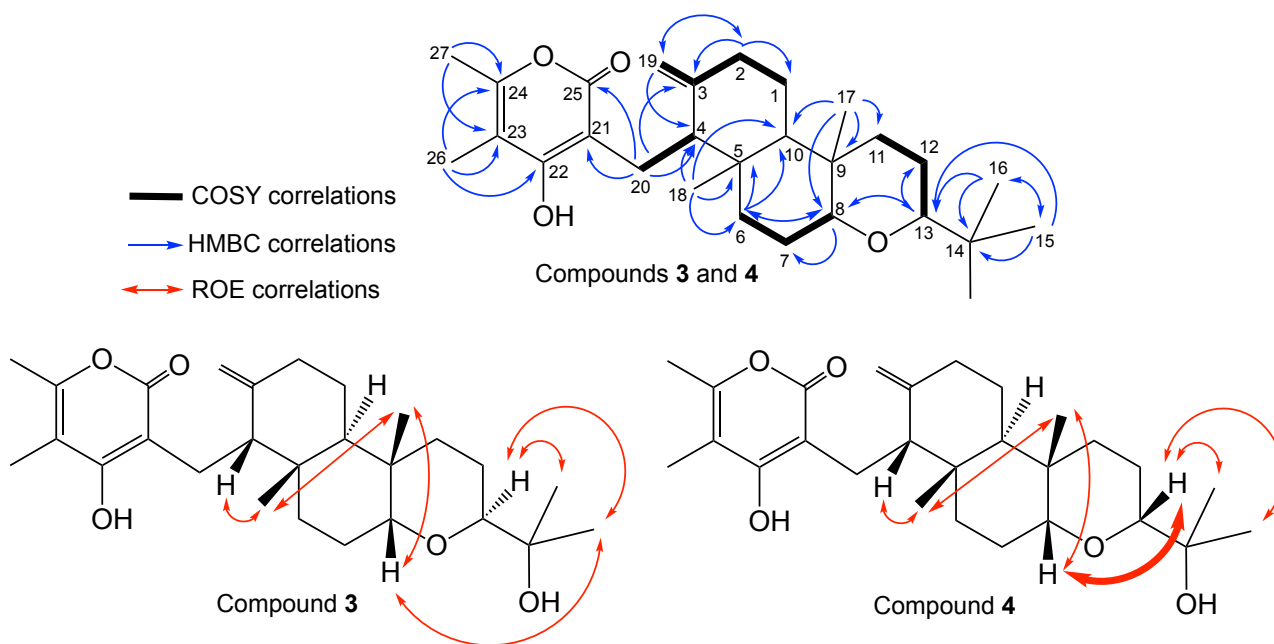


Figure 3. Key COSY, HMBC and ROE correlations for compounds **3** and **4**

The main difference between higginsianin A **10** and compound **3** lies in ring C. In **10**, ring C is a tetrahydrofuran substituted at C-12 by a isobutenyl group, while in **3**, ring C is a tetrahydropyran substituted at C-13 by a isopropanol group. Ring C of compound **3** was built and connected to ring B through C-8 and C-9, observing COSY correlations between H-11, H-12 and H-13 and HMBC correlations from Me-17 to C-8, C-9 and C-11 and from H-13 to C-12 and C-8.

The C-13 position was substituted by an isopropanol group, observing correlations from Me-15 to C-13, C-14 and C-16 and from Me-16 to C-13, C-14 and C-15.

The configuration of **3** was established according to ROE correlations and comparison with the absolute configuration of higginsanin A (**10**), obtained from reported X-ray analysis.¹⁴ The common ROE correlations between Me-18, H-4, Me-17 and H-8 and the absence of correlation with H-10 supported that the configurations of C-4, C-5, C-8, C-9, and C-10 are similar to those reported for higginsanin A. Concerning the configuration of C-13, no ROE correlation was observed between H-8 and H-13, suggesting a *trans* orientation of these two protons. Compound **3** is a new diterpenoid α -pyrone and was named higginsianin C.

Compound **4** was obtained as a white powder. Its molecular formula, C₂₇H₄₀O₅, was identical to those found for higginsianin C and was deduced by HRESIMS with *m/z* 445.2958 [M+H]⁺. The ¹H and ¹³C NMR spectra of **4** were very similar to those of **3** (Table 2). Moreover, COSY and HMBC data confirmed that **4** had the same connectivities, supporting a similar planar scaffold (Figure 3).

The configuration of **4** was established according to ROE correlations and comparison with compound **3**. Here again, we noticed common ROE correlations between Me-18, H-4, Me-17 and H-8 and the absence of correlation with H-10 supported that the configuration of C-4, C-5, C-8, C-9, and C-10 are similar to those deduced for **3**. A key ROE correlation was observed in **4** between H-8 and H-13, suggesting a *cis* configuration of these two protons. Compound **4** was named 13-*epi*-higginsianin C.

The diterpenoid moiety of **3** and **4** is similar to the previously reported γ -pyrone candelalide C.²⁸

The absolute configuration at C-13 is similar to the established configuration of **4** due to the common key ROE correlation between H-8 and H-13.

In order to validate the configuration of compounds **3** and **4** established by ROESY experiments, molecular modeling studies were carried out to evaluate the conformational flexibility of different conformers for compounds **3** and **4** and to compare these results with the experimental NMR data.

The most stable conformers of compounds **3** and **4** are presented in Figure 4.

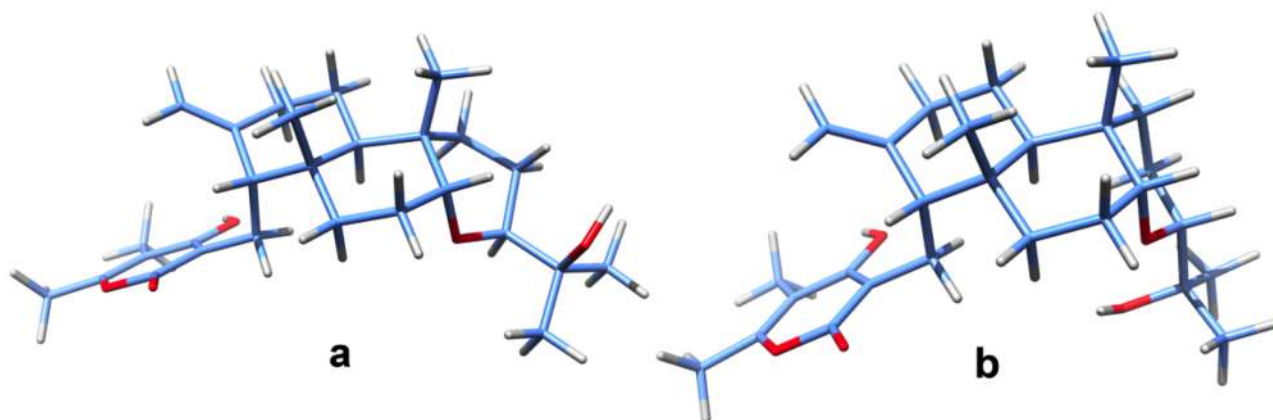


Figure 4. Three-dimensional structures of the most stable conformers of compounds **3** (a) and **4** (b)

Their structures are in full agreement with the relative configurations and ROE correlations mentioned above. The atoms H-4, C-18, C-17 and H-8 are indeed on the same side in both compounds **3** and **4**, with all the corresponding distances compatible with the ROE correlations observed: H-4 to C-18 2.57 Å and 2.59 Å, C-18 to C-17 3.42 Å and 3.37 Å, C-17 to H-8 2.64 Å and 2.56 Å, respectively. Additionally, in compound **4** the distance from H-8 to H13 is 2.42 Å, thus confirming the configuration of this chiral center. The absolute stereochemistry of these compounds was further confirmed by the computation of TDDFT ECD spectra, which proved to be very similar with the experimental ones and with those reported for higginsianins A and B (Supporting Information, S46).¹⁴

The ¹H and ¹³C NMR chemical shifts corresponding to these conformers were computed using the DFT-NMR approach that we used previously.²⁹ The chemical shifts were generally well predicted, with mean unsigned errors (MUEs) of 0.09 and 0.11 for ¹H NMR and of 2.68 and 2.51 for ¹³C NMR, respectively, and with root mean square errors (RMSEs) of 0.11 and 0.14 for ¹H NMR and of 3.15 and 3.03 for ¹³C NMR, respectively (Tables S41 and S42 in Supp. Info.).

The tetracyclic higginsianins A and C may derive from the tricyclic analog B through classical enzymatic reactions as depicted in Figure 5.

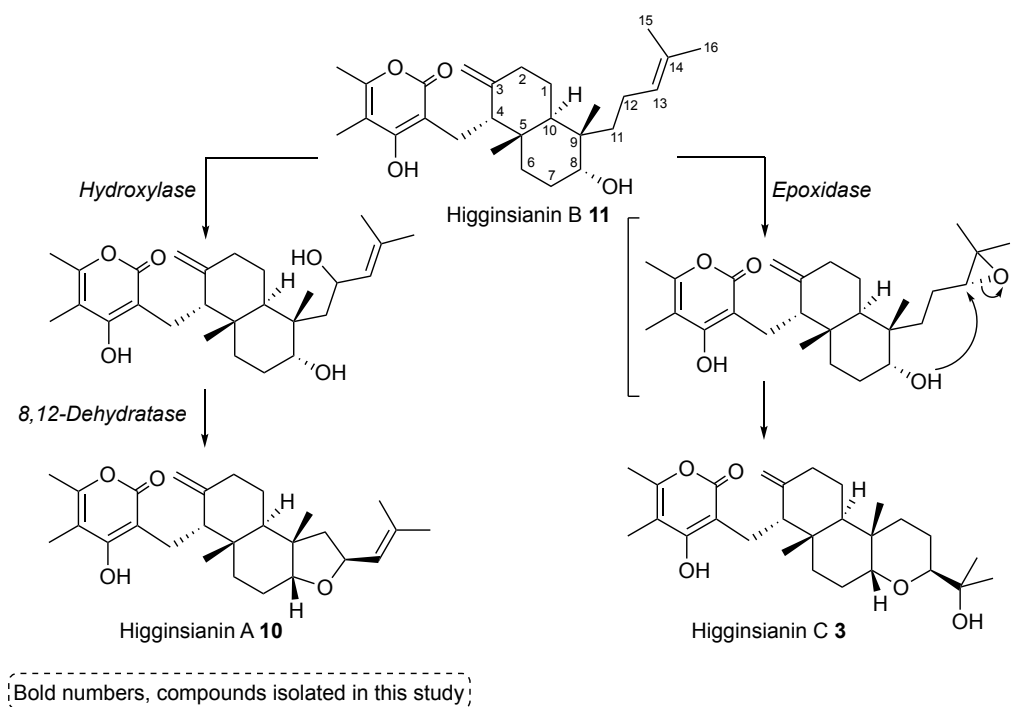


Figure 5. Proposed biosynthesis of the higginsianin family starting from the B form.

Compound **5** was obtained as a transparent oil. Its molecular formula, $C_{23}H_{36}O_7$, was deduced by HRESIMS with m/z 425.2552 $[M+H]^+$. This formula was corroborated by the ^{13}C NMR spectrum and revealed six degrees of unsaturation. Based on the following spectroscopic data, these degrees of unsaturation corresponded to an α -cadinene sesquiterpene moiety, an ester carbonyl group and an inositol derivative ring.

The ^{13}C NMR spectrum revealed the presence of 23 carbons which, in combination with the HSQC spectrum, can be attributed to five methyl carbons, including two methoxy groups (δ_C 15.5, 21.7, 24.0, 58.0 and 61.2 ppm), three methylene groups (δ_C 26.5, 26.8 and 31.7 ppm), 12 methine groups: 10 sp^3 methines including six bonded to oxygen (δ_C 27.7, 35.8, 37.4, 41.8, 70.9, 71.6, 74.0, 74.5, 81.7 and 86.5), two sp^2 methines (δ_C 124.3 and 141.5) and three non-protonated carbons including one carbonyl group at δ_C 168.1 ppm and two sp^2 carbons (δ_C 134.5 and 136.2). The $^nJ_{1H-13C}$ connectivities given by an HMBC NMR experiment are listed in Table 3.

Table 3. NMR Spectroscopic Data of Compound **5**

Compound 5 (500 MHz, CD ₃ OD)			
N ^o	δ _C , type	δ _H , mult, <i>J</i> in Hz	HMBC
1	35.8, CH	2.55, d (11.1)	-
2	26.8, CH ₂	1.42, dd (5.0, 12.2); 2.00, m	1, 2, 6
3	31.7, CH ₂	1.91, m; 2.08, m	1, 2, 4
4	136.2, C	-	-
5	124.3 CH	5.55, br m	1, 15
6	37.4, CH	2.01, m	-
7	41.8, CH	1.55, m	6, 11, 12
8	26.5, CH ₂	2.16, td (3.9, 19.1)	6, 7, 9, 10
9	141.5, CH	6.99, m	1, 7, 14
10	134.5, C	-	-
11	27.7, CH	2.05, m	-
12	15.5, CH ₃	0.87, d (6.6)	7, 11, 13
13	21.7, CH ₃	0.95, d (6.6)	7, 11, 12
14	168.1, C	-	-
15	24.0, CH ₃	1.70, s	3, 4, 5
1'	70.9, CH	5.66, br t (2.3)	1', 6', 14
2'	81.7, CH	3.18, dd (2.3, 9.6)	1', 3', 7'
3'	74.0, CH	3.62, m	-
4'	86.5, CH	2.94, br t (9.4)	3', 5', 8'
5'	74.5, CH	3.64, m	-
6'	71.6, CH	3.65, m	-
7'	58.0, CH ₃	3.41, s	2'
8'	61.2, CH ₃	3.65, s	4'

HMBC correlations observed from Me-15 to C-3, C-4 and C-5, from H-2 to C-1, C-3 and C-6, in combination with the COSY correlations between H-1 and H-2 and between H-5 and H-6 allowed us to build the first six-membered ring of the cadinene skeleton. The COSY data revealed the spin system spanning Me-12/Me-13/H-7/H-8/H-9 and observing HMBC correlations from H-7 to C-6 and from H-9 to H-7 and H-1, we were able to connect the second isopropyl substituted six-membered ring at the C-1/C-6 positions to give the α -cadinene sesquiterpene moiety (Figure 6). The third six-membered ring consisted of a dimethoxy-inositol derivative according to COSY correlations between H-4' and H-5' and between H-6', H-1' and H-2' via H-1' and HMBC correlations from H-1' to C-2' and C-6', from H-2' to C-1' and C-3' and from H-4' to C-3' and C-5'. The methoxy groups MeO-7' and MeO-8' were linked to C-2' and C-3' respectively, according to HMBC correlations from Me-7' to C-2' and from Me-8' to C-3'. Finally, this dimethoxy-inositol derivative was linked to the α -cadinene sesquiterpene moiety through an ester group between C-10 and C-1' according to HMBC correlations from H-9 and H-1' to C-14.

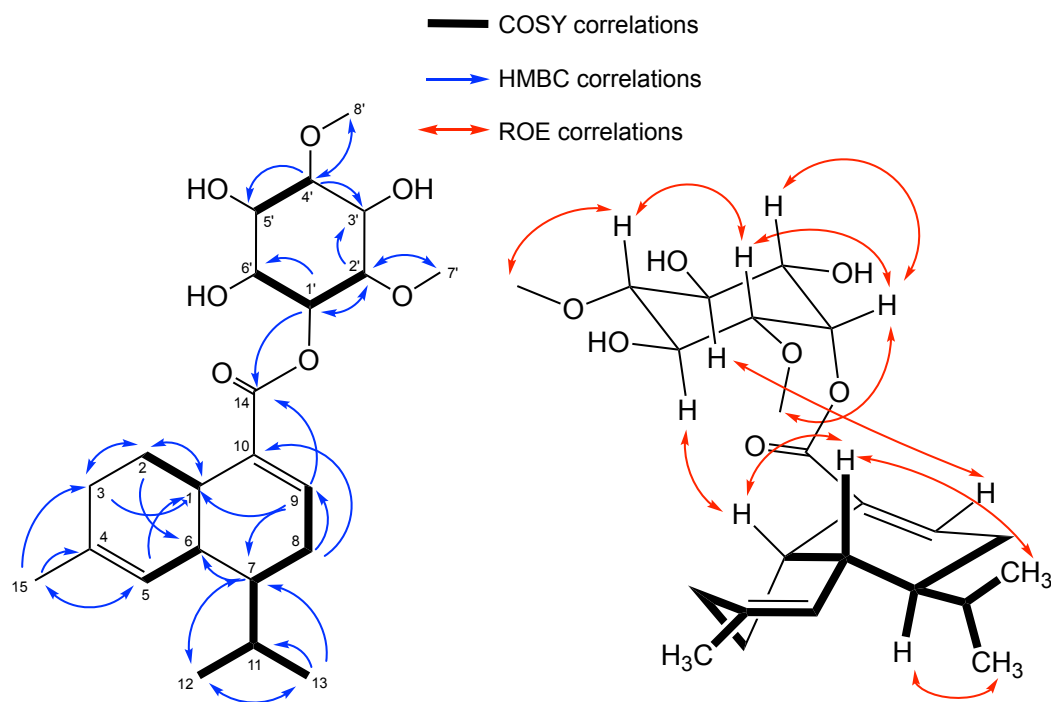


Figure 6. Key COSY, HMBC and ROE (mixing time = 300 ms) correlations for compound **5**

The ROESY spectrum allowed us to determine the relative configuration of C-1, C-6 and C-7. ROE correlations were observed between H-1 and H-6 and absence of correlation was noticed between H-1 and H-7 and H-6 and H-7.

A time-dependent density functional theory (TDDFT) ECD calculation of compound **5** with the stereogenic centers on the bicyclic system assigned as *1S*, *6R*, *7S* resulted in a spectrum nearly identical with the experimental ECD spectrum determined for this compound, with a positive peak at 217 nm (Figure 7). The absolute configurations of the carbons at the bicyclic junction and the ECD spectrum are opposite with those reported for (+)-sclerosporin and analogs³⁴ and therefore compound **5** is a (–)-sclerosporin derivative. The *S-cis* and *S-trans* conformation of the unsaturated ester has no significant influence on the overall shape of the ECD spectrum (data not shown).

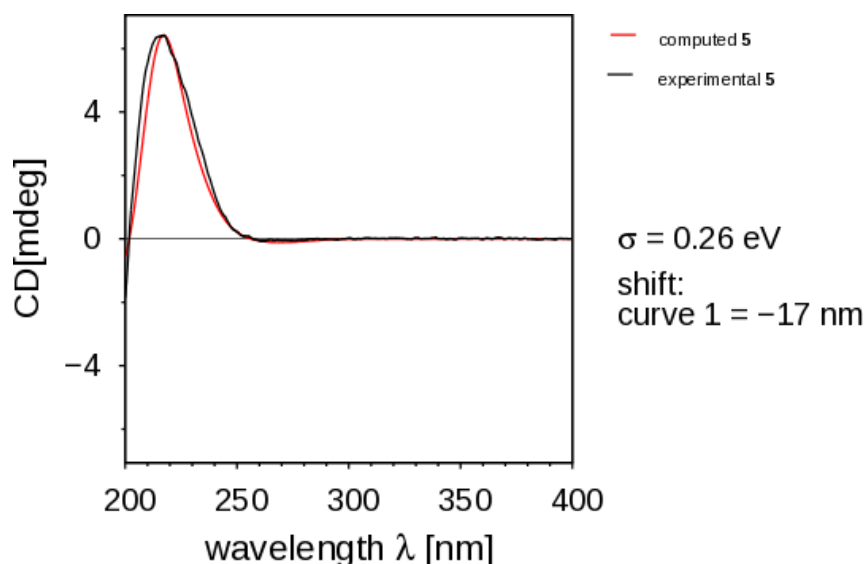


Figure 7. Superposed experimental ECD spectrum (black) with the computed ECD spectrum (red) for compound **5**.

Concerning the inositol moiety, the configuration was established based on the ROE correlation and the 3J_H coupling constants (Table 3). H-1' (δ_H 5.66) gave a broad triplet with a 3J_H of 2.3 Hz, suggesting an eq-ax conformation of H-1' with H-2' and H-6'. Moreover, H-2' (δ_H 3.18, dd) showed two 3J_H of 2.3 Hz and 9.6 Hz, corroborating an equatorial position for H-1' and so axial positions of H-2' and H-3'. H-4' gave a broad triplet with a 3J_H of 9.6 Hz, suggesting an ax-ax conformation of H-3', H-4' and H-5'. This conformation was consistent with the ROE correlations observed between H-1' with H-2', Me-7' and H-6', H-2' with H-4' and H-6', H-1 with H-3' and H-9 with H-5'. Compound **5** was named sclerosporide.

The most stable conformer of compound **5** is presented in Figure 8.

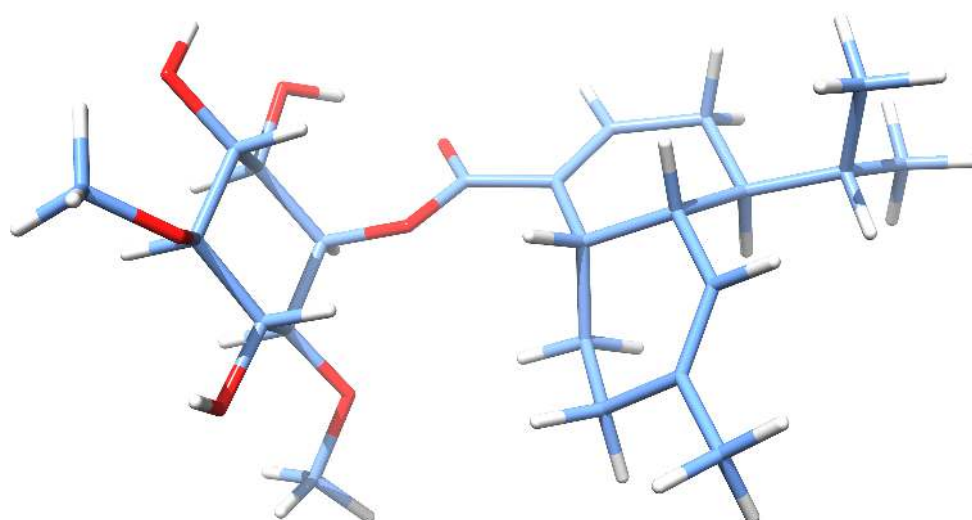


Figure 8. Three-dimensional structure of the most stable conformer of compound **5**

The main feature of this structure is the hydrogen bond between the OH group in position 6' and the carbonyl oxygen atom from the ester group which brings the two fragments, cadinene and inositol, closer and allows them to interact, according to the ROE correlations. The distances H-1' to H-2', C-7' to H-6', H-2' to H-4', H-2' to H-6', H-1 to H-3' and H-9 to H-5' are 2.46 Å, 4.66 Å, 2.64 Å, 2.44 Å, 3.04 Å, 5.45 Å, respectively. The relative configuration of the chiral centers is in agreement with the coupling constants determined experimentally.

As for compounds **3** and **4**, the ^1H and ^{13}C NMR chemical shifts corresponding to **5** were computed using the DFT-NMR approach (Tables S43 and S44 supporting information). Again, a good correlation was observed between the experimental and computed values of the chemical shifts, with mean unsigned errors (MUEs) of 0.14 for ^1H NMR and of 2.83 for ^{13}C NMR, respectively, and with root mean square errors (RMSEs) of 0.22 for ^1H NMR and of 4.03 for ^{13}C NMR, respectively.

Sclerosporin was first isolated from *Sclerotinia fructicula* as an inducer of asexual arthrospore formation,³¹ and from *Diplocarpon mali*, the Marssonina apple blotch disease agent.^{32,33}

Sclerosporin has been reported in less than eight publications so far, half of them focused on the isolation of the compound and analogs from various fungal strains,^{31,33,34} while the others are dedicated to chemical synthesis.³⁵⁻³⁷ The sclerosporin family contains oxido-reduction derivatives of the original compound, sclerosporal was isolated from *Sclerotinia fructicula*, polygosumic acid from *Polygonum viscosum*, and four hydroxylated derivatives from *Cadophora malorum*.

Compound **5** is the first example of a conjugated sclerosporin; more unexpected is its conjugation with dimethoxy inositol because until now methoxy inositol derivatives have been exclusively reported from the plant kingdom. (+)-Pinpollitol, a di-O-methyl D-(+)-chiro-inositol was isolated from the pollen of *Pinus radiata* exhibiting growth regulating properties.³⁸ Mono methoxy inositols isolated from plants like D-pinitol, L-quebrachitol and *O*-methyl-*scyllo*-inositol exhibit valuable biological activities.³⁹⁻⁴¹

This is the first time that a sclerosporin-based compound has been reported from any

Colletotrichum species, and the first time that an O-alkylated inositol has been found in a phylum other than plants.

Compounds were assayed for different biological and enzymatic activities. Antibacterial activity was tested against *Escherichia coli* ATCC 25922, *Bacillus subtilis* ATCC 6633 and *Micrococcus luteus* ATCC 10240 by the broth microdilution method according to Clinical and Laboratory Standards Institute (CLSI) guidelines. Antifungal activity was tested against *Rhizopus oryzae* ATCC 11145, *Aspergillus ochraceus* ATCC 1009 and *Botrytis cinerea* B05.10 according to the European Committee for Antimicrobial Susceptibility Testing method (EUCAST). For antibacterial and antifungal bioassays, the minimal inhibitory concentrations (MIC) are higher than 225 μM (antibacterial control MIC_{chloramphenicol} = 10 μM ; antifungal control MIC_{amphotericin B} = 2 μM).

Compounds were also screened on a panel of cosmetic targets as anti-tyrosinase, anti-collagenase, anti-hyaluronidase, anti-elastase and antioxidant (DPPH method). We used the following controls at concentrations giving 50 % inhibition in our condition: tyrosinase inhibition, kojic acid for (20 μM); elastase inhibition, elastatinal (15 μM); collagenase inhibition, 1,10-phenanthroline (100 μM); hyaluronidase inhibition, ascorbic acid (5mM); DPPH method, trolox (20 μM). Compounds were tested from 10 to 200 μM and the inhibition never exceeded 20% at the higher concentrations.

Our findings demonstrate the major impact that chromatin status has on the production of secondary metabolites by *C. higginsianum*. Deletion of *cclA* drastically altered the profile of metabolites produced in liquid cultures of this fungus, as shown by the massive over-production of some known terpenoid compounds, and the identification of new analogs of these compounds and novel structural scaffolds that were uniquely produced by the mutant. Our work highlights the enormous potential of genetic manipulation of key chromatin regulators as a strategy for unlocking the chemical diversity encoded by fungal genomes.

EXPERIMENTAL SECTION

General Experimental Procedures.

Optical rotations were measured at 25 °C on a JASCO P1010 polarimeter. UV spectra were measured in a 1 cm quartz tank using a Varian Cary 100 scan spectrophotometer. ECD spectra were measured with a Jasco J-810 CD Spectrometer. IR spectra were obtained on a Perkin-Elmer Spectrum100 model instrument. ¹H and ¹³C spectra were recorded using a Bruker Avance-500 and 600 instrument operating at 500 and 600 MHz respectively. The Bruker Avance 600 MHz was equipped with a microprobe (1.7 TXI). LC-ESI-MS analysis were performed on a simple-stage quadrupole Waters-Micromass ZQ 2000 mass spectrometer equipped with an ESI (electrospray ionization) interface coupled to an Alliance Waters 2695 HPLC instrument with PDA and ELS detection. The HRESIMS spectra were recorded on a Waters-Micromass mass spectrometer equipped with ESI-TOF (electrospray-time of flight). HPLC chromatograph consisted of a Waters system including an autosampler 717, a pump 600, a photodiode array 2998 and an evaporative light-scattering detector, ELSD 2420. The HPLC analytical column used was a 3.5 μm, C-18 column (Sunfire 150 x 4.6 mm) operating at 0.7 mL/min. The semipreparative column was a 5 μm, C-18 (Sunfire 250mm x 10mm) operating at 4 mL/min. On both columns, the gradient consisted of a linear gradient for 50 min from H₂O to CH₃CN, both containing 0.1% formic acid. Silica gel 60 (6–35 and 35–70 μm) and analytical TLC plates (Si gel 60 F 254) were purchased from SDS (France). Prepacked silica gel 80 g Redisep columns were used for flash chromatography using a Combiflash-Companion apparatus (Serlabo). The Antibase database was used for rapid dereplication and characterization of known compounds. All other chemicals and solvents were purchased from SDS (France).

Fungal Strains

Colletotrichum higginsianum IMI 349063 was used as the wild-type strain. The strain called $\Delta cclA$ used in this study was obtained by deleting the gene CH63R_04661 coding the sole ortholog of the *Aspergillus nidulans* CclA protein (AN9399) in *C. higginsianum*. Complete details about the generation and phenotyping of this deletion mutant are reported elsewhere (Dallery et al.,

submitted). Both strains were routinely maintained on Mathur's medium as previously described.¹ When necessary *ΔcclA* was propagated on potato dextrose agar supplemented with 100 μg·mL⁻¹ of hygromycin B as a selection agent.

Fermentation, Extraction and Isolation

Fungal strains were cultivated in Potato Dextrose Broth (PDB, Difco) amended with 30 g·L⁻¹ of XAD-16 resin. The inoculum originated from potato dextrose agar plates and consisted of a mixture of spores and mycelium. A total of four Erlenmeyer flasks of 2L each containing 1L of PDB medium were inoculated and allowed to grow at 25 °C with shaking (150 rpm) for 5 days. At the end of the incubation period, fungal biomass and resin were recovered and separated from the supernatant by filtration.

The mix of biomass and resin was extracted with 3 × 500 mL of EtoAc. The extract was dried over Na₂SO₄ and evaporated under reduced pressure yielding 390 mg of organic extract. The extract was subjected to flash chromatography using a gradient of n-heptane:EtoAc (100:0–0:100) at 40 mL/min during 75 min to afford 9 fractions, according to their TLC profiles. Fractions 1-5 were pooled and purified from a preparative C-18 column (Sunfire, 250mm x 10mm x 5μm) using a linear gradient for 40 min from H₂O to CH₃CN, both containing 0.1% formic acid followed by 10 min of CH₃CN containing 0.1% formic acid to afford 1 mg of eremophilane, 3 mg of colletorin A **6**, 2.5 mg of **2**, 2 mg of **1**, 3 mg of colletochlorin D **9** and 1 mg of colletochlorin B **8**. Fraction 6 (70.9 mg, n-heptane:EtoAc 40:60) was purified from a preparative C-18 column (Sunfire, 250mm x 10mm x 5μm) using an isocratic elution of water: CH₃CN (30:70), both containing 0.1% formic acid to afford 4 mg of colletochlorin A **7**, 3 mg of **3**, 4 mg of higginsianin A **10** and 17 mg of higginsianin B **11**. Fraction 8 (14.1 mg, n-heptane: EtoAc 20:80) was purified from a preparative C-18 column (Sunfire, 250mm x 10mm x 5μm) using a linear gradient for 40 min from H₂O to CH₃CN, both containing 0.1% formic acid followed by 10 min of acetonitrile containing 0.1% formic acid to afford 1.5 mg of **4**. Fraction 9 (24 mg, n-heptane: EtoAc 0:100) was purified from a

preparative C-18 column (Sunfire, 250mm x 10mm x 5 μ m) using a linear gradient for 40 min from H₂O to CH₃CN, both containing 0.1% formic acid followed by 10 min of CH₃CN containing 0.1% formic acid to afford 1.5 mg of **5**.

Colletorin D (1): yellow solid, UV λ_{\max} nm (log ϵ) 228 (4.2), 292 (4.1), 337 (3.6); IR ν_{\max} 3325, 2913, 1724, 1655, 1593, 1216 cm⁻¹; NMR data, Table 1; HRESIMS m/z 221.1174 [M+H]⁺ (calcd for C₁₃H₁₇O₃, 221.1178).

Colletorin D acid (2): yellow oil, UV λ_{\max} nm (log ϵ) 228 (4.2), 292 (4.1), 337 (3.6); IR ν_{\max} 3325, 1644, 1531, 1201, 1121 cm⁻¹; NMR data, Table 1; HRESIMS m/z 235.0964 [M-H]⁻ (calcd for C₁₃H₁₅O₄, 235.0970).

Higginsianin C (3): white amorphous solid, $[\alpha]_D^{25}$ -29 (*c* 0.1, MeOH); UV λ_{\max} nm (log ϵ) 291 (3.1); IR ν_{\max} 3388, 2932, 2893, 1676, 1644, 1568, 1383, 1234, 1074 cm⁻¹; NMR data, Table 2; HRESIMS m/z 445.2974 [M+H]⁺ (calcd for C₂₇H₄₁O₅, 445.2954).

13-epi-higginsianin C (4): white amorphous solid, $[\alpha]_D^{25}$ -19 (*c* 0.1, MeOH); UV λ_{\max} nm (log ϵ) 291 (3.1); IR ν_{\max} 3388, 2932, 2893, 1676, 1644, 1568, 1383, 1234, 1074 cm⁻¹; NMR data, Table 2; HRESIMS m/z 445.2958 [M+H]⁺ (calcd for C₂₇H₄₁O₅, 445.2954).

Sclerosporide (5): transparent oil, $[\alpha]_D^{25}$ -8.3 (*c* 0.1, MeOH); UV λ_{\max} nm (log ϵ) 234 (2.8); ECD (1 % w/v, MeOH), λ_{\max} ($\Delta\epsilon$) 217.2 (6.42) nm, IR ν_{\max} 3396, 2928, 1717, 1652, 1379, 1238, 1075, 980 cm⁻¹; NMR data, see table 3 and supporting information; HRESIMS m/z 425.2552 [M+H]⁺ (calcd for C₂₃H₃₇O₇, 425.2539).

Molecular Modeling

Three-dimensional coordinates of compounds **3**, **4** and **5** were generated from SMILES using CORINA version 3.60 (Molecular Networks GmbH, <http://www.molecular-networks.com/products/corina>).

The conformational analysis of these compounds was carried out using MacroModel v9.5, as implemented in the Schrödinger Suite (<http://www.schrodinger.com>). Default values were used except the allowed energy window (42 kJ/mol) and the number of evaluations per rotatable bond (500). The resulting conformers were clustered using a 2.0 Å cut-off.

The geometries of all conformers were optimized in gas-phase using the Gaussian 09 package (Gaussian 09, Revision D.1, Gaussian Inc., <http://www.gaussian.com>)⁴⁶ with the Becke's three-parameter hybrid exchange functional (B3LYP);⁴⁷⁻⁴⁸ and the 6-31+G(d,p) basis set. Subsequent vibrational frequency calculations confirmed that these conformations were local minima.

NMR chemical shifts and coupling constants were calculated at the B3LYP/6-31+G(d,p) level following the protocol described by Tantillo and colleagues at the CHESHIRE Chemical Shift Repository (<http://cheshirenmr.info/>)⁴⁹ using the Gaussian09 package. The analysis of results was performed using an in-house-developed script.

ECD spectra were computed at the B3LYP/TZVP level (60 excited states), using Gaussian09.⁴⁶ The computed and experimental ECD spectra were superimposed using SpecDis.⁵⁰

Structure images were obtained with Chimera⁵¹ using the Pov-Ray rendering feature.

ASSOCIATED CONTENT.

Supporting Information. The Supporting Information is available free of charge on the ACS Publications website at DOI:”..

AUTHOR INFORMATION.

Corresponding Author

ACKNOWLEDGMENT.

R.J.O. received funding from the French National Research Agency (grant ANR-12-CHEX-0008-01)

REFERENCES AND NOTES

REFERENCES AND NOTES

(1) O'Connell, R.; Herbert, C.; Sreenivasaprasad, S.; Khatib, M.; Esquerre-Tugaye, M. T.; Dumas, B. *Mol Plant Microbe Interact* **2004**, *17*, 272-82.

(2) Birker, D.; Heidrich, K.; Takahara, H.; Narusaka, M.; Deslandes, L.; Narusaka, Y.; Reymond, M.; Parker, J. E.; O'Connell, R. *Plant J* **2009**, *60*, 602-13.

(3) Dallery, J.-F.; Lapalu, N.; Zampounis, A.; Pigné, S.; Luyten, I.; Amselem, J.; Wittenberg, A. H. J.; Zhou, S.; de Queiroz, M. V.; Robin, G. P.; Auger, A.; Hainaut, M.; Henrissat, B.; Kim, K.-T.; Lee, Y.-H.; Lespinet, O.; Schwartz, D. C.; Thon, M. R.; O'Connell, R. J. *BMC Genomics* **2017**, *18*, 667.

(4) Giles, S. S.; Soukup, A. A.; Lauer, C.; Shaaban, M.; Lin, A.; Oakley, B. R.; Wang, C. C. C.; Keller, N. P. *Appl. Environ. Microbiol.* **2011**, *77*, 3669-3675.

(5) Bok, J. W.; Chiang, Y. M.; Szewczyk, E.; Reyes-Dominguez, Y.; Davidson, A. D.; Sanchez, J. F.; Lo, H. C.; Watanabe, K.; Strauss, J.; Oakley, B. R.; Wang, C. C.; Keller, N. P. *Nat Chem Biol* **2009**, *5*, 462-4.

(6) Reyes-Dominguez, Y.; Boedi, S.; Sulyok, M.; Wiesenberger, G.; Stoppacher, N.; Krska, R.; Strauss, J. *Fungal Genet Biol* **2012**, *49*, 39-47.

(7) Chujo, T.; Scott, B. *Mol Microbiol* **2014**, *92*, 413-34.

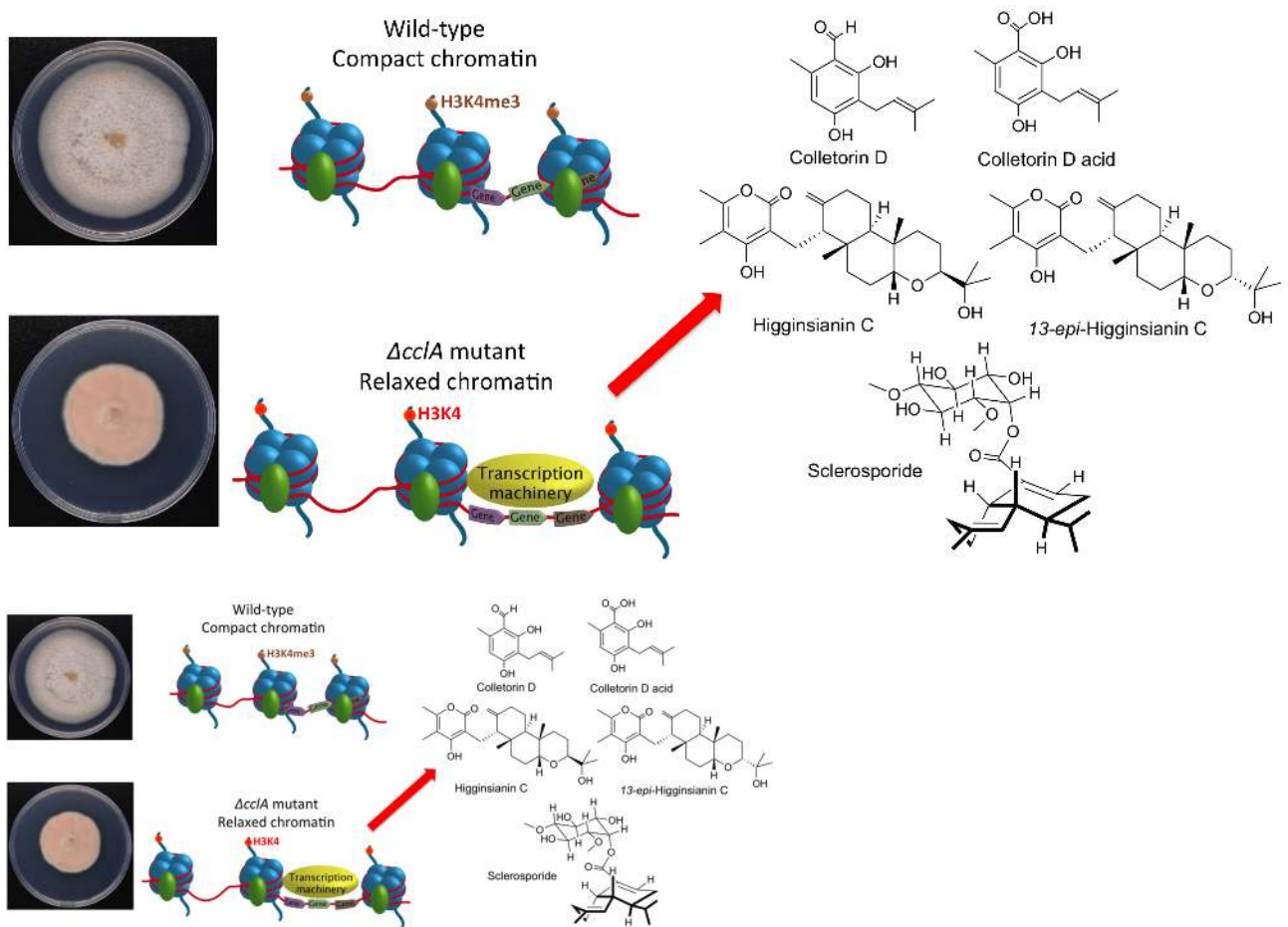
(8) Wu, G.; Zhou, H.; Zhang, P.; Wang, X.; Li, W.; Zhang, W.; Liu, X.; Liu, H.-W.; Keller, N. P.; An, Z.; Yin, W.-B. *Org. Lett.* **2016**, *18*, 1832-1835.

- (9) Miller, T.; Krogan, N. J.; Dover, J.; Erdjument-Bromage, H.; Tempst, P.; Johnston, M.; Greenblatt, J. F.; Shilatifard, A. *Proc. Natl. Acad. Sci. U.S.A.* **2001**, *98*, 12902-12907.
- (10) Palmer, J. M.; Bok, J. W.; Lee, S.; Dagenais, T. R.; Andes, D. R.; Kontoyiannis, D. P.; Keller, N. P. *PeerJ* **2013**, *1*, e4.
- (11) Kosuge, Y.; Suzuki, A.; Hirata, S.; Tamura, S. *Agric. Biol. Chem.* **1973**, *37*, 455-456.
- (12) Kosuge, Y.; Suzuki, A.; Tamura, S. *Agric. Biol. Chem.* **1974**, *38*, 1265-1267.
- (13) Kosuge, Y.; Suzuki, A.; Tamura, S. *Agric. Biol. Chem.* **1974**, *38*, 1553-1554.
- (14) Cimmino, A.; Mathieu, V.; Masi, M.; Baroncelli, R.; Boari, A.; Pescitelli, G.; Ferderin, M.; Lisy, R.; Evidente, M.; Tuzi, A.; Zonno, M. C.; Kornienko, A.; Kiss, R.; Evidente, A. *J. Nat. Prod.* **2016**, *79*, 116-125.
- (15) Masi, M.; Cimmino, A.; Boari, A.; Tuzi, A.; Zonno, M. C.; Baroncelli, R.; Vurro, M.; Evidente, A. *J. Agric. Food Chem.* **2017**, *65*, 1124-1130.
- (16) Le Goff, G.; Adelin, E.; Cortial, S.; Servy, C.; Ouazzani, J. *Bioprocess Biosyst. Eng.* **2013**, *36*, 1285-1290.
- (17) Le Goff, G.; Martin, M.-T.; Iorga, B. I.; Adelin, E.; Servy, C.; Cortial, S.; Ouazzani, J. *J. Nat. Prod.* **2013**, *76*, 142-149.
- (18) Kawagishi, H.; Sato, H.; Sakamura, S.; Kobayashi, K.; Tadao, U. *Agric. Biol. Chem.* **1984**, *48*, 1903-1904.
- (19) Masi, M.; Zonno, M. C.; Cimmino, A.; Reveglia, P.; Berestetskiy, A.; Boari, A.; Vurro, M.; Evidente, A. *Nat. Prod. Res.* **2017**, *32*, 1537-1547.
- (20) Masi, M.; Cimmino, A.; Boari, A.; Zonno, M. C.; Górecki, M.; Pescitelli, G.; Tuzi, A.; Vurro, M.; Evidente, A. *Tetrahedron* **2017**, *73*, 6644-6650.
- (21) Fujii, I.; Mori, Y.; Watanabe, A.; Kubo, Y.; Tsuji, G.; Ebizuka, Y. *Biosci. Biotechnol. Biochem.* **1999**, *63*, 1445-1452.
- (22) Nawata, Y.; Ando, K.; Tamura, G.; Arima, K.; Iitaka, Y. *J. Antibiot (Tokyo)* **1969**, *22*, 511-2.

- (23) Tamura, G.; Suzuki, S.; Takatsuki, A.; Ando, K.; Arima, K. *J Antibiot (Tokyo)* **1968**, *21*, 539-44.
- (24) Cagnoli-Bellavita, N.; Ceccherelli, P.; Fringuelli, R.; Ribaldi, M. *Phytochemistry* **1975**, *14*, 807.
- (25) Singh, S. B.; Zink, D. L.; Bills, G. F.; Jenkins, R. G.; Silverman, K. C.; Lingham, R. B. *Tetrahedron Lett.* **1995**, *36*, 4935-4938.
- (26) Sasaki, H.; Okutomi, T.; Hosokawa, T.; Nawata, Y.; Ando, K. *Tetrahedron Lett.* **1972**, *13*, 2541-2544.
- (27) Gutiérrez, M.; Theoduloz, C.; Rodríguez, J.; Lolas, M.; Schmeda-Hirschmann, G. *J. Agric. Food Chem.* **2005**, *53*, 7701-7708.
- (28) Singh, S. B.; Zink, D. L.; Dombrowski, A. W.; Dezeny, G.; Bills, G. F.; Felix, J. P.; Slaughter, R. S.; Goetz, M. A. *Org. Lett.* **2001**, *3*, 247-250.
- (29) Nothias-Scaglia, L. F.; Gallard, J. F.; Dumontet, V.; Roussi, F.; Costa, J.; Iorga, B. I.; Paolini, J.; Litaudon, M. *J Nat Prod* **2015**, *78*, 2423-31.
- (30) Katayama, M.; Marumo, S.; Hattori, H. *Tetrahedron Lett.* **1983**, *24*, 1703-1706.
- (31) Katayama, M.; Marumo, S. *Agric. Biol. Chem.* **1978**, *42*, 505-506.
- (32) Harada, Y.; Sawamura, K.; Konno, K. *J. J. Phytopath.* **1974**, *40*, 412-418.
- (33) Sawai, K.; Okuno, T.; Yoshikawa, E. *Agric. Biol. Chem.* **1985**, *49*, 2501-2503.
- (34) Almeida, C.; Eguereva, E.; Kehraus, S.; Siering, C.; König, G. M. *J. Nat. Prod.* **2010**, *73*, 476-478.
- (35) Kitahara, T.; Kurata, H.; Matsuoka, T.; Mori, K. *Tetrahedron* **1985**, *41*, 5475-5485.
- (36) Okada, K.; Koseki, K.; Kitahara, T.; Mori, K. *Agric. Biol. Chem.* **1985**, *49*, 487-493.
- (37) Kitahara, T.; Matsuoka, T.; Katayama, M.; Marumo, S.; Mori, K. *Tetrahedron Lett.* **1984**, *25*, 4685-4688.
- (38) Gallagher, R. T. *Phytochemistry* **1975**, *14*, 755-757.

- (39) Shakeel, U. R.; Sofi, S. N.; Khuroo, M. A.; Taneja, S. C.; Bhat, K. A.; Vishwakarma, R. *Nat Prod Res* **2013**, *27*, 2033-8.
- (40) Sureshan, K. M.; Murakami, T.; Watanabe, Y. *Tetrahedron* **2009**, *65*, 3998-4006.
- (41) De Almeida, M. V.; Couri, M. R. C.; De Assis, J. V.; Anconi, C. P. A.; Dos Santos, H. F.; De Almeida, W. B. *Magn. Reson. Chem.* **2012**, *50*, 608-614.
- (42) Newton, G. L.; Fahey, R. C. *Arch. Microbiol.* **2002**, *178*, 388-394.
- (43) Mo, E.; Ahn, J.; Jo, Y.; Kim, S.; Hwang, B.; Lee, M. *Molecules* **2017**, *22*, 1349.
- (44) Wu, T.; Liang, Y.; Zhu, X.; Zhao, M.; Liu, H. *Anal. Bioanal. Chem.* **2014**, *406*, 3239-3247.
- (45) Wu, J.; Tang, C.; Yao, S.; Zhang, L.; Ke, C.; Feng, L.; Lin, G.; Ye, Y. *J. Nat. Prod.* **2015**, *78*, 2332-2338.
- (46) Frisch, M. J.; Trucks, G. W.; Schlegel, H. B.; Scuseria, G. E.; Robb, M. A.; Cheeseman, J. R.; Scalmani, G.; Barone, V.; Mennucci, B.; Petersson, G. A.; et al. *Gaussian 09, Revision D.01*. Gaussian Inc.: Wallingford CT, USA (<http://www.gaussian.com>).
- (47) Lee, C.; Yang, W.; Parr, R. G. *Phys. Rev. B* **1988**, *37*, 785-789.
- (48) Becke, A. D. *J. Chem. Phys.* **1993**, *98*, 5648-5652.
- (49) Lodewyk, M. W.; Siebert, M. R.; Tantillo, D. J. *Chem Rev* **2012**, *112*, 1839-62.
- (50) Bruhn, T.; Schaumlöffel, A.; Hemberger, Y.; Bringmann, G. *Chirality* **2013**, *25*, 243-249.
- (51) Pettersen, E. F.; Goddard, T. D.; Huang, C. C.; Couch, G. S.; Greenblatt, D. M.; Meng, E. C.; Ferrin, T. E. *J Comput Chem* **2004**, *25*, 1605-12.

For Table of Contents Only (Graphical Abstract)



Supporting Information

Deleting a chromatin remodeling gene increases the diversity of secondary metabolites produced by *Colletotrichum higginsianum*

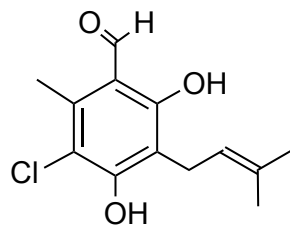
Jean-Félix Dallery,[†] Géraldine Le Goff,[†] Emilie Adelin,[†] Bogdan I. Iorga,[†] Sandrine Pigné,[‡]
Richard O'Connell,[‡] Jamal Ouazzani^{†*}

[†] Centre National de la Recherche Scientifique, Institut de Chimie des Substances Naturelles ICSN, Avenue de la Terrasse 91198, Gif-sur-Yvette, cedex, France.

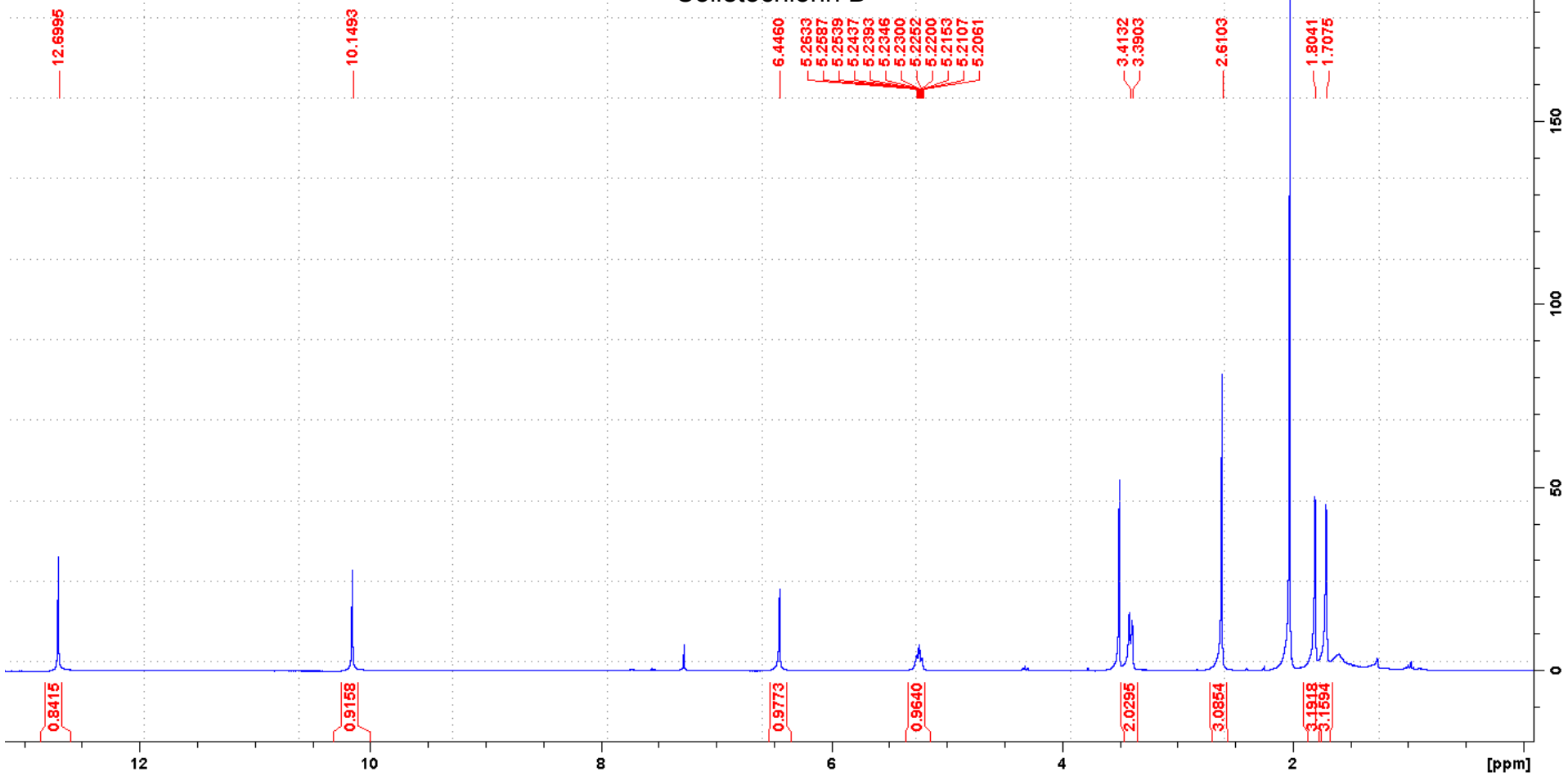
[‡] UMR BIOGER, INRA, AgroParisTech, Université Paris-Saclay, Avenue Lucien Brétignières, 78850, Thiverval-Grignon, France.

TABLE OF CONTENT

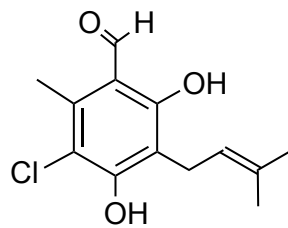
- S1.** ¹H NMR spectrum of colletochlorin D (CDCl₃, 500 MHz).
S2. ¹³C NMR spectrum of colletochlorin D (CDCl₃, 125 MHz).
S3. 1H-1H COSY spectrum of colletochlorin D (CDCl₃, 500 MHz).
S4. 1H-¹³C HSQC-ED spectrum of colletochlorin D (CDCl₃, 500 MHz).
S5. 1H-¹³C HMBC spectrum of colletochlorin D (CDCl₃, 500 MHz).
S6. ¹H NMR spectrum of colletorin D (**1**) (CDCl₃, 500 MHz).
S7. ¹³C NMR spectrum of colletorin D (**1**) (CDCl₃, 125 MHz).
S8. 1H-1H COSY spectrum of colletorin D (**1**) (CDCl₃, 500 MHz).
S9. 1H-¹³C HSQC-ED spectrum of colletorin D (**1**) (CDCl₃, 500 MHz).
S10. 1H-¹³C HMBC spectrum of colletorin D (**1**) (CDCl₃, 500 MHz).
S11. HRESIMS of colletorin D (**1**)
S12. ¹H NMR spectrum of colletorin D acid (**2**) (CD₃OD, 500 MHz).
S13. ¹³C NMR spectrum of colletorin D acid (**2**) (CD₃OD, 125 MHz).
S14. 1H-1H COSY spectrum of colletorin D acid (**2**) (CD₃OD, 500 MHz).
S15. 1H-¹³C HSQC-ED spectrum of colletorin D acid (**2**) (CD₃OD, 500 MHz).
S16. 1H-¹³C HMBC spectrum of colletorin D acid (**2**) (CD₃OD, 500 MHz).
S17. HRESIMS of colletorin D acid (**2**)
S18. ¹H NMR spectrum of Higginsianin C (**3**) (CD₃OD, 500 MHz).
S19. ¹³C NMR spectrum of Higginsianin C (**3**) (CD₃OD, 125 MHz).
S20. 1H-1H COSY spectrum of Higginsianin C (**3**) (CD₃OD, 500 MHz).
S21. 1H-¹³C HSQC-ED spectrum of Higginsianin C (**3**) (CD₃OD, 500 MHz).
S22. 1H-¹³C HMBC spectrum of Higginsianin C (**3**) (CD₃OD, 500 MHz).
S23. 1H-1H ROESY spectrum of Higginsianin C (**3**) (CD₃OD, 500 MHz).
S24. HRESIMS of Higginsianin C (**3**)
S25. IR spectrum of Higginsianin C (**3**)
S26. ¹H NMR spectrum of 13-*epi*-higginsianin C (**4**) (CD₃OD, 500 MHz).
S27. ¹³C NMR spectrum of 13-*epi*-higginsianin C (**4**) (CD₃OD, 125 MHz).
S28. 1H-1H COSY spectrum of 13-*epi*-higginsianin C (**4**) (CD₃OD, 500 MHz).
S29. 1H-¹³C HSQC-ED spectrum of 13-*epi*-higginsianin C (**4**) (CD₃OD, 500 MHz).
S30. 1H-¹³C HMBC spectrum of 13-*epi*-higginsianin C (**4**) (CD₃OD, 500 MHz).
S23. 1H-1H ROESY spectrum of 13-*epi*-higginsianin C (**4**) (CD₃OD, 500 MHz).
S31. HRESIMS of 13-*epi*-higginsianin C (**4**)
S32. IR spectrum of 13-*epi*-higginsianin C (**4**)
S33. ¹H NMR spectrum of sclerosporide (**5**) (CD₃OD, 500 MHz).
S34. ¹³C NMR spectrum of sclerosporide (**5**) (CD₃OD, 125 MHz).
S35. 1H-1H COSY spectrum of sclerosporide (**5**) (CD₃OD, 500 MHz).
S36. 1H-¹³C HSQC-ED spectrum of sclerosporide (**5**) (CD₃OD, 500 MHz).
S37. 1H-¹³C HMBC spectrum of sclerosporide (**5**) (CD₃OD, 500 MHz).
S38. 1H-1H ROESY spectrum of sclerosporide (**5**) (CD₃OD, 500 MHz).
S39. HRESIMS of sclerosporide (**5**)
S40. IR spectrum of sclerosporide (**5**)
S41. Comparison of ¹H NMR Data from Experimental Chemical Shifts (δ_{exp}) vs Calculated Chemical Shifts by DFT-NMR (δ_{calcd}) for compounds **3** and **4** (δ_{H} in ppm)
S42. Comparison of ¹³C NMR Data from Experimental Chemical Shifts (δ_{exp}) vs Calculated Chemical Shifts by DFT-NMR (δ_{calcd}) for compounds **3** and **4** (δ_{H} in ppm)
S43. Comparison of ¹H NMR Data from Experimental Chemical Shifts (δ_{exp}) vs Calculated Chemical Shifts by DFT-NMR (δ_{calcd}) for compound **5** (δ_{H} in ppm)
S44. Comparison of ¹³C NMR Data from Experimental Chemical Shifts (δ_{exp}) vs Calculated Chemical Shifts by DFT-NMR (δ_{calcd}) for compound **5** (δ_{H} in ppm)
From page 48 to page 54, Energy, Coordinates and Frequencies for compounds **3**, **4** and **5**.
From page 55 to 57, 3D dynamic structures of compounds **3**, **4** and **5**.
S45. Experimental data for known compounds isolated in this study.
S46. Superposed experimental ECD spectrum (black) with the ECD computed spectrum (red) for compounds **3** (left) and **4** (right).



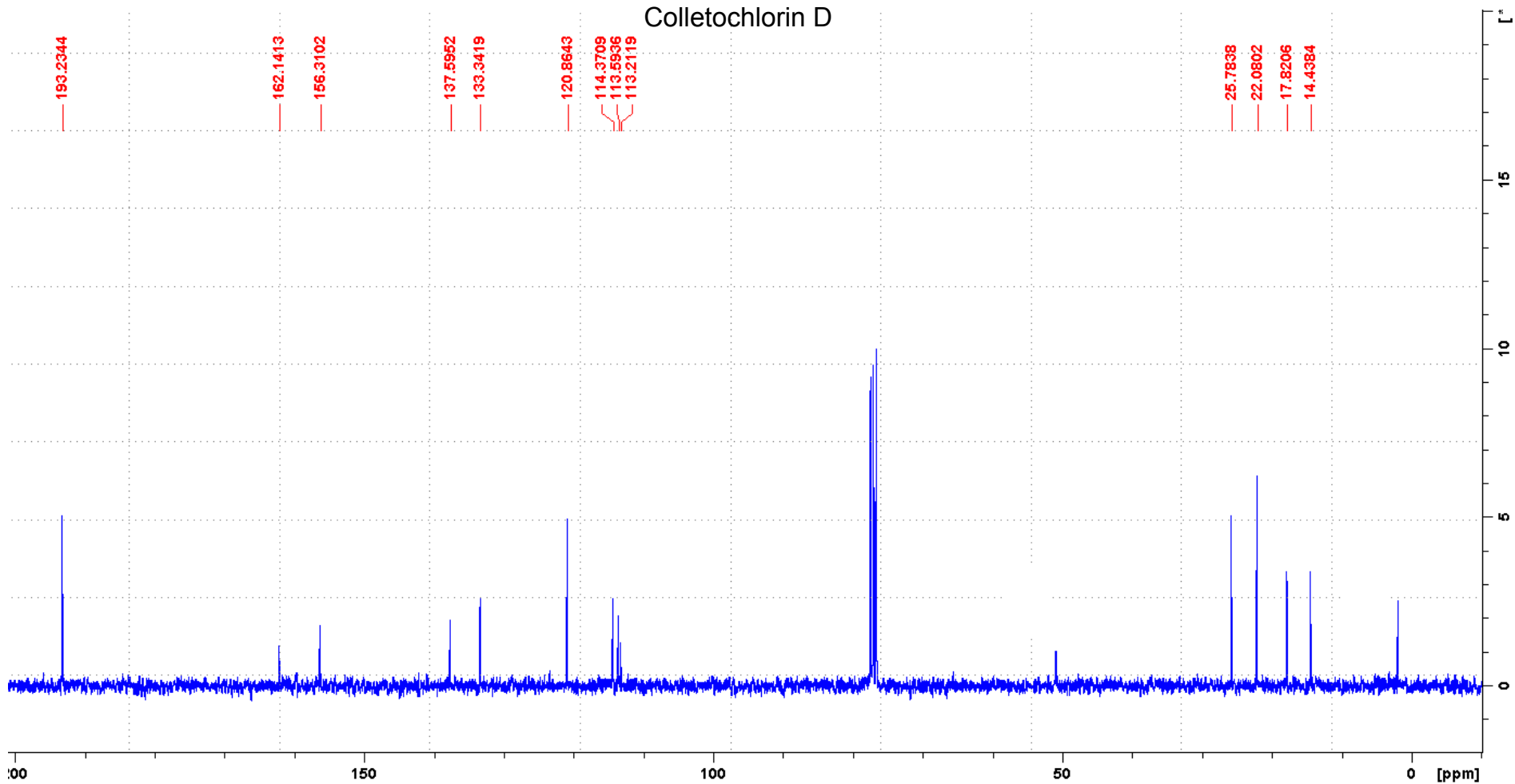
Colletochlorin D



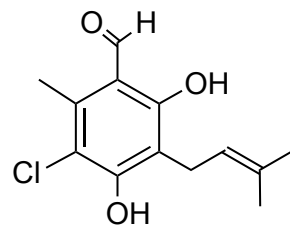
S1. ¹H NMR spectrum of colletochlorin D (CDCl₃, 500 MHz).



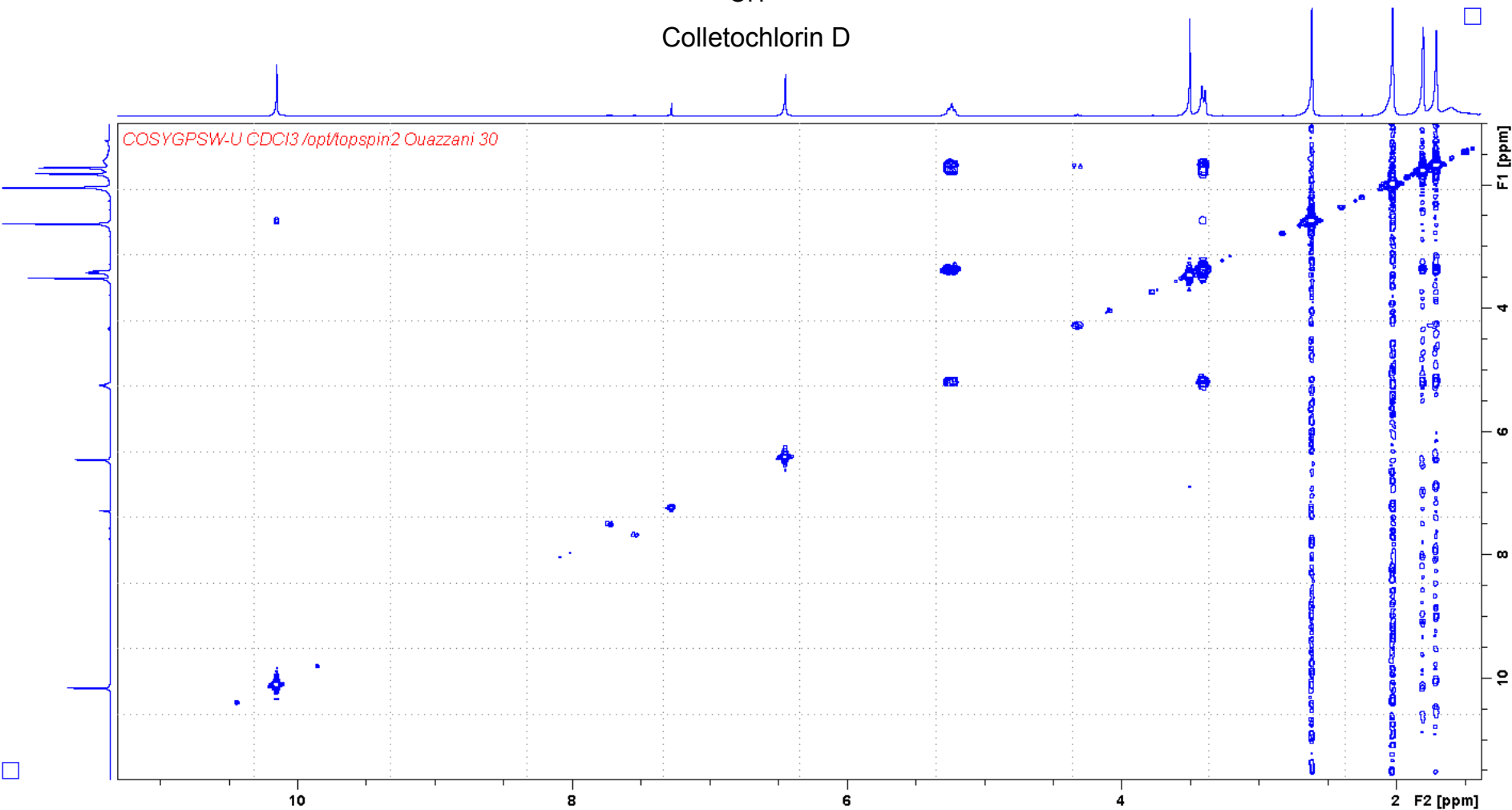
Colletochlorin D



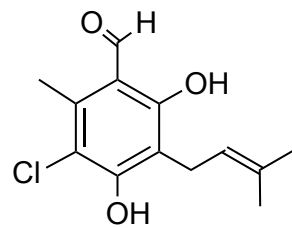
S2. ¹³C NMR spectrum of colletochlorin D (CDCl₃, 125 MHz).



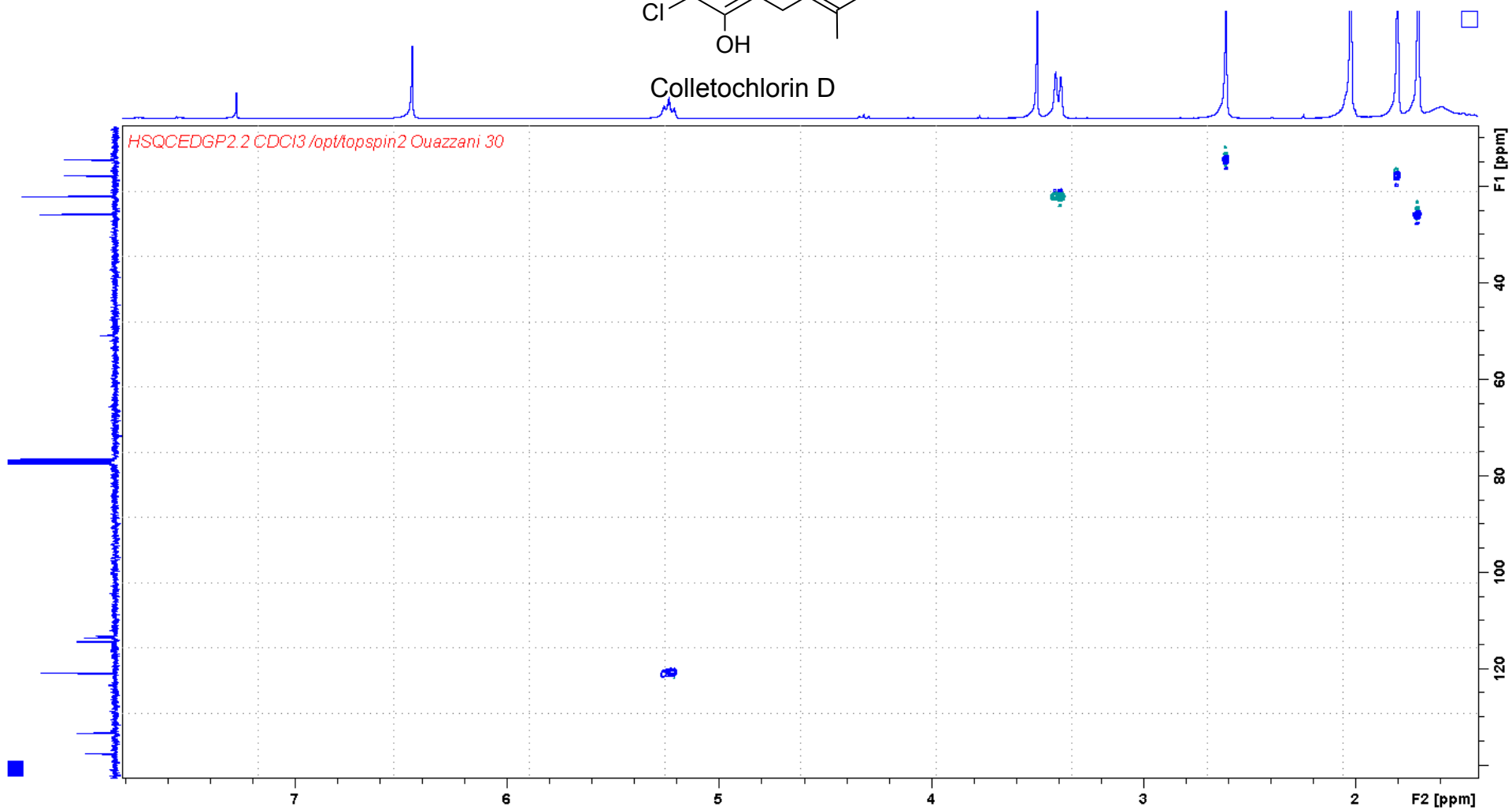
Colletochlorin D



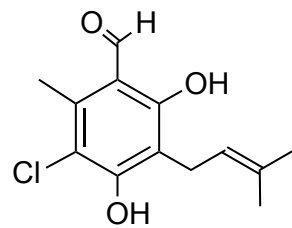
S3. ¹H-¹H COSY spectrum of colletochlorin D (CDCl₃, 500 MHz).



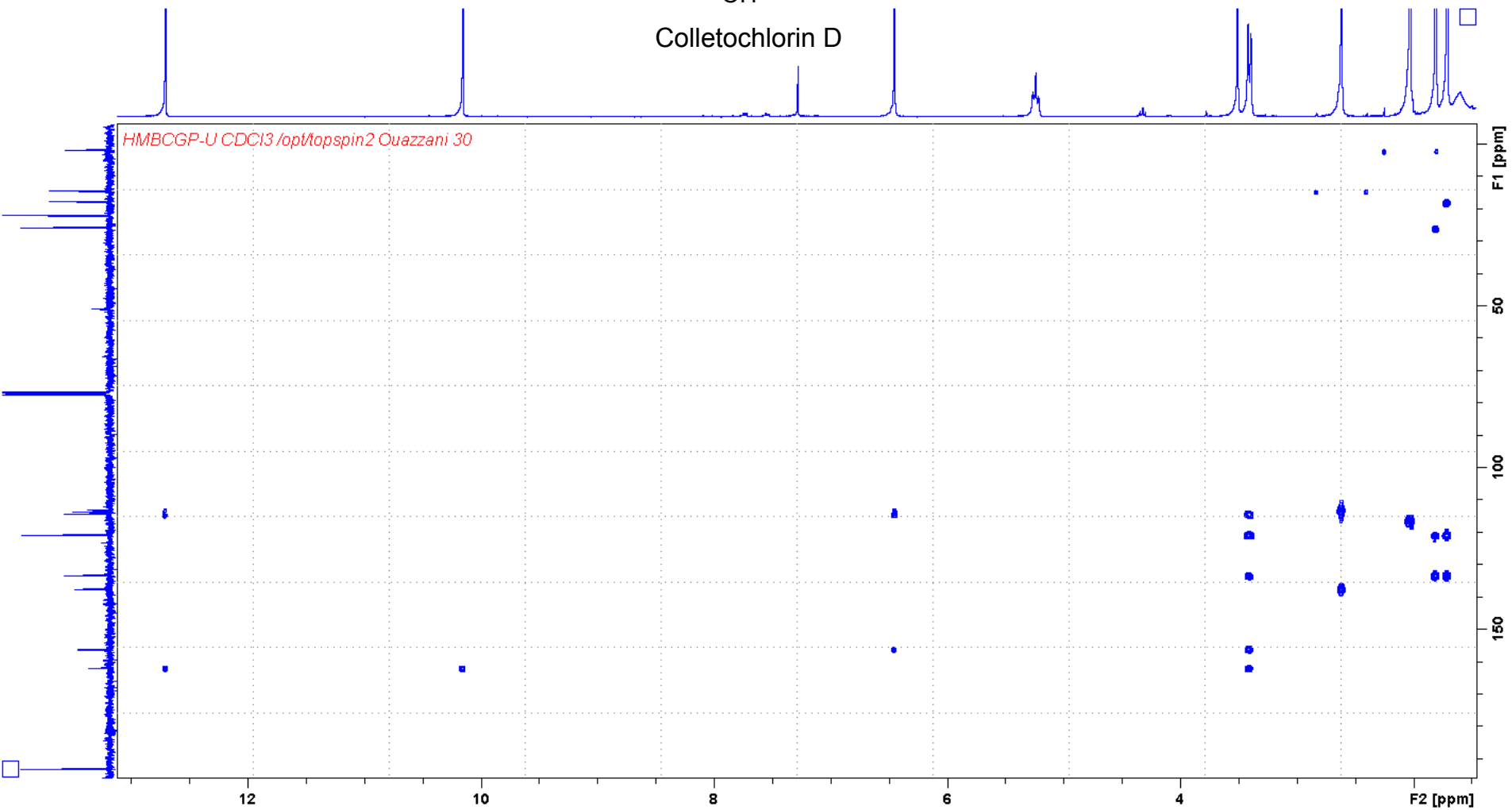
Colletochlorin D



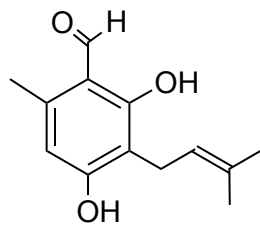
S4. ^1H - ^{13}C HSQC-ED spectrum of colletochlorin D (CDCl_3 , 500 MHz).



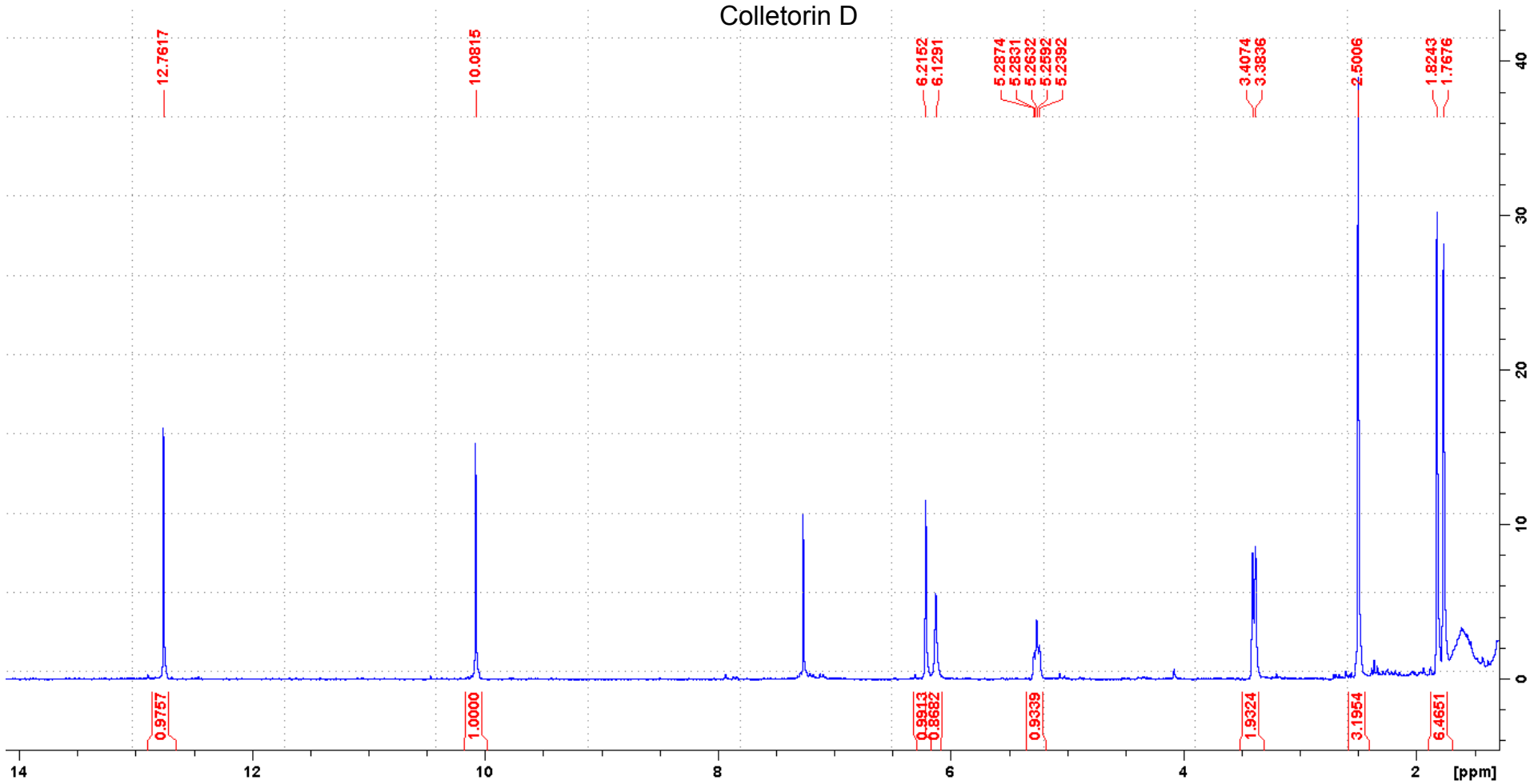
Colletochlorin D



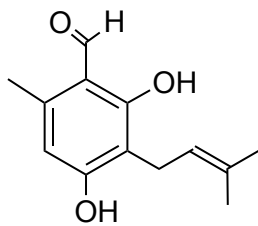
S5. ^1H - ^{13}C HMBC spectrum of colletochlorin D (CDCl_3 , 500 MHz).



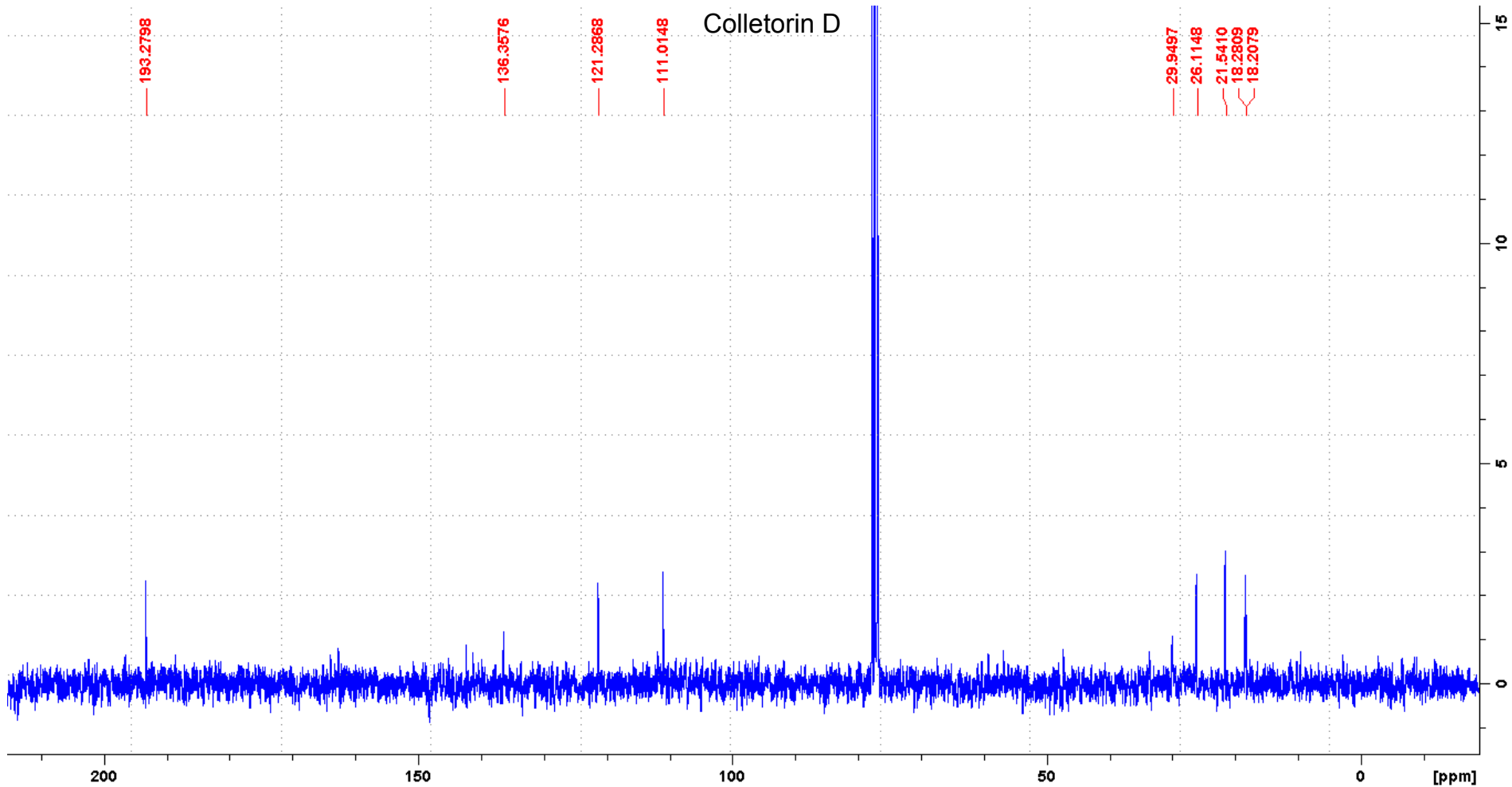
Colletorin D



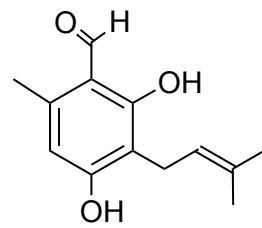
S6. ¹H NMR spectrum of colletorin D (1) (CDCl₃, 500 MHz).



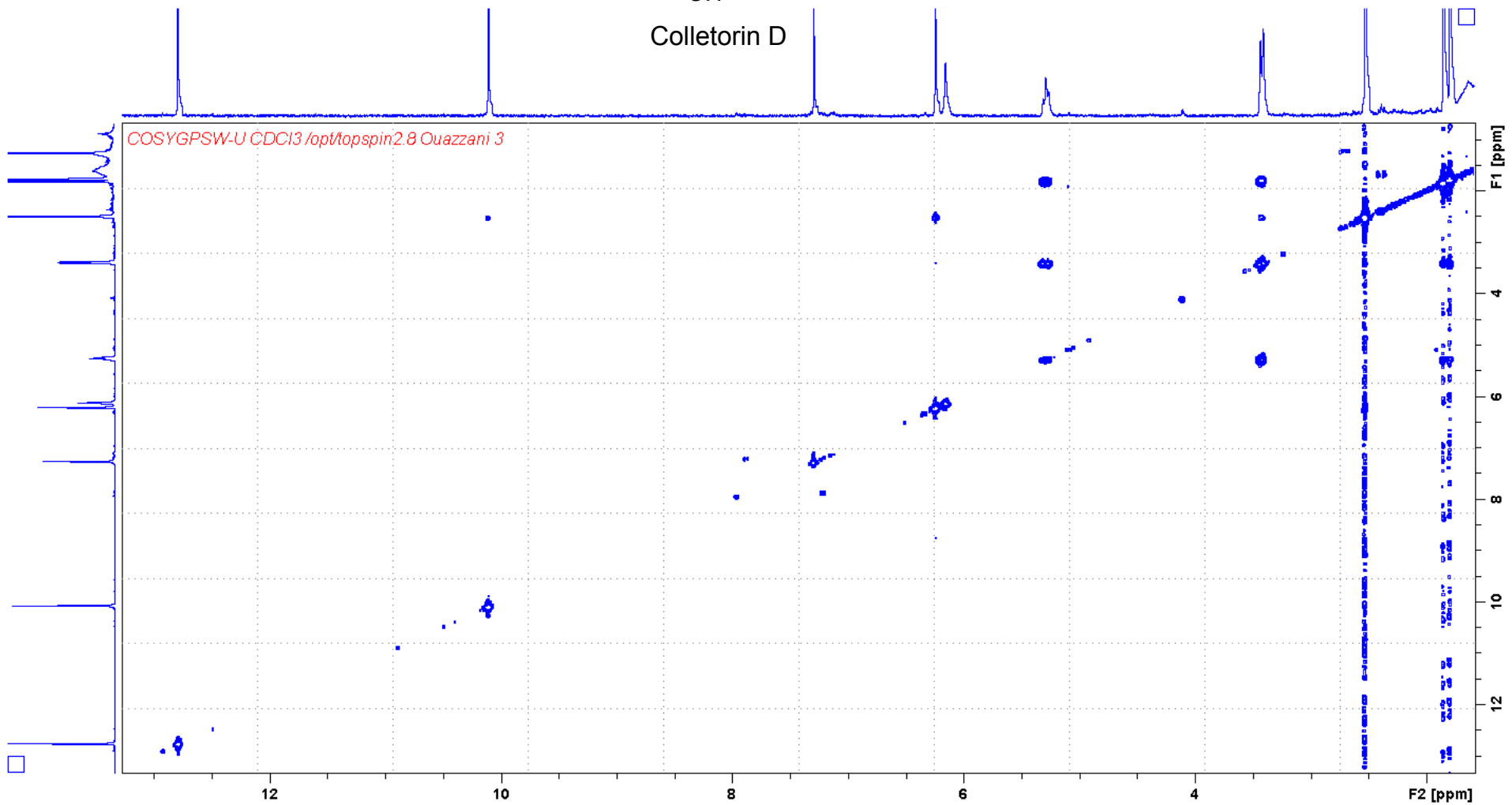
Colletorin D



S7. ^{13}C NMR spectrum of colletorin D (1) (CDCl_3 , 125 MHz).



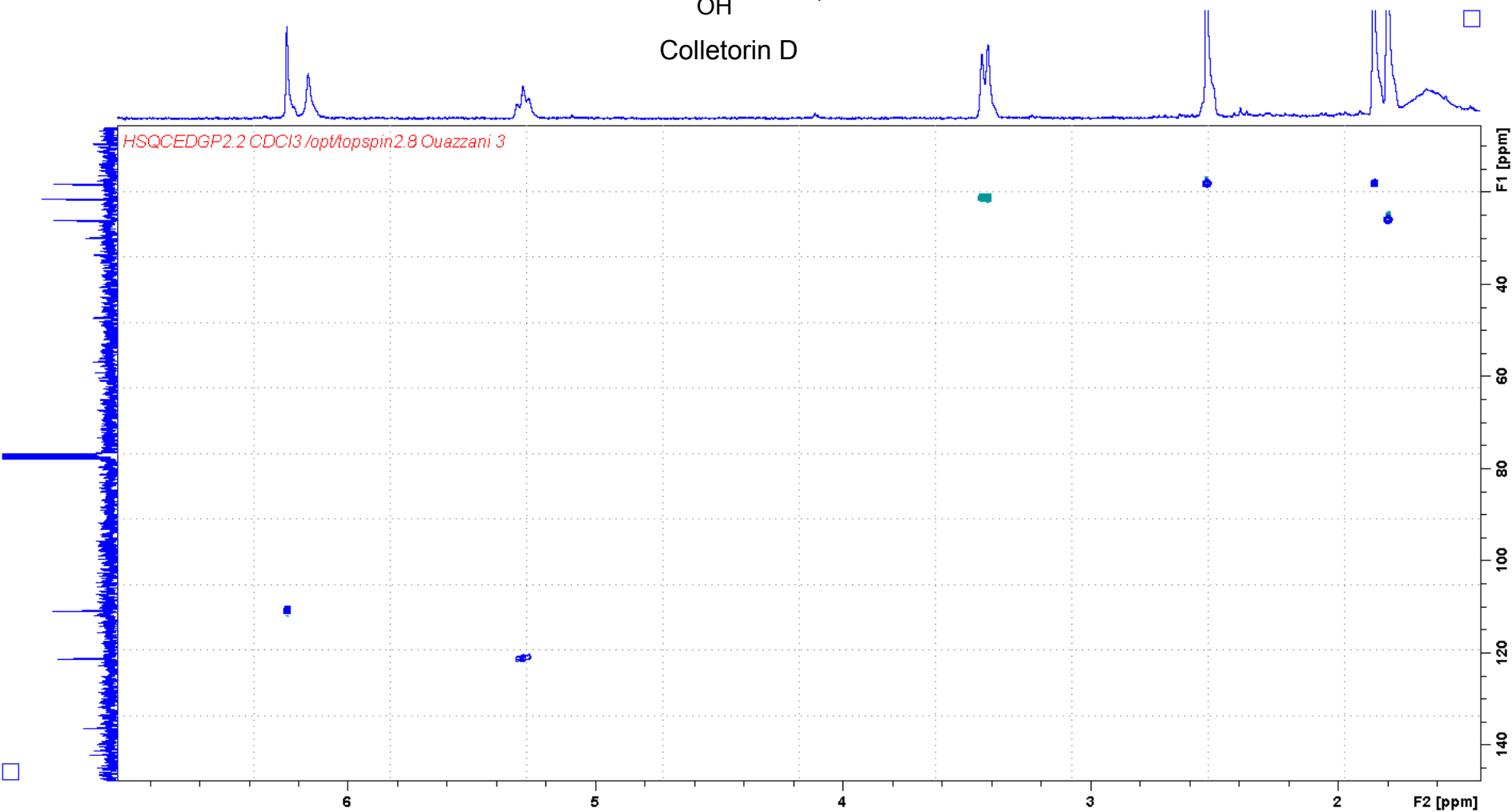
Colletorin D



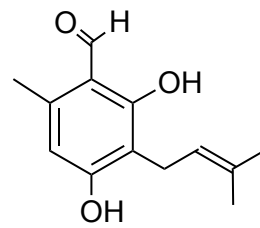
S8. ^1H - ^1H COSY spectrum of colletorin D (**1**) (CDCl_3 , 500 MHz).



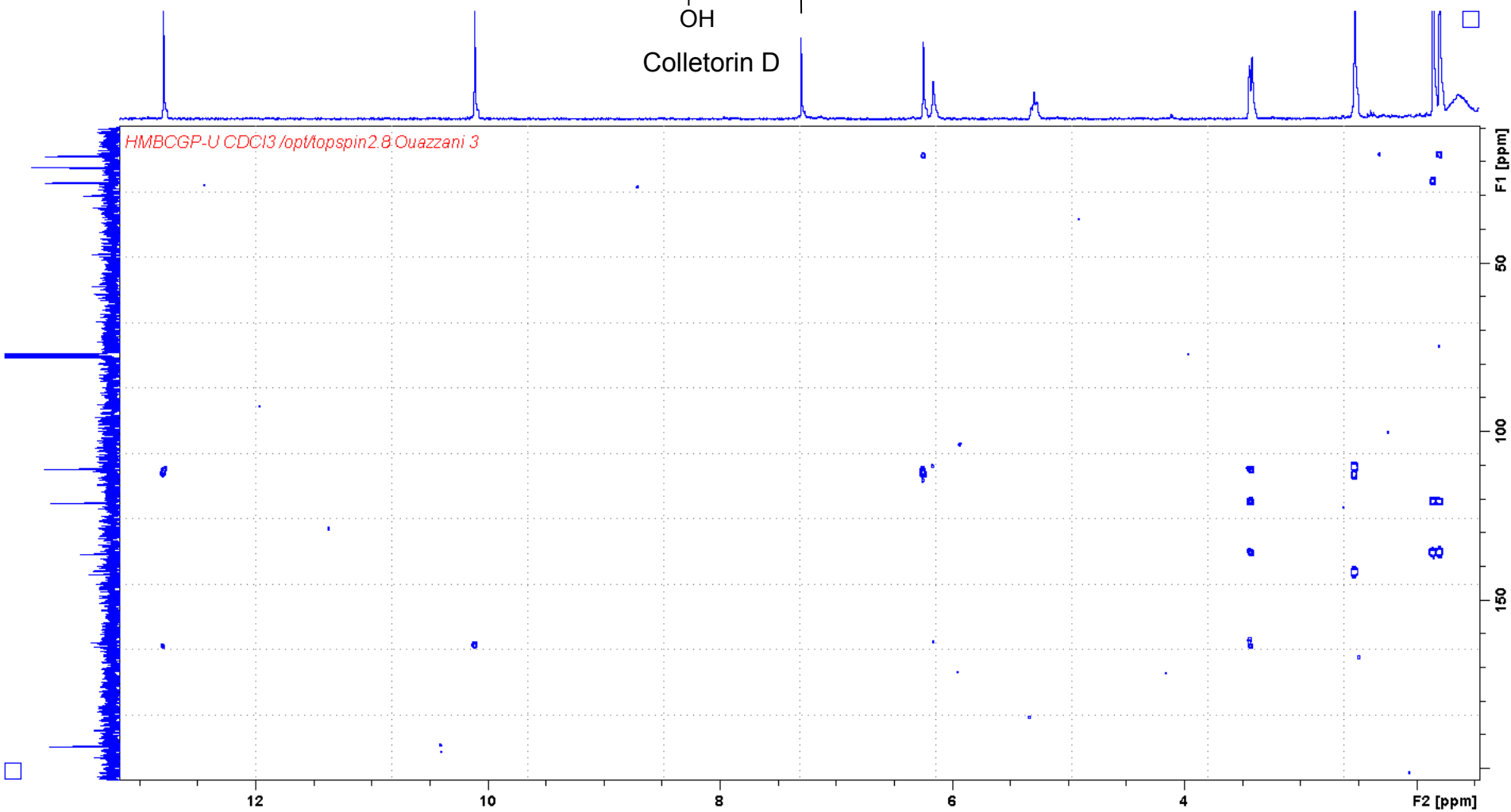
Colletorin D



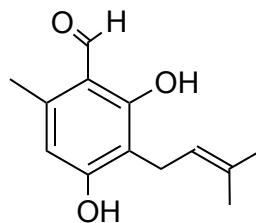
S9. ^1H - ^{13}C HSQC-ED spectrum of colletorin D (**1**) (CDCl_3 , 500 MHz).



Colletorin D



S10. ^1H - ^{13}C HMBC spectrum of colletorin D (**1**) (CDCl_3 , 500 MHz).



Colletorin D

Elemental Composition Report

Single Mass Analysis

Tolerance = 10.0 PPM / DBE: min = -1.5, max = 100.0

Element prediction: Off

Number of isotope peaks used for i-FIT = 9

Monoisotopic Mass, Even Electron Ions

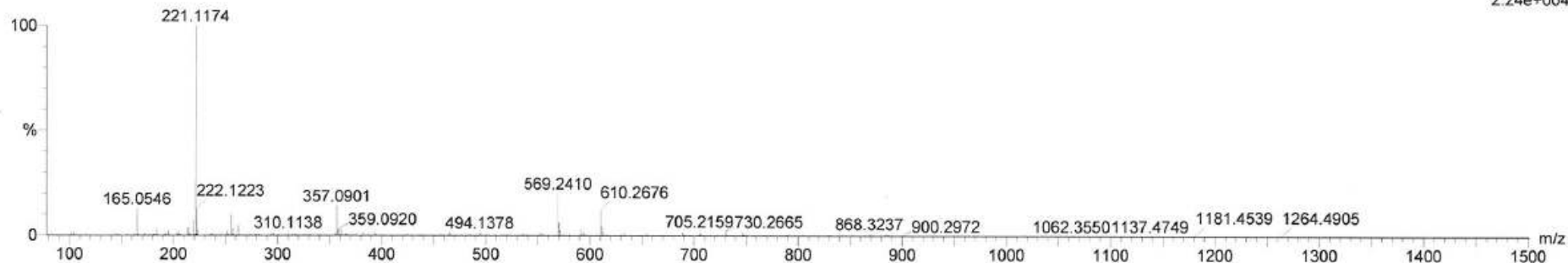
247 formula(e) evaluated with 1 results within limits (all results (up to 1000) for each mass)

Elements Used:

C: 0-50 H: 0-100 N: 0-10 O: 0-10

OUAZZANI_adelin53-1 22 (0.588) Cm (16:28-41:64x2.000)

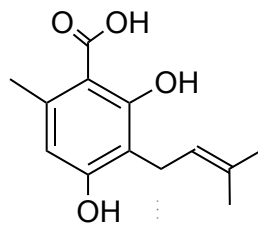
1: TOF MS ES+
2.24e+004



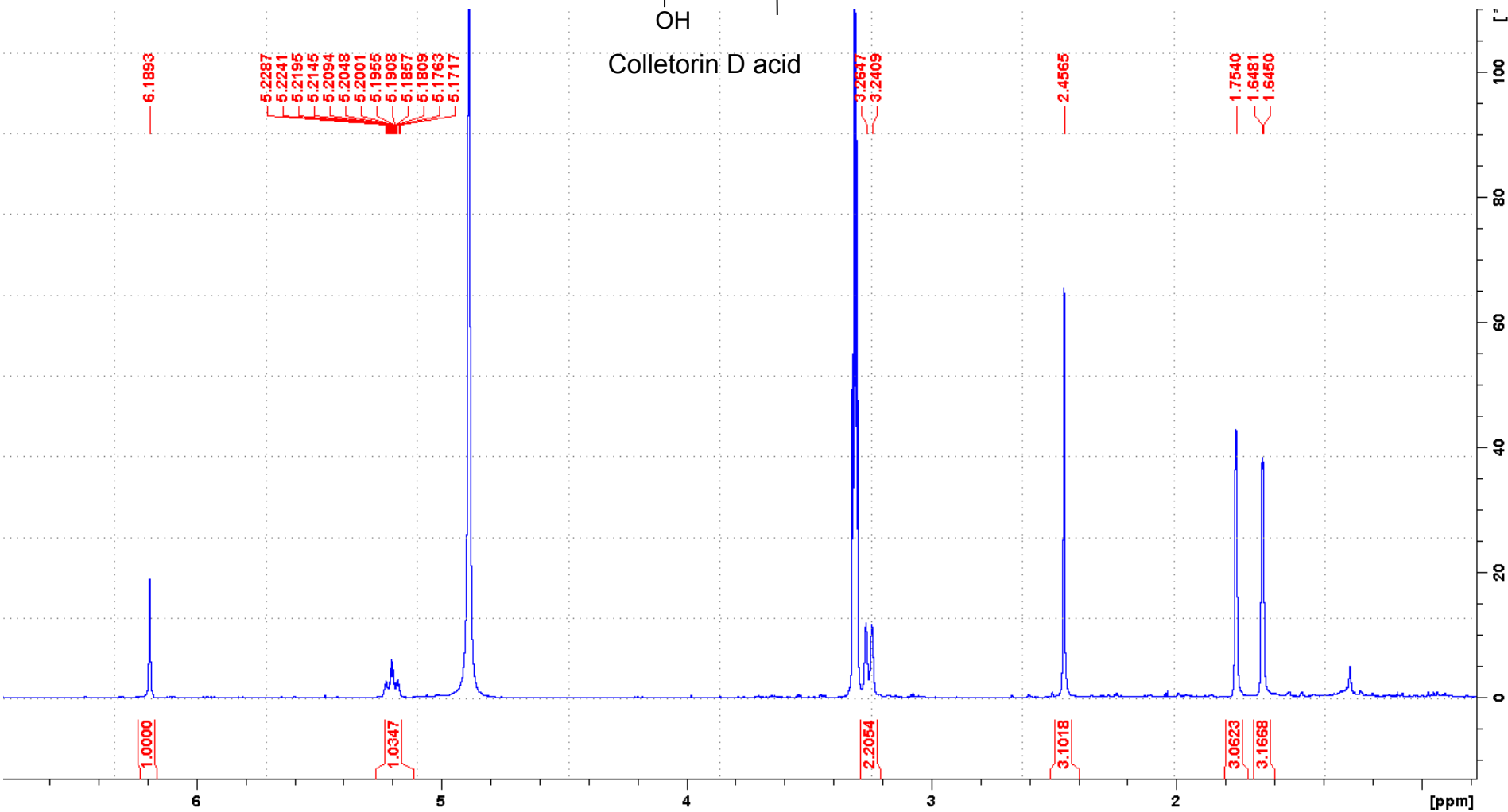
Minimum: -1.5
Maximum: 100.0

Mass	Calc. Mass	mDa	PPM	DBE	i-FIT	i-FIT (Norm)	Formula
221.1174	221.1178	-0.4	-1.8	5.5	367.9	0.0	C13 H17 O3

S11. HRESIMS of colletorin D (1)

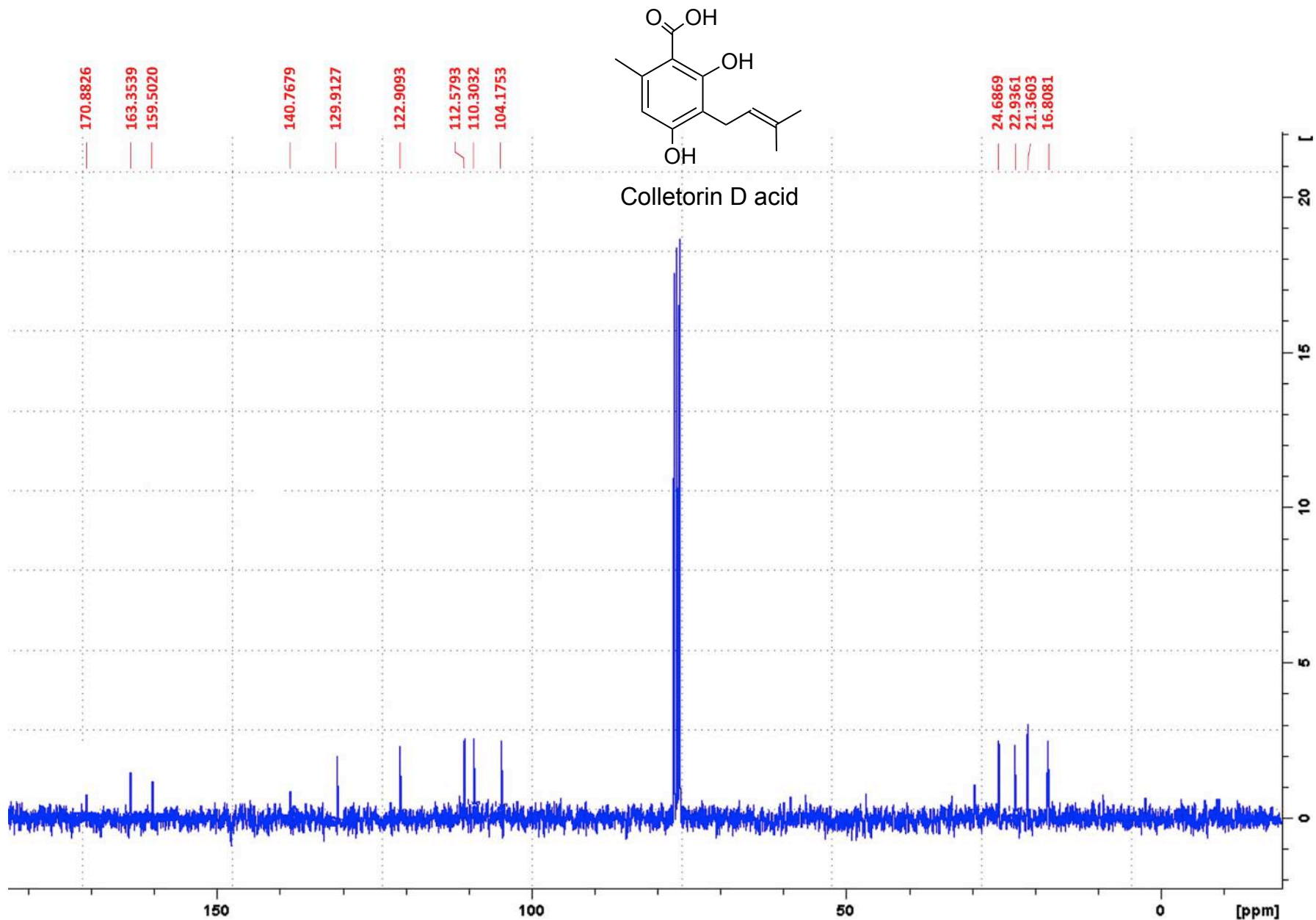


Colletorin D acid

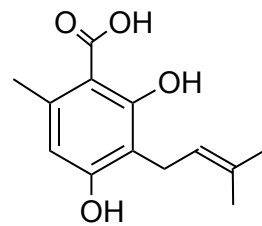


S12. ¹H NMR spectrum of colletorin D acid (**2**) (CD₃OD, 500 MHz).

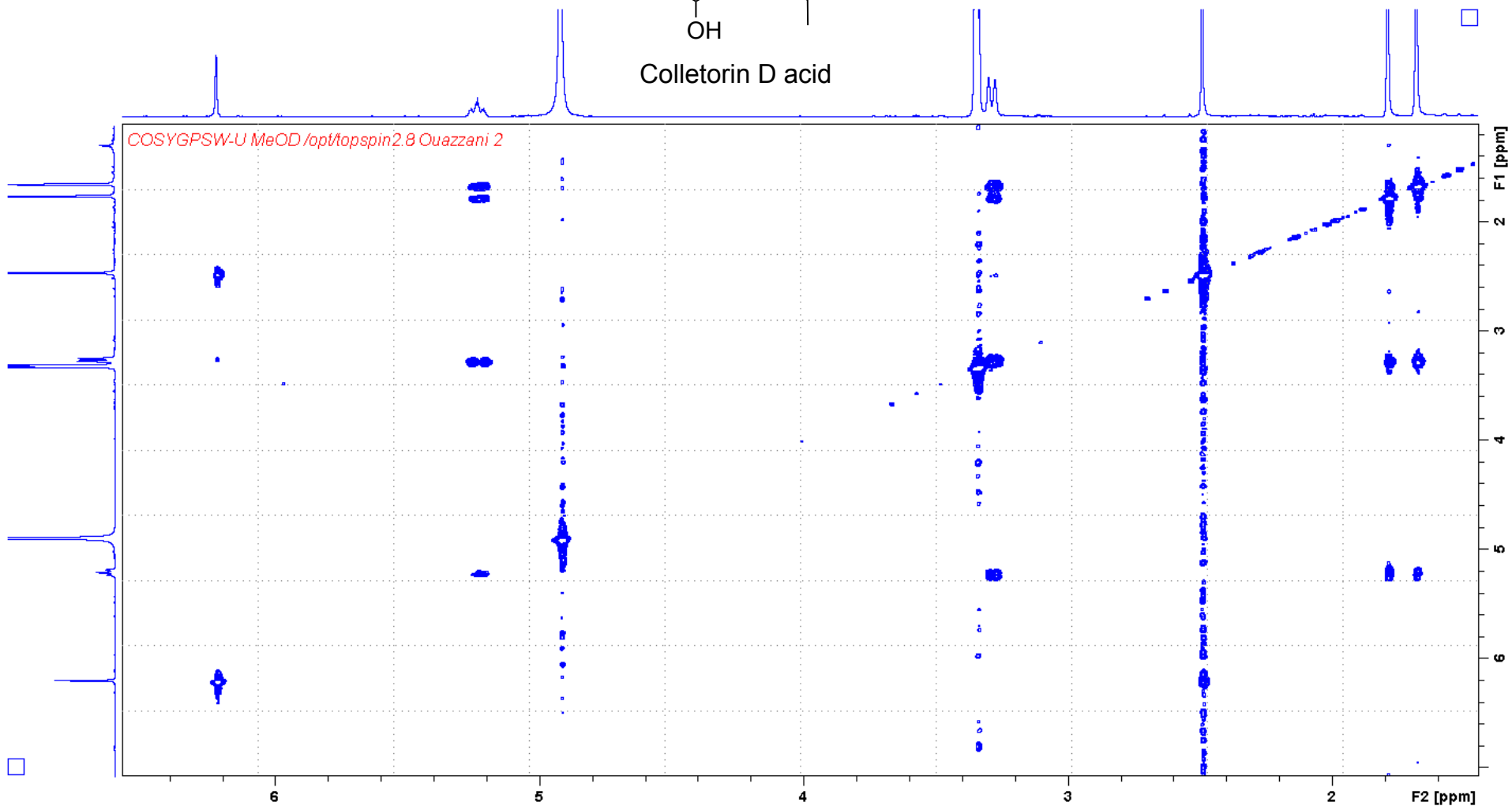
Difficult to solubilize in chloroform (Exchangeable aldehyde and hydroxyl protons not seen in the spectrum)



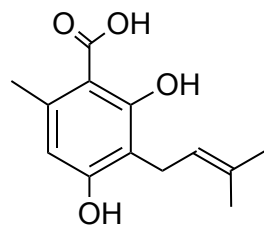
S13. ¹³C NMR spectrum of colletorin D acid (**2**) (CD₃OD, 125 MHz).



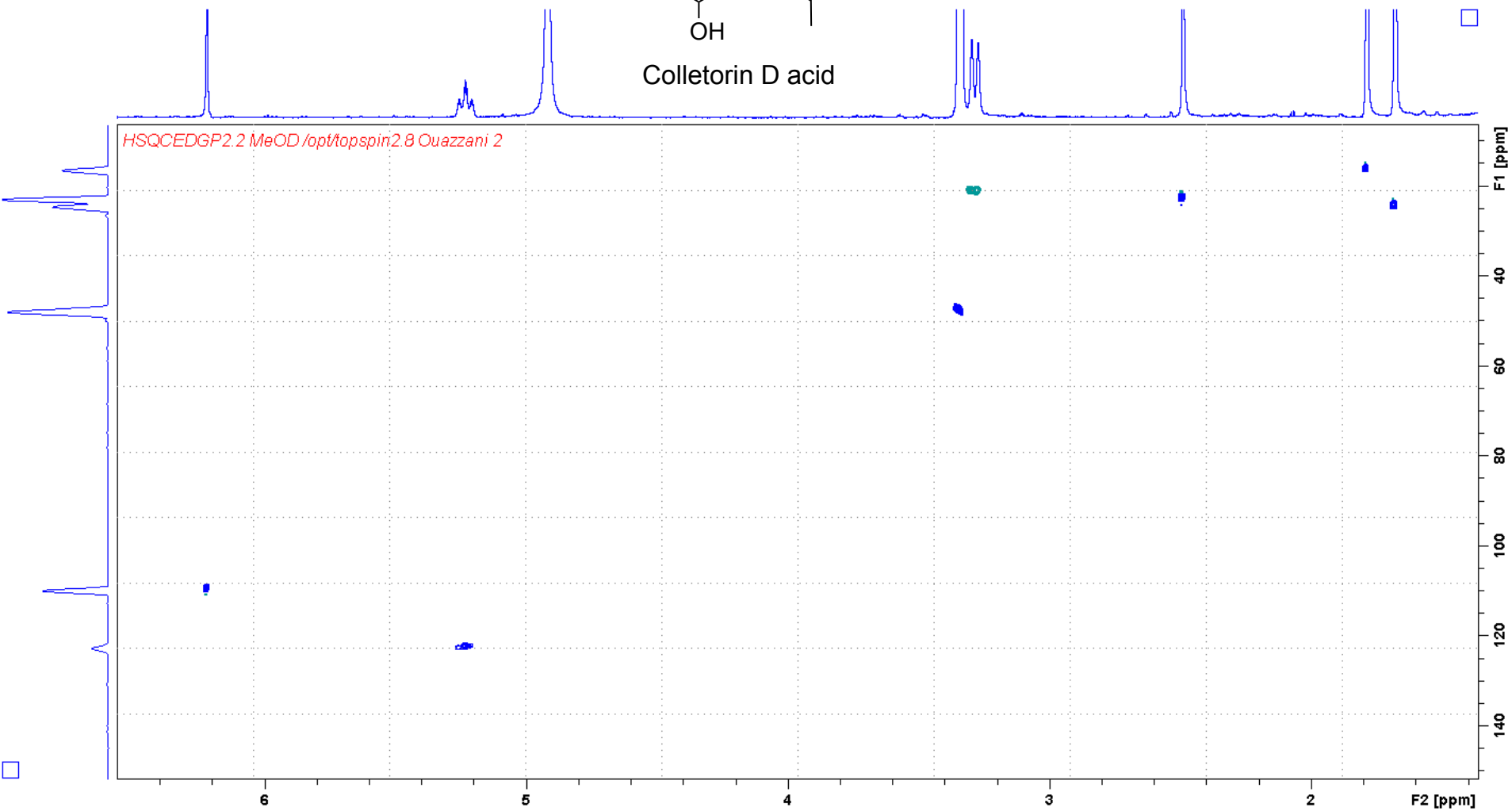
Colletorin D acid



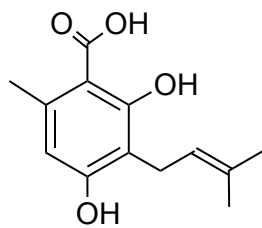
S14. ^1H - ^1H COSY spectrum of colletorin D acid (**2**) (CD_3OD , 500 MHz).



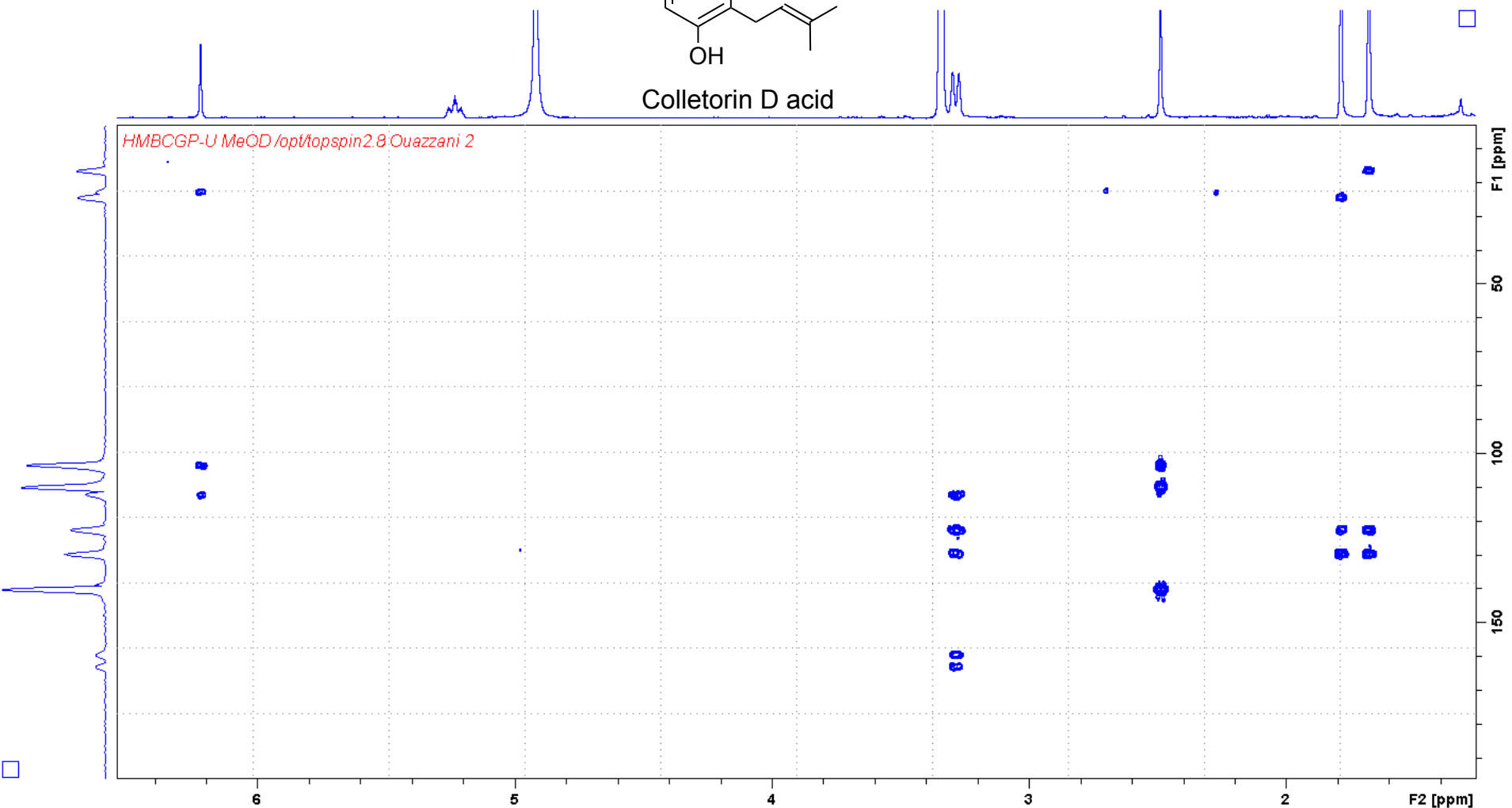
Colletorin D acid



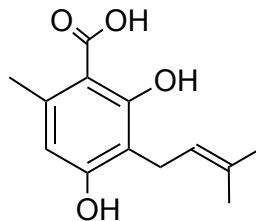
S15. ^1H - ^{13}C HSQC-ED spectrum of colletorin D acid (**2**) (CD_3OD , 500 MHz).



Colletorin D acid



S16. ^1H - ^{13}C HMBC spectrum of colletorin D acid (**2**) (CD_3OD , 500 MHz).



Colletorin D acid

Elemental Composition Report

Single Mass Analysis

Tolerance = 10.0 PPM / DBE: min = -1.5, max = 100.0

Element prediction: Off

Number of isotope peaks used for i-FIT = 9

Monoisotopic Mass, Even Electron Ions

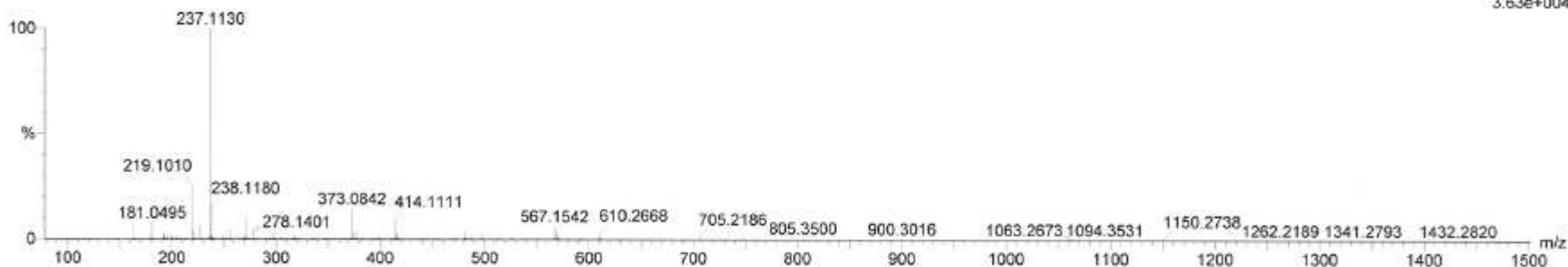
278 formula(e) evaluated with 2 results within limits (all results (up to 1000) for each mass)

Elements Used:

C: 0-50 H: 0-100 N: 0-10 O: 0-10

OUAZZANI_adelin54-1 22 (0.591) Cm (17:28-36:59x2.000)

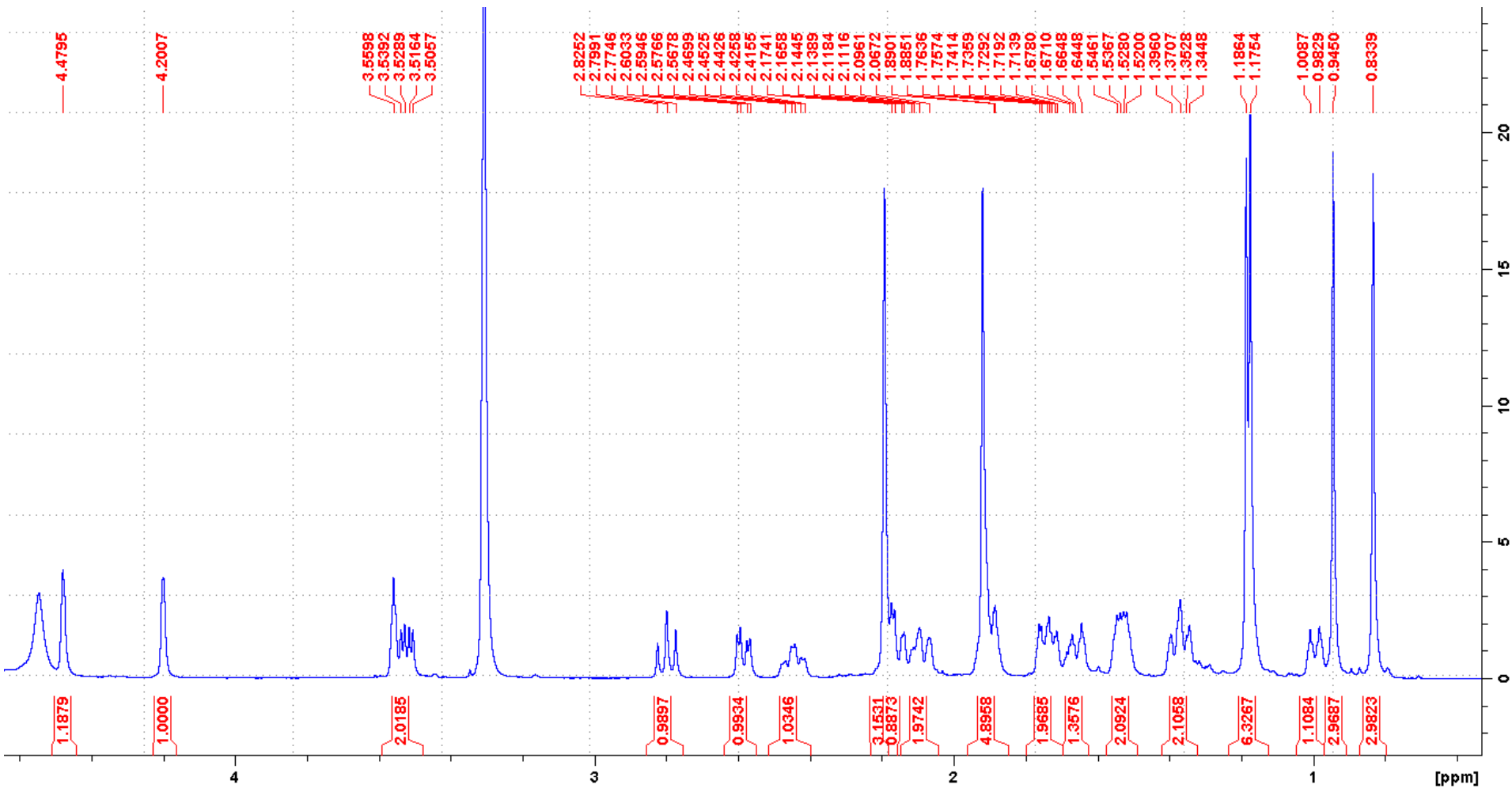
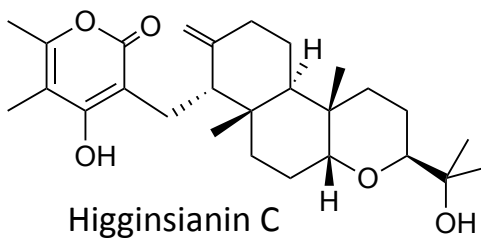
1: TOF MS ES+
3.63e+004



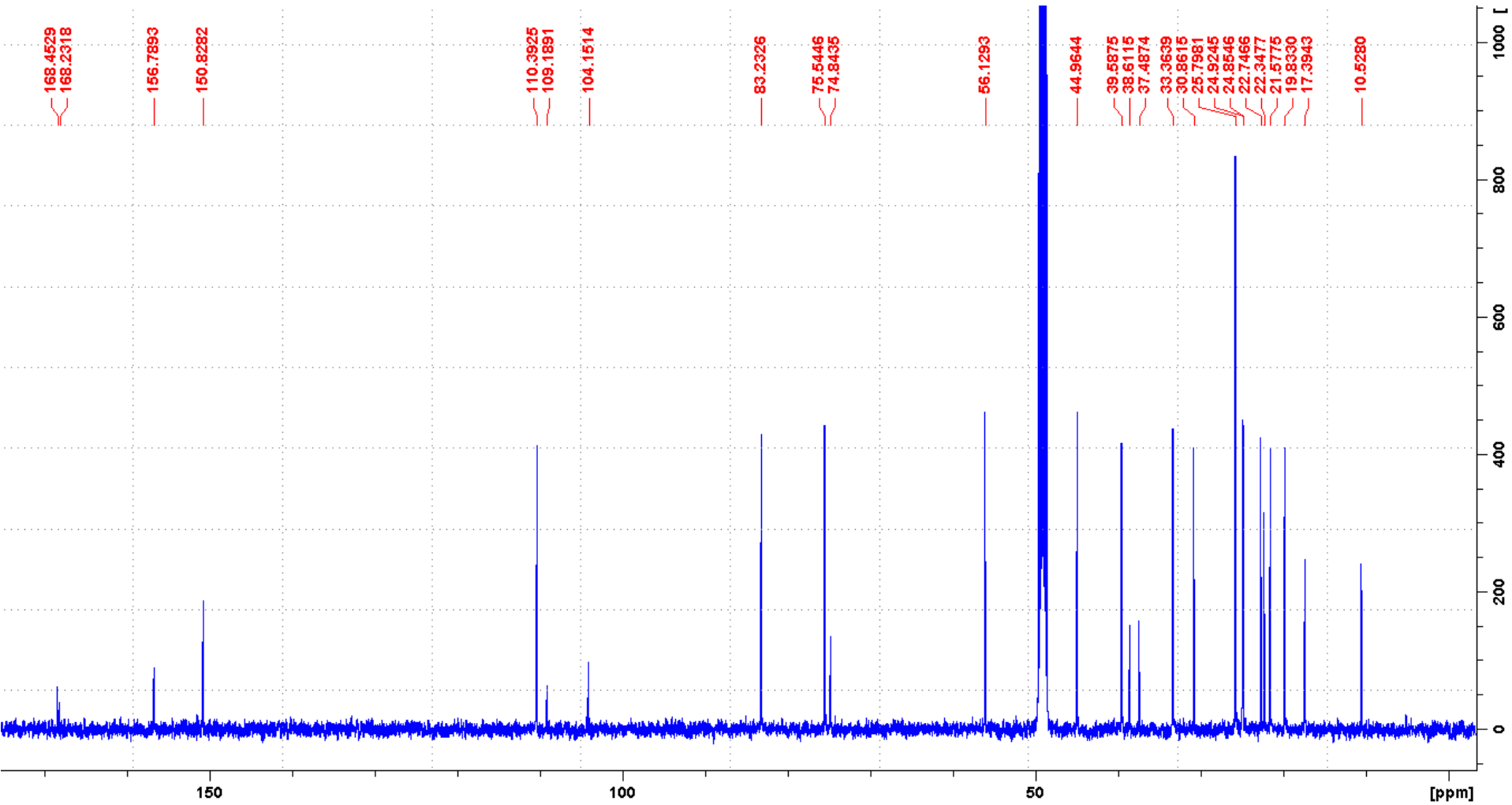
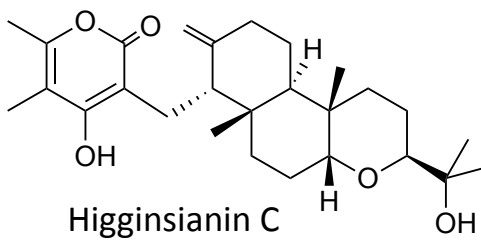
Minimum: -1.5
Maximum: 5.0 10.0 100.0

Mass	Calc. Mass	mDa	PPM	DBE	i-FIT	i-FIT (Norm)	Formula
237.1130	237.1127	0.3	1.3	5.5	581.6	0.0	C13 H17 O4
	237.1140	-1.0	-4.2	10.5	586.3	4.7	C14 H13 N4

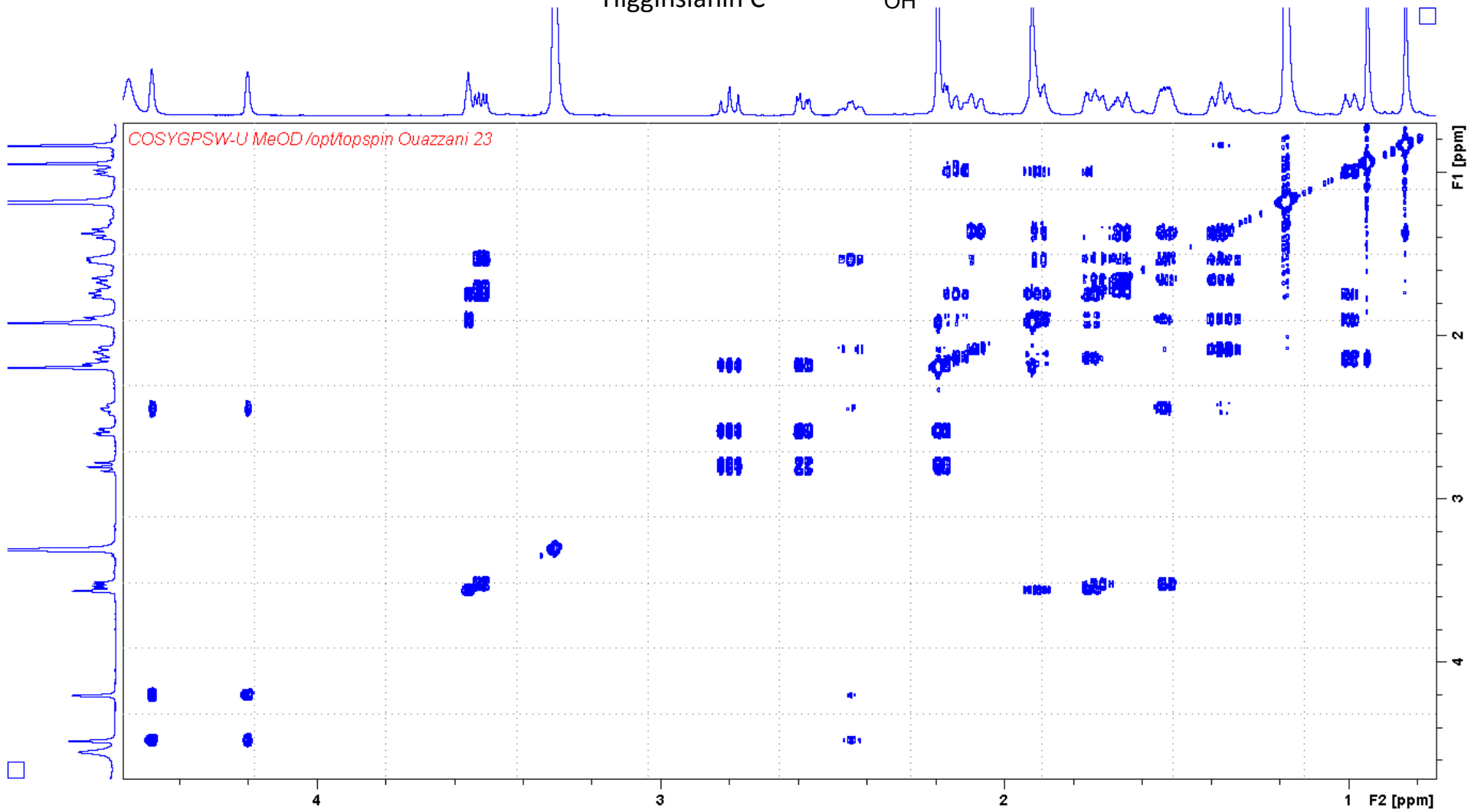
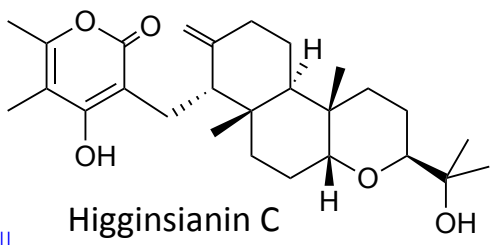
S17. HRESIMS of colletorin D acid (2)



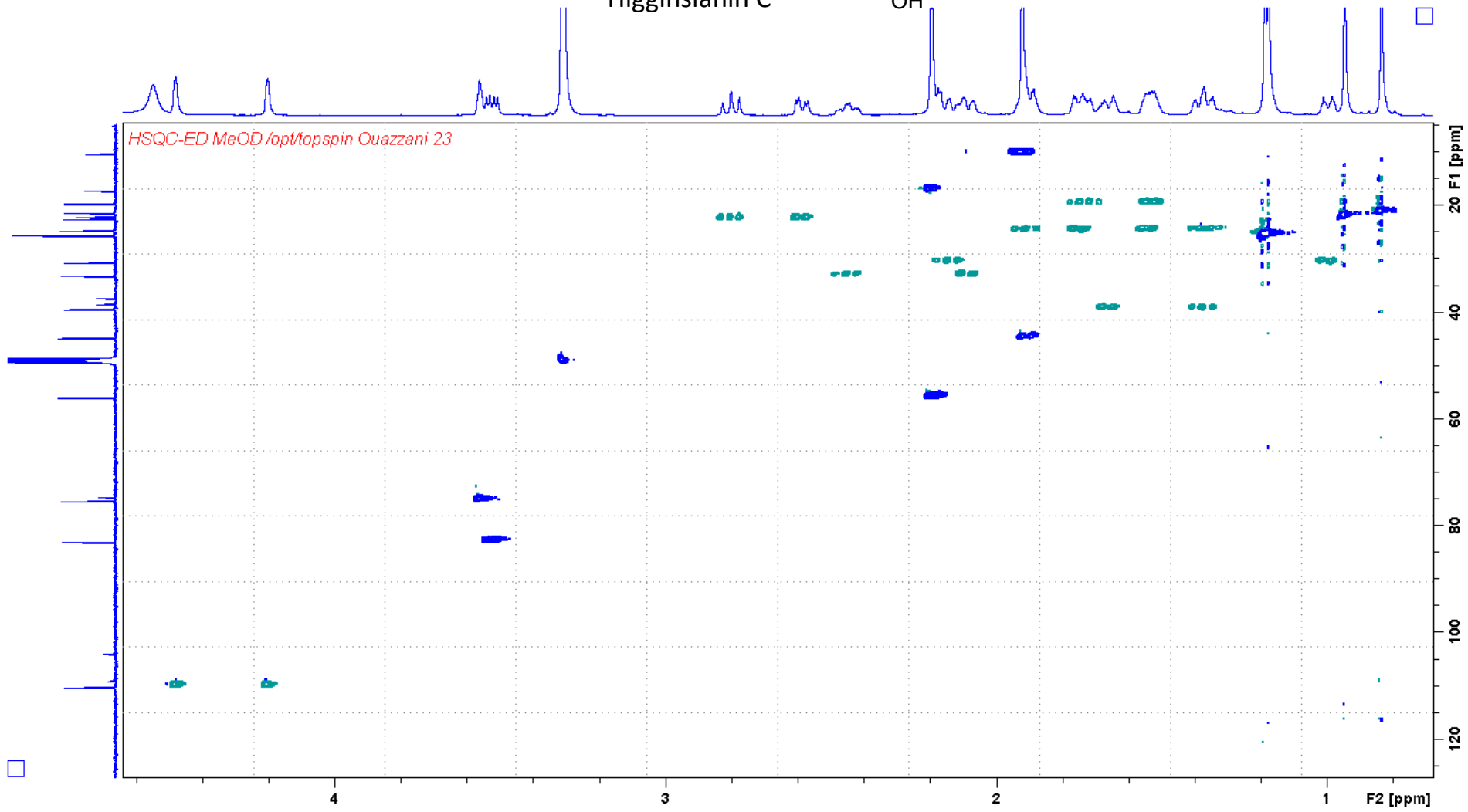
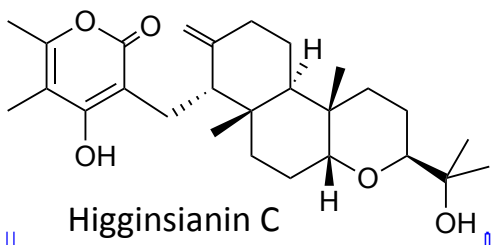
S18. ¹H NMR spectrum of Higginsianin C (**3**) (CD₃OD, 500 MHz).



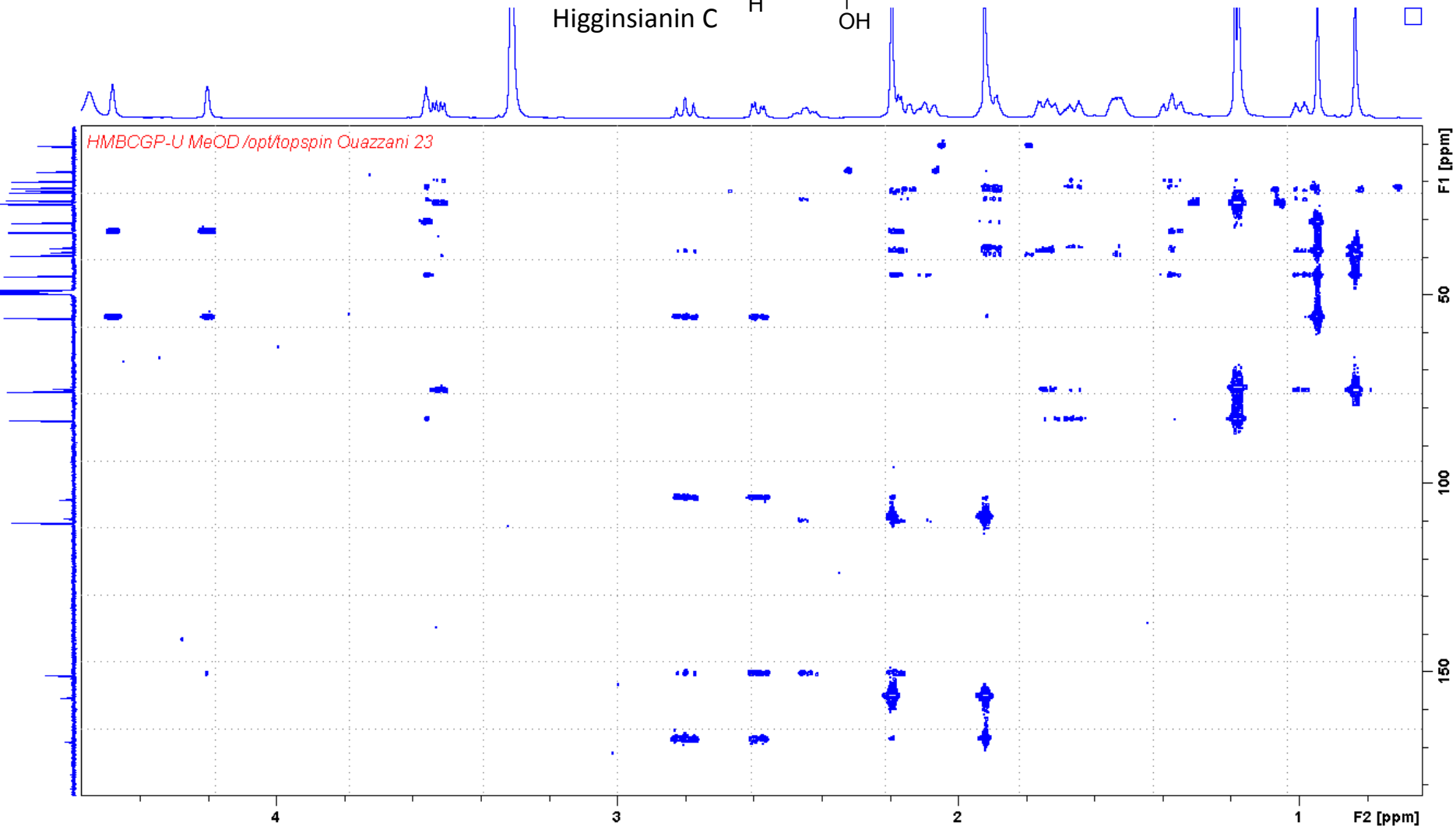
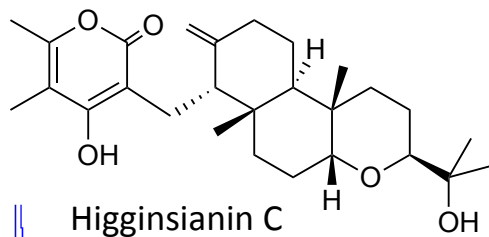
S19. ¹³C NMR spectrum of Higginsianin C (**3**) (CD₃OD, 125 MHz).



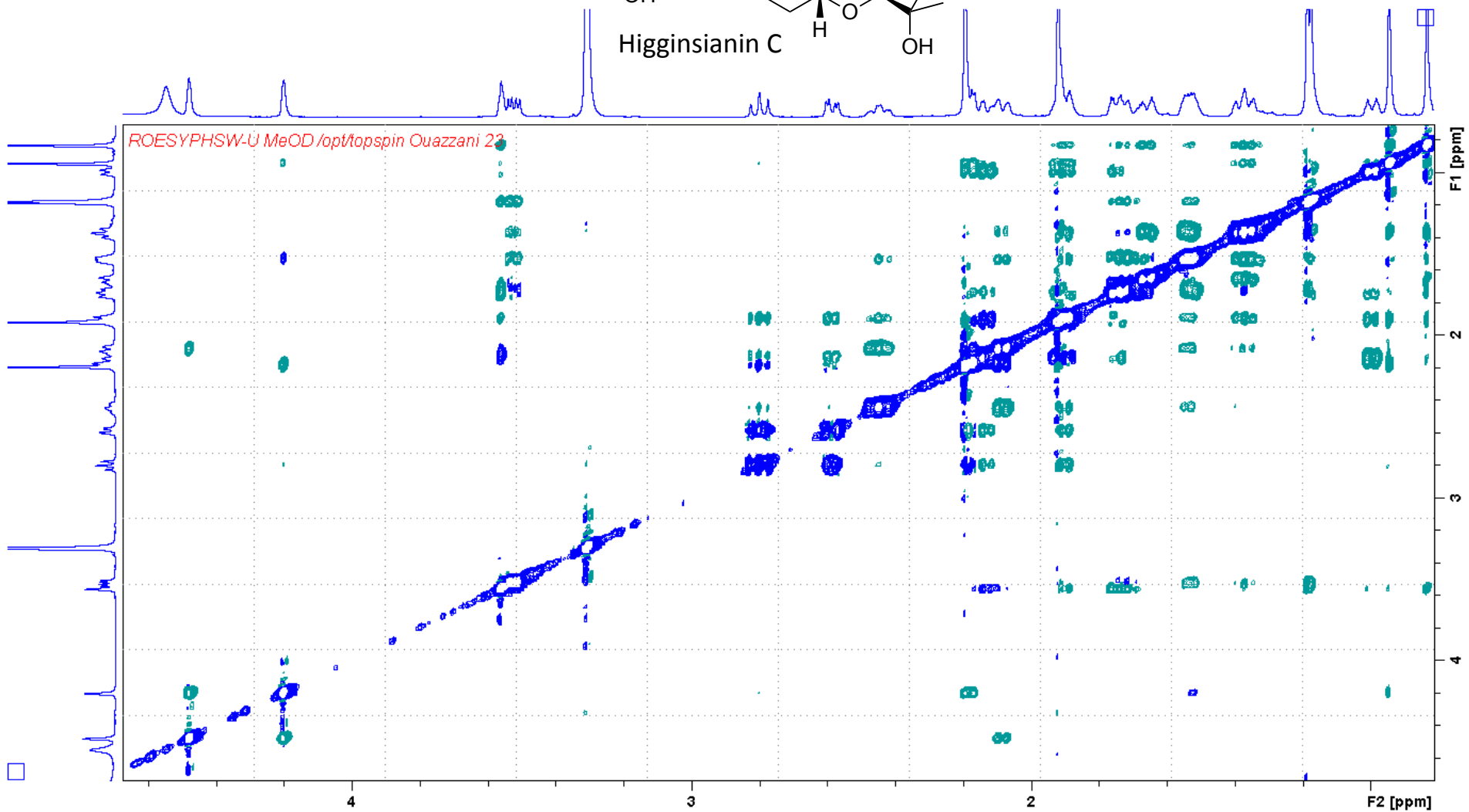
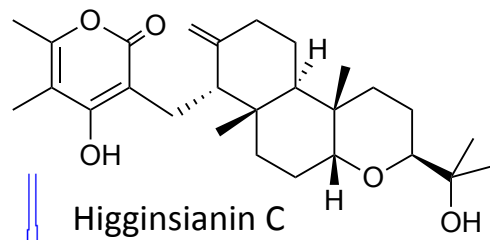
S20. ¹H-¹H COSY spectrum of Higginsianin C (**3**) (CD₃OD, 500 MHz).



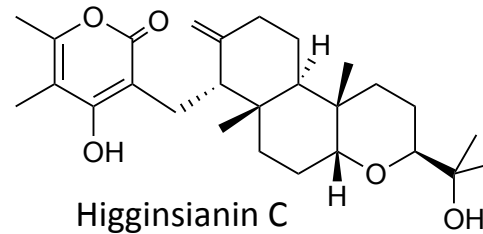
S21. ¹H-¹³C HSQC-ED spectrum of Higginsianin C (3) (CD₃OD, 500 MHz).



S22. ^1H - ^{13}C HMBC spectrum of Higginsianin C (3) (CD_3OD , 500 MHz).



S23. ^1H - ^1H ROESY spectrum of Higginsianin C (**3**) (CD_3OD , 500 MHz).



Elemental Composition Report

Single Mass Analysis

Tolerance = 10.0 PPM / DBE: min = -1.5, max = 100.0

Element prediction: Off

Number of isotope peaks used for i-FIT = 9

Monoisotopic Mass, Even Electron Ions

2418 formula(e) evaluated with 12 results within limits (all results (up to 1000) for each mass)

Elements Used:

C: 0-30 H: 0-50 N: 0-10 O: 0-10 Cl: 0-5

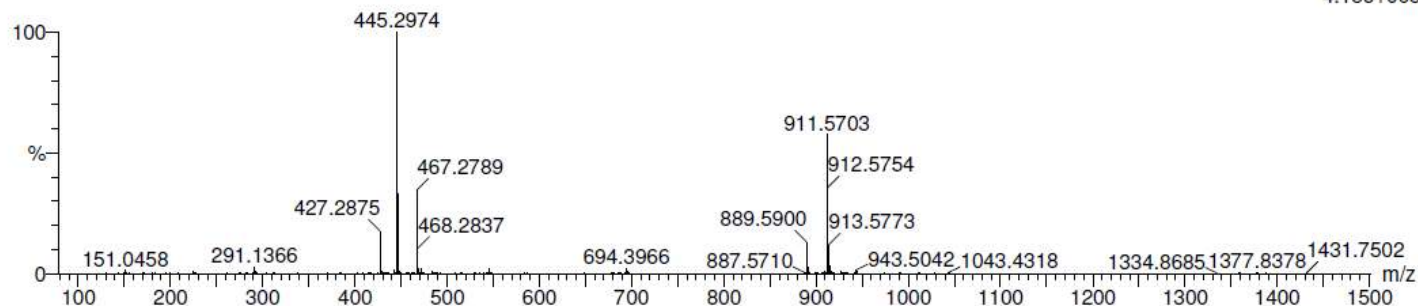
17-Jan-2018 3:::2:4

LCT Premier XE KE483

OUAZZANI_dallery1-5 25 (0.662) Cm (17:35)

1: TOF MS ES+

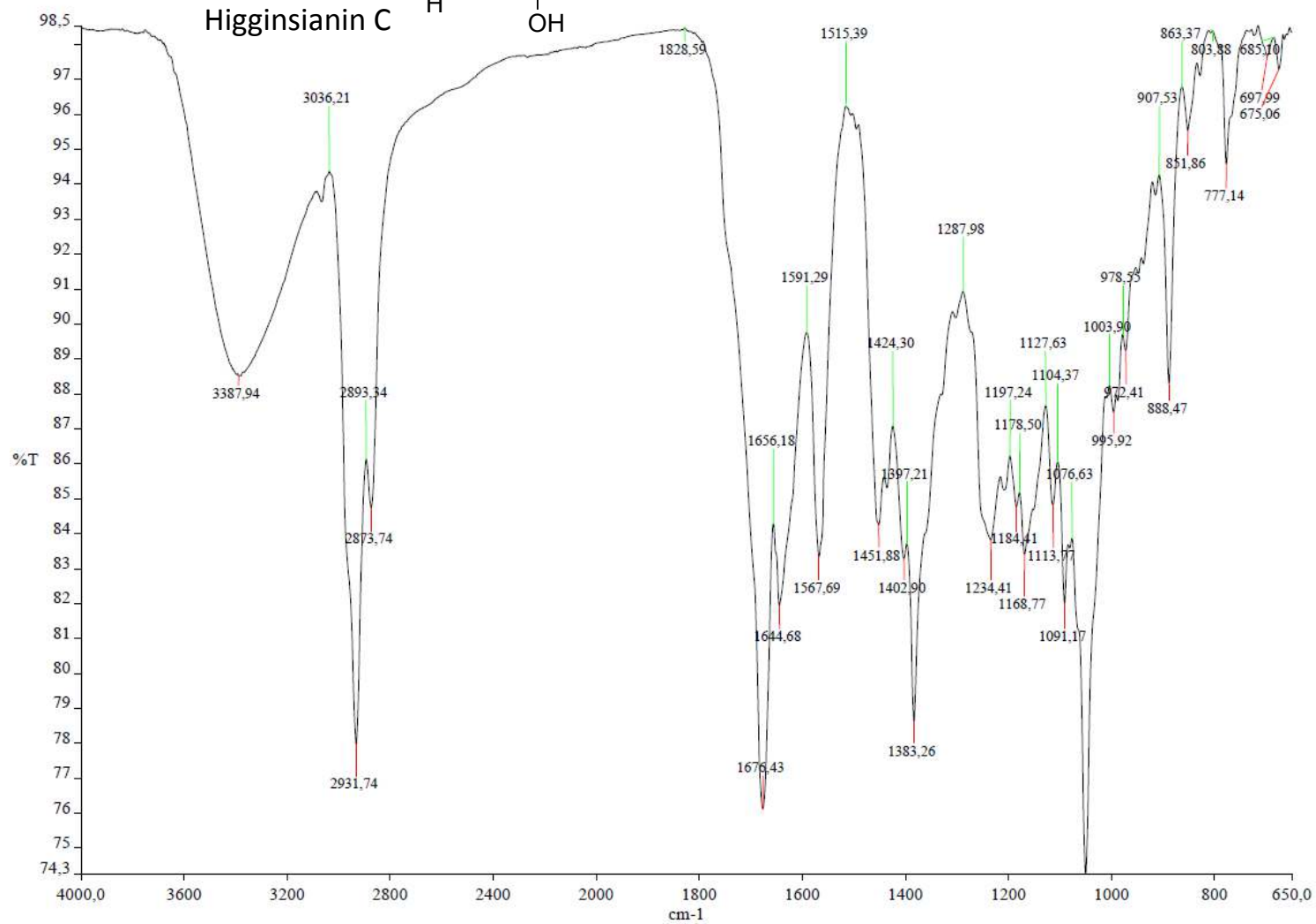
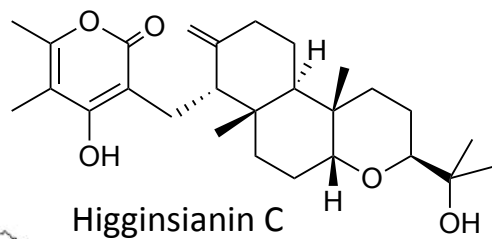
4.15e+005



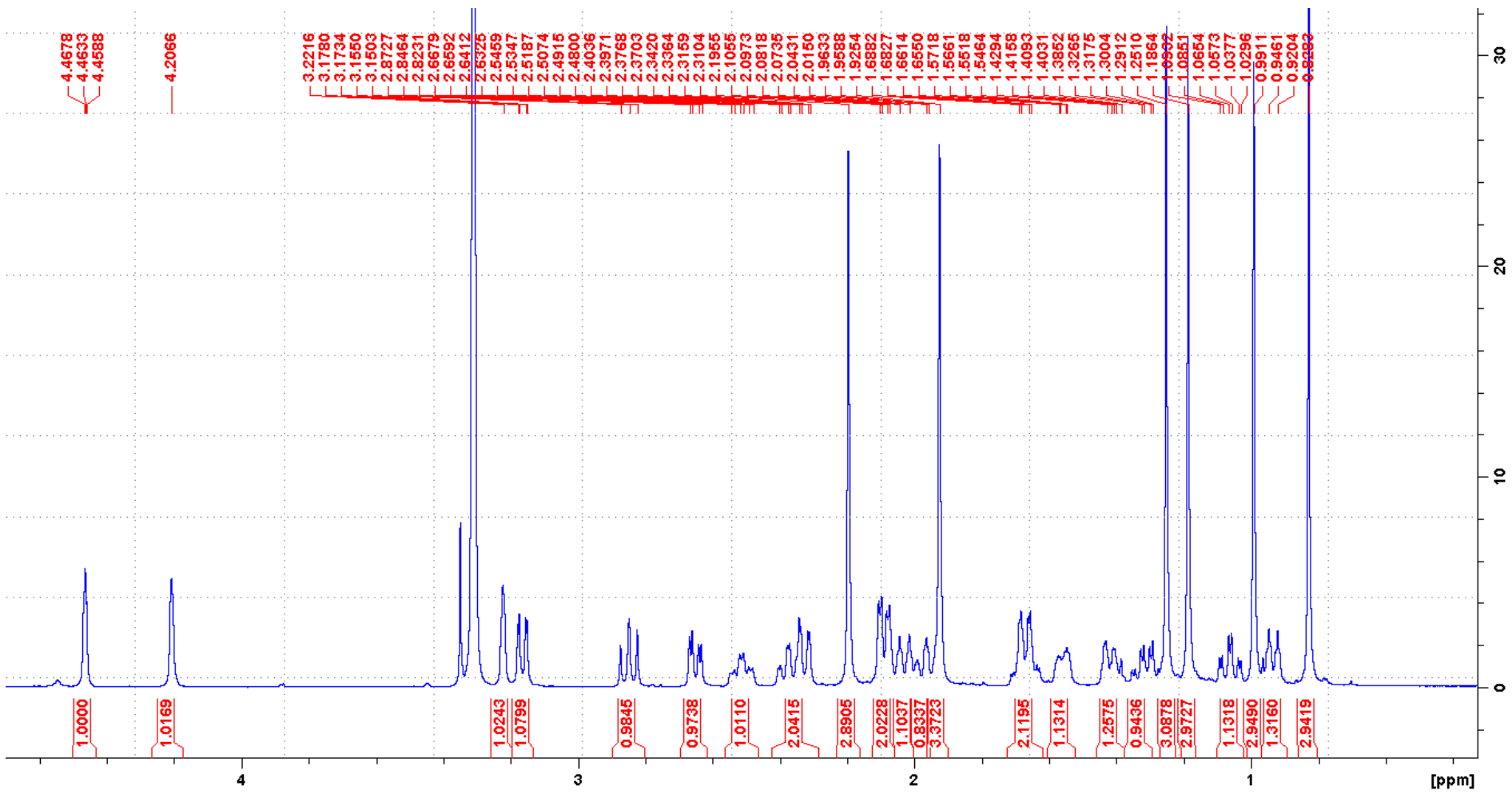
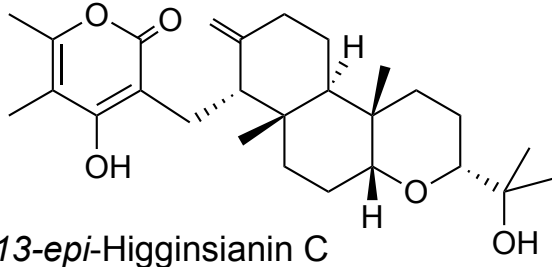
Minimum: -1.5
Maximum: 5.0 10.0 100.0

Mass	Calc. Mass	mDa	PPM	DBE	i-FIT	i-FIT (Norm)	Formula
445.2974	445.2954	2.0	4.5	7.5	1520.6	0.6	C27 H41 O5
	445.2967	0.7	1.6	12.5	1520.9	0.9	C28 H37 N4 O
	445.3013	-3.9	-8.8	-1.5	1533.6	13.6	C20 H45 O10
	445.2999	-2.5	-5.6	4.5	1536.3	16.3	C17 H37 N10 O4
	445.2986	-1.2	-2.7	-0.5	1537.0	17.0	C16 H41 N6 O8

S24. HRESIMS of Higginsianin C (3)

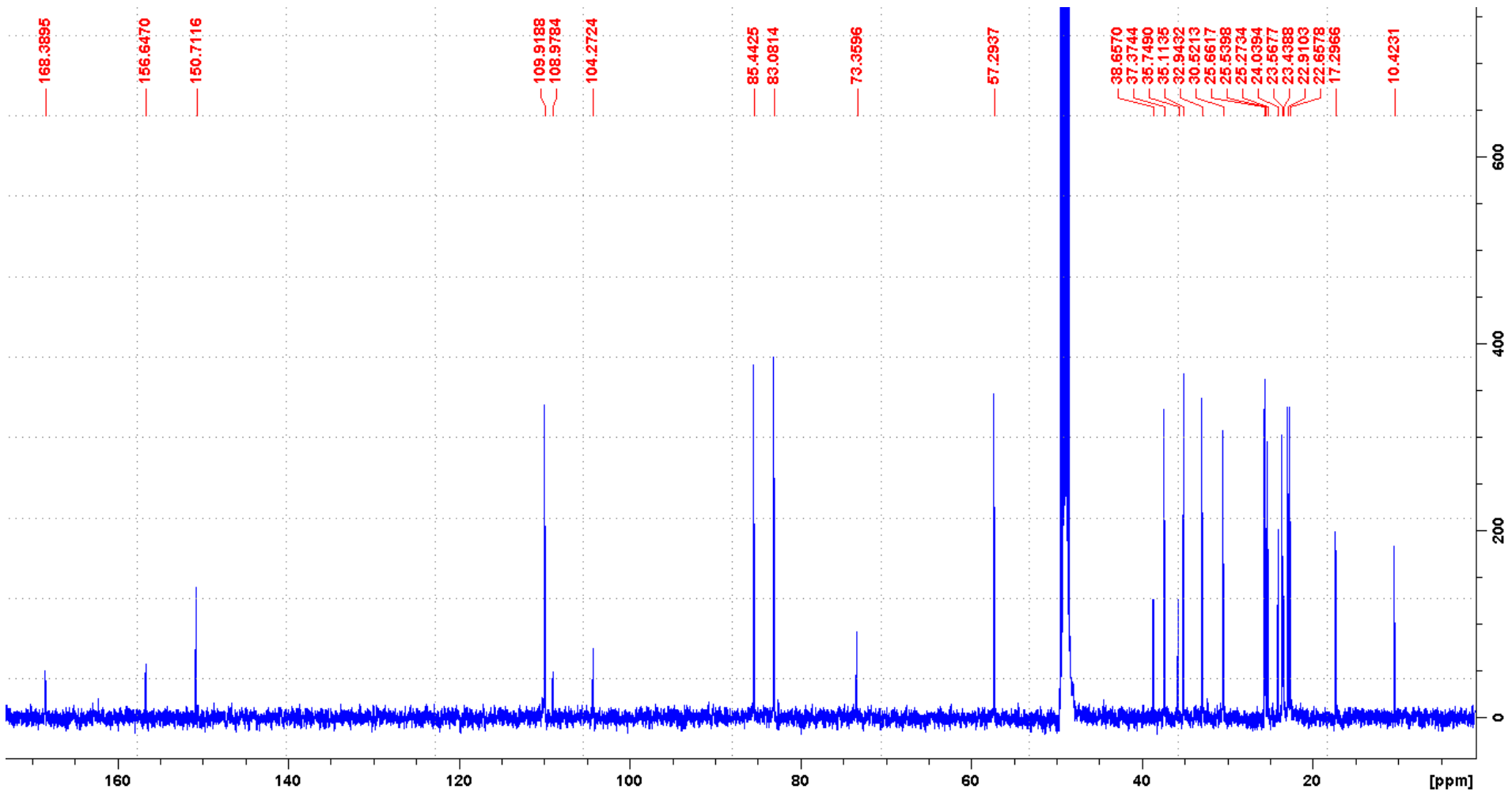
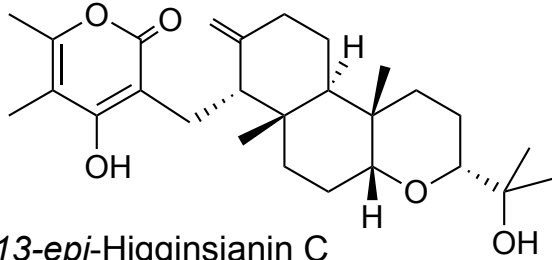


S25. IR spectrum of Higginsianin C (**3**)

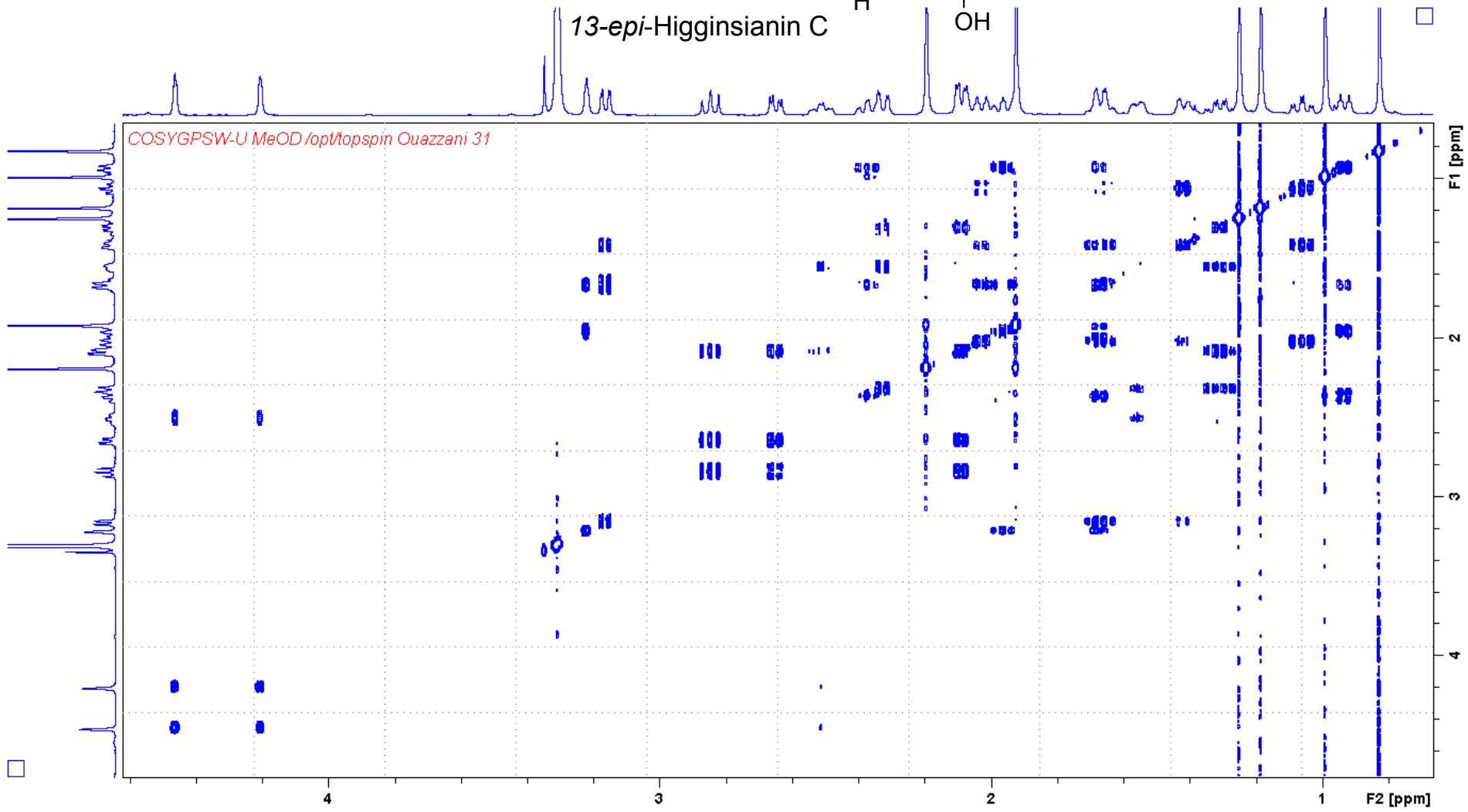
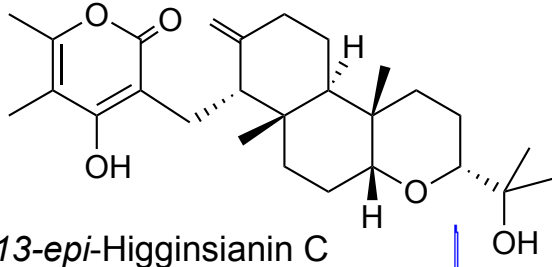


S26. ¹H NMR spectrum of 13-*epi*-higginsianin C (**4**) (CD₃OD, 500 MHz).

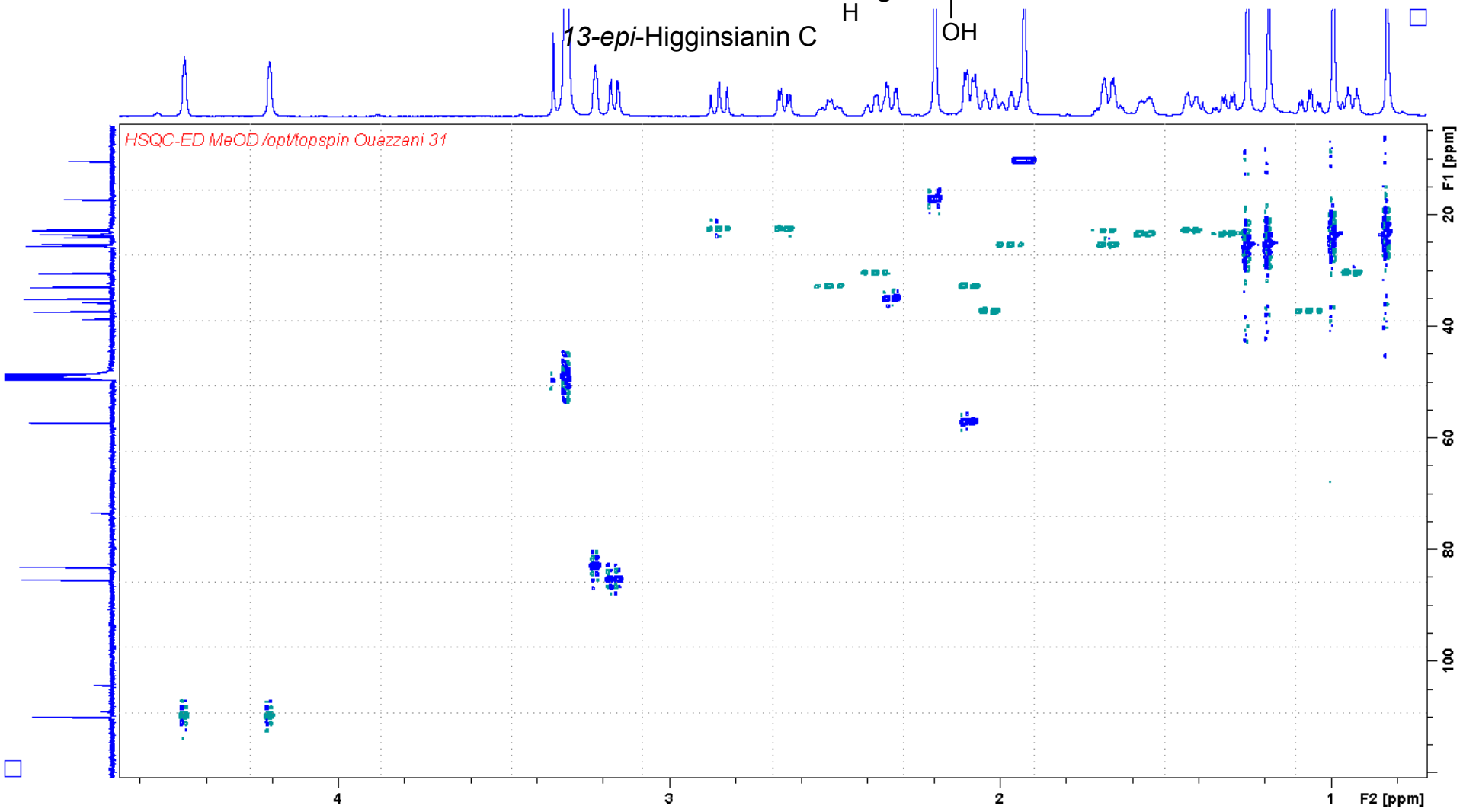
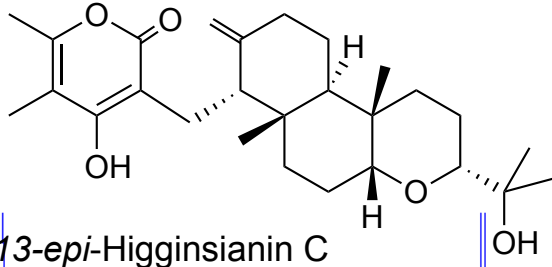
13-*epi*-Higginsianin C



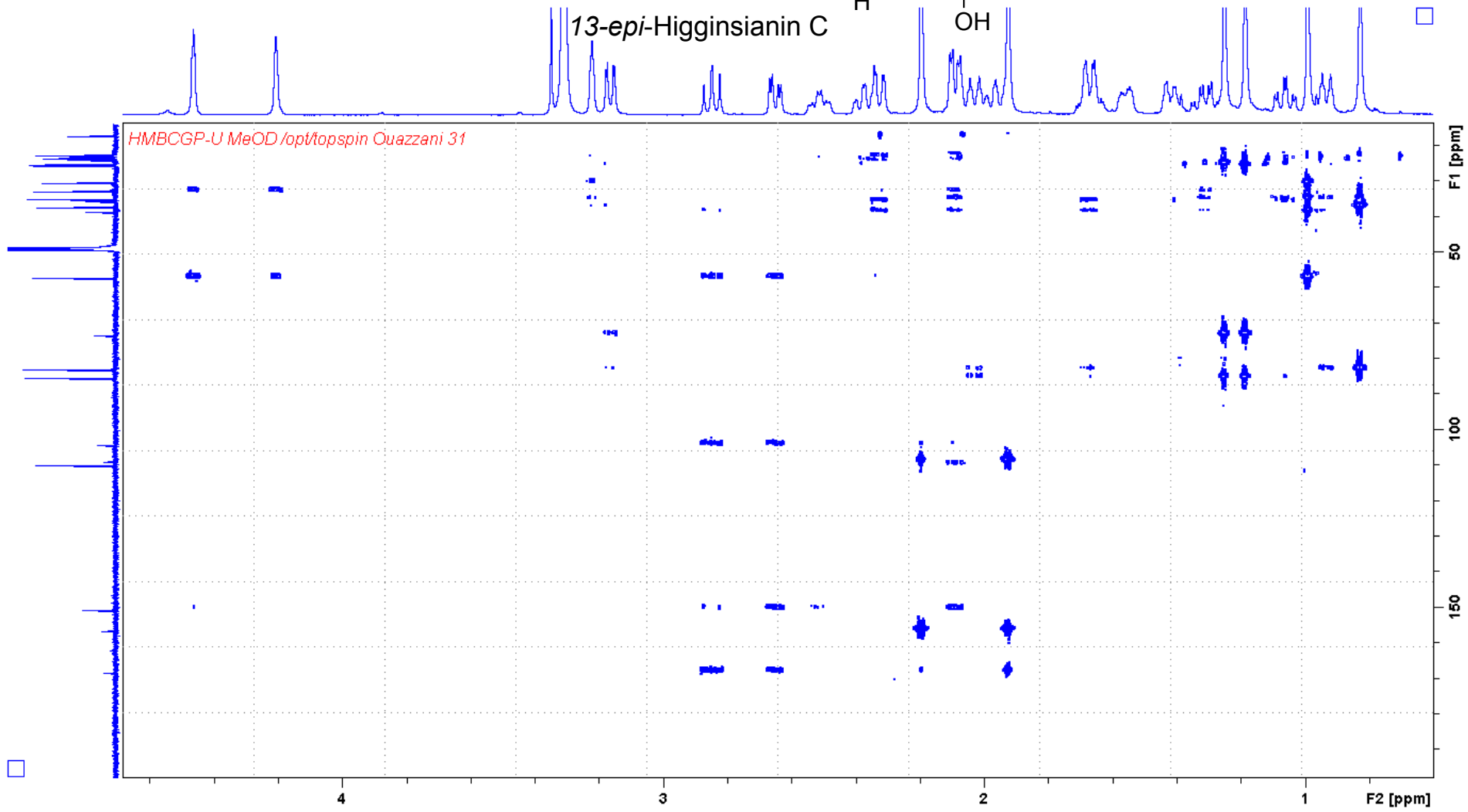
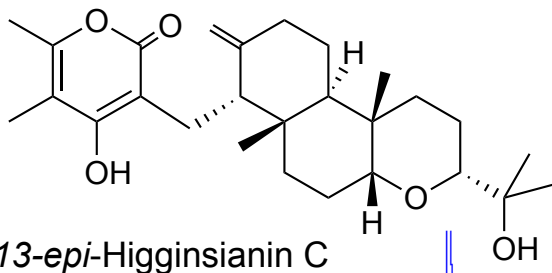
S27. ¹³C NMR spectrum of 13-*epi*-higginsianin C (4) (CD₃OD, 125 MHz).



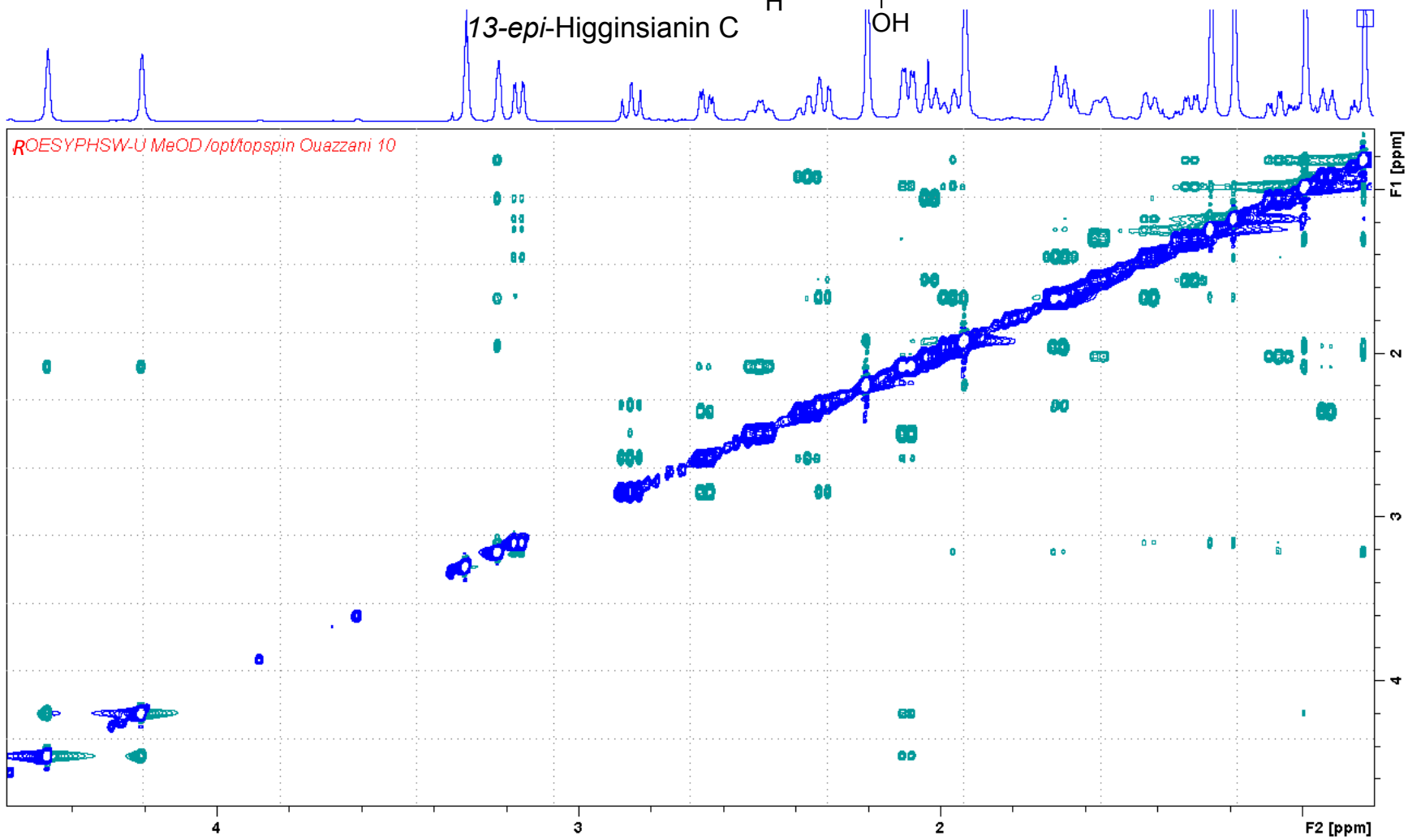
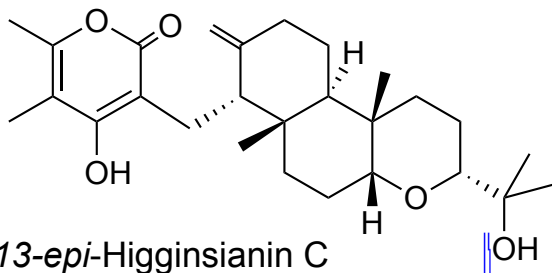
S28. ¹H-¹H COSY spectrum of 13-*epi*-higginsianin C (4) (CD₃OD, 500 MHz).



S29. ^1H - ^{13}C HSQC-ED spectrum of 13-*epi*-higginsianin C (4) (CD_3OD , 500 MHz).



S30. ^1H - ^{13}C HMBC spectrum of 13-*epi*-higginsianin C (**4**) (CD_3OD , 500 MHz).



S23. ^1H - ^1H ROESY spectrum of 13-*epi*-higginsianin C (**4**) (CD_3OD , 500 MHz).

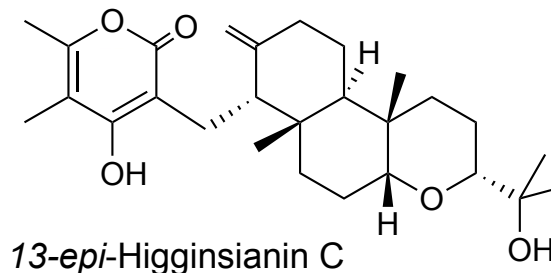
Elemental Composition Report

Single Mass Analysis

Tolerance = 10.0 PPM / DBE: min = -1.5, max = 100.0

Element prediction: Off

Number of isotope peaks used for i-FIT = 9



Monoisotopic Mass, Even Electron Ions

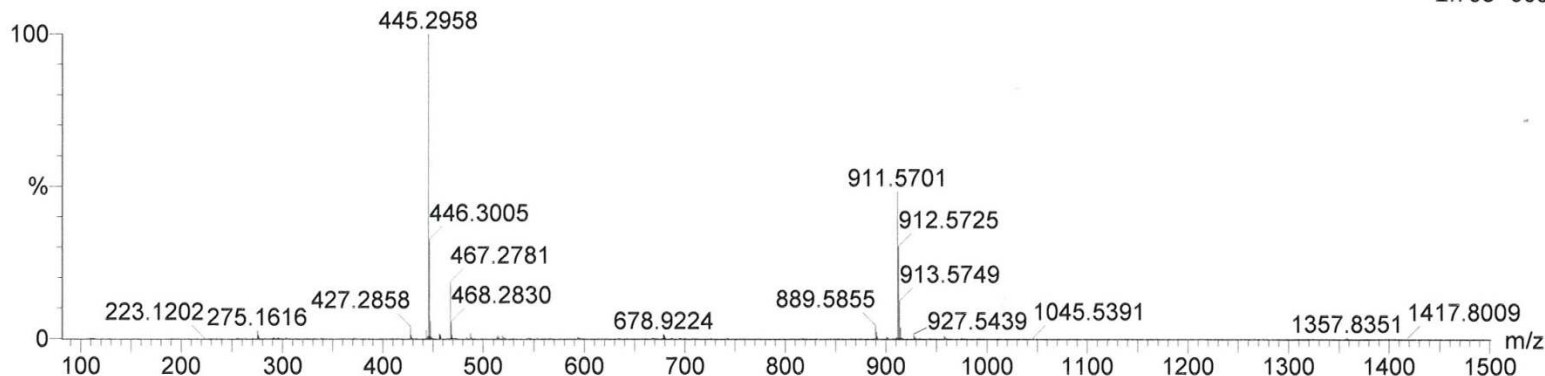
462 formula(e) evaluated with 6 results within limits (all results (up to 1000) for each mass)

Elements Used:

C: 0-30 H: 0-50 N: 0-10 O: 0-10

OUAZZANI_glegoff54-3 23 (0.608) Cm (17:28-37:69x2.000)

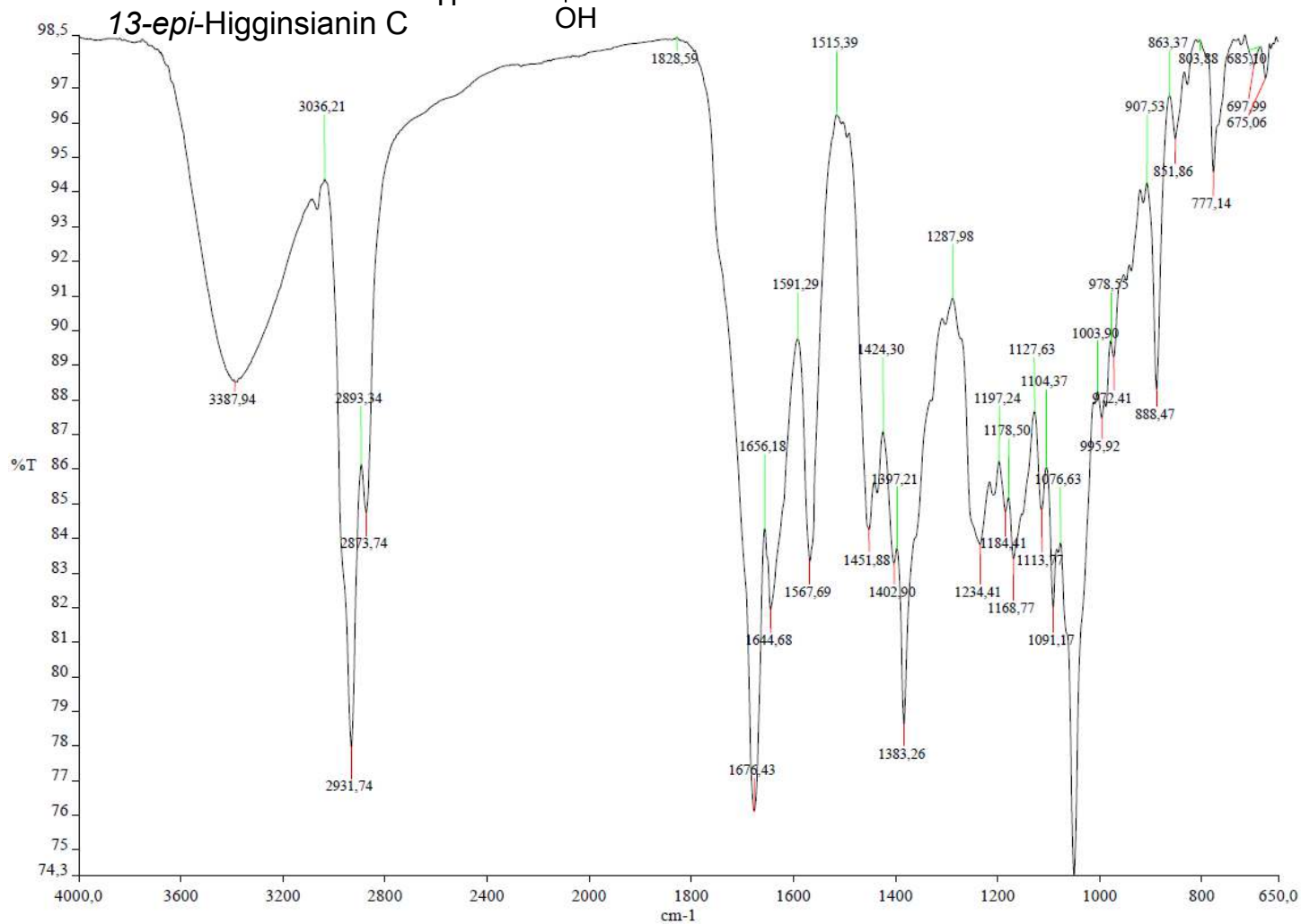
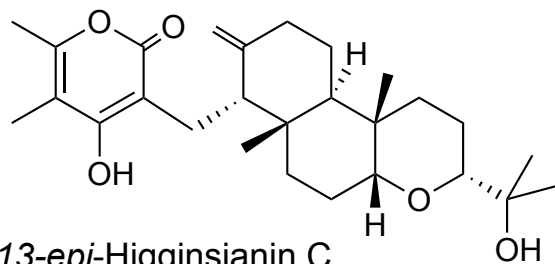
1: TOF MS ES+
2.75e+005



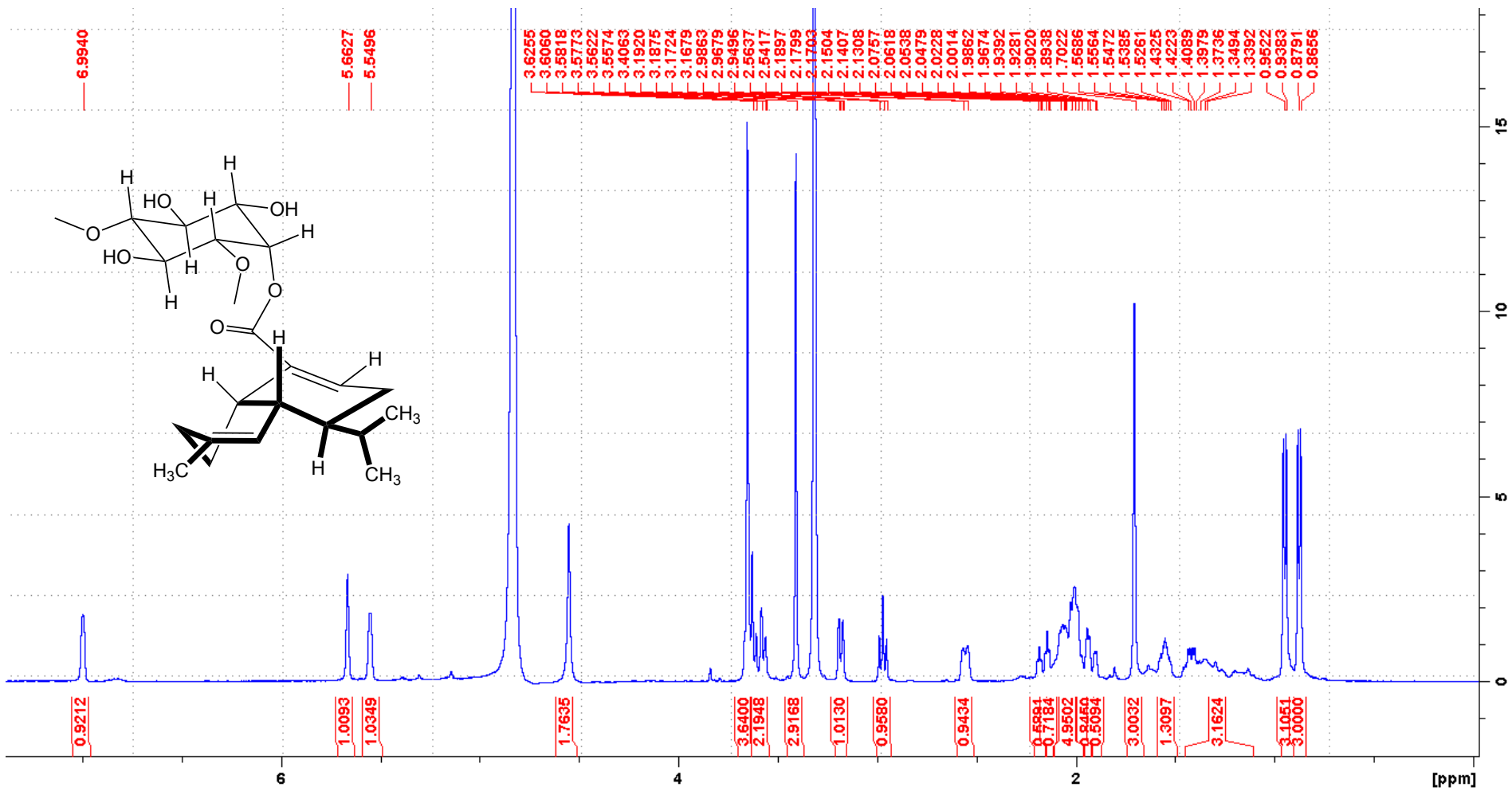
Minimum: -1.5
Maximum: 5.0 10.0 100.0

Mass	Calc. Mass	mDa	PPM	DBE	i-FIT	i-FIT (Norm)	Formula
445.2958	445.2954	0.4	0.9	7.5	1039.5	0.1	C27 H41 O5 ✓
	445.2967	-0.9	-2.0	12.5	1041.8	2.4	C28 H37 N4 O
	445.2986	-2.8	-6.3	-0.5	1058.4	19.1	C16 H41 N6 O8
	445.2927	3.1	7.0	8.5	1050.3	10.9	C23 H37 N6 O3
	445.2999	-4.1	-9.2	4.5	1057.6	18.3	C17 H37 N10 O4
	445.2914	4.4	9.9	3.5	1052.5	13.1	C22 H41 N2 O7

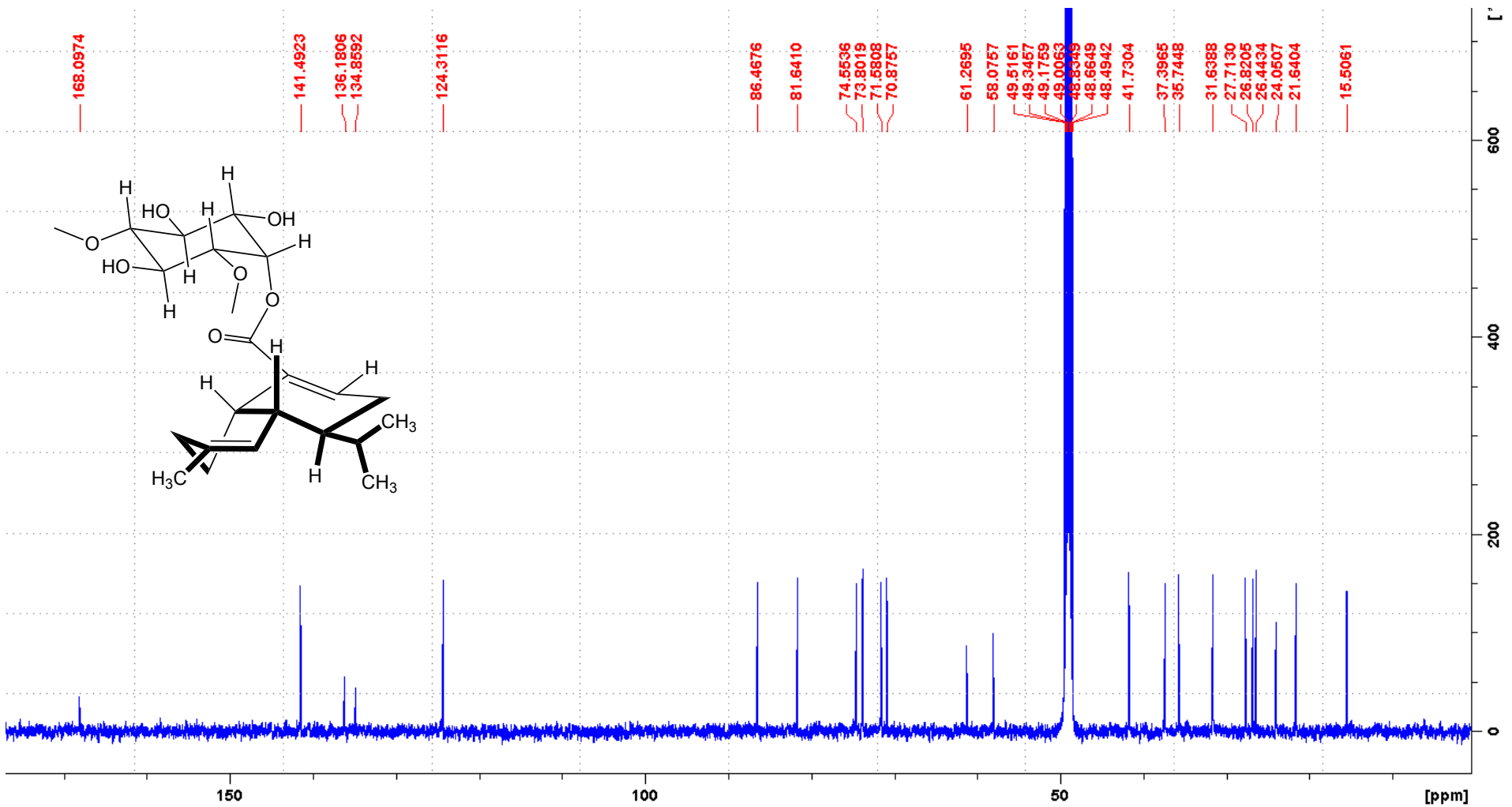
S31. HRESIMS of 13-epi-higginsianin C (4)



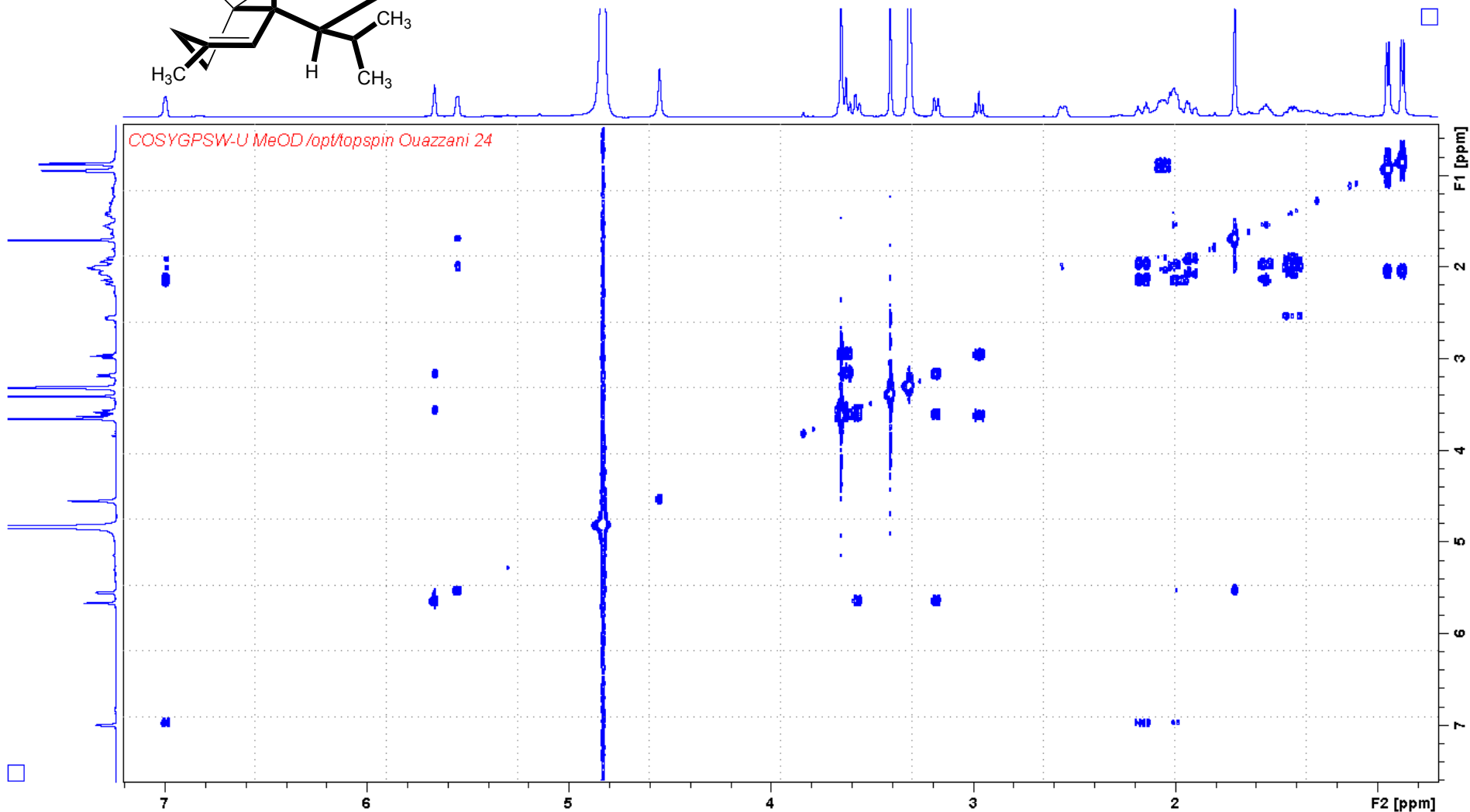
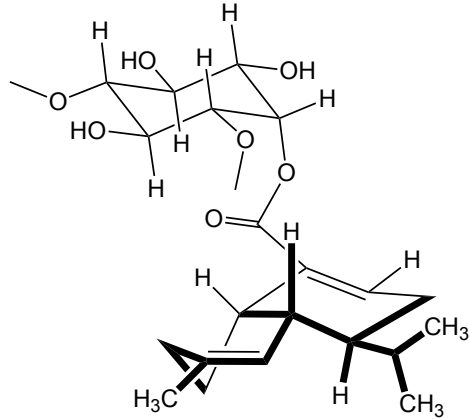
S32. IR spectrum of 13-*epi*-higginsianin C (4)



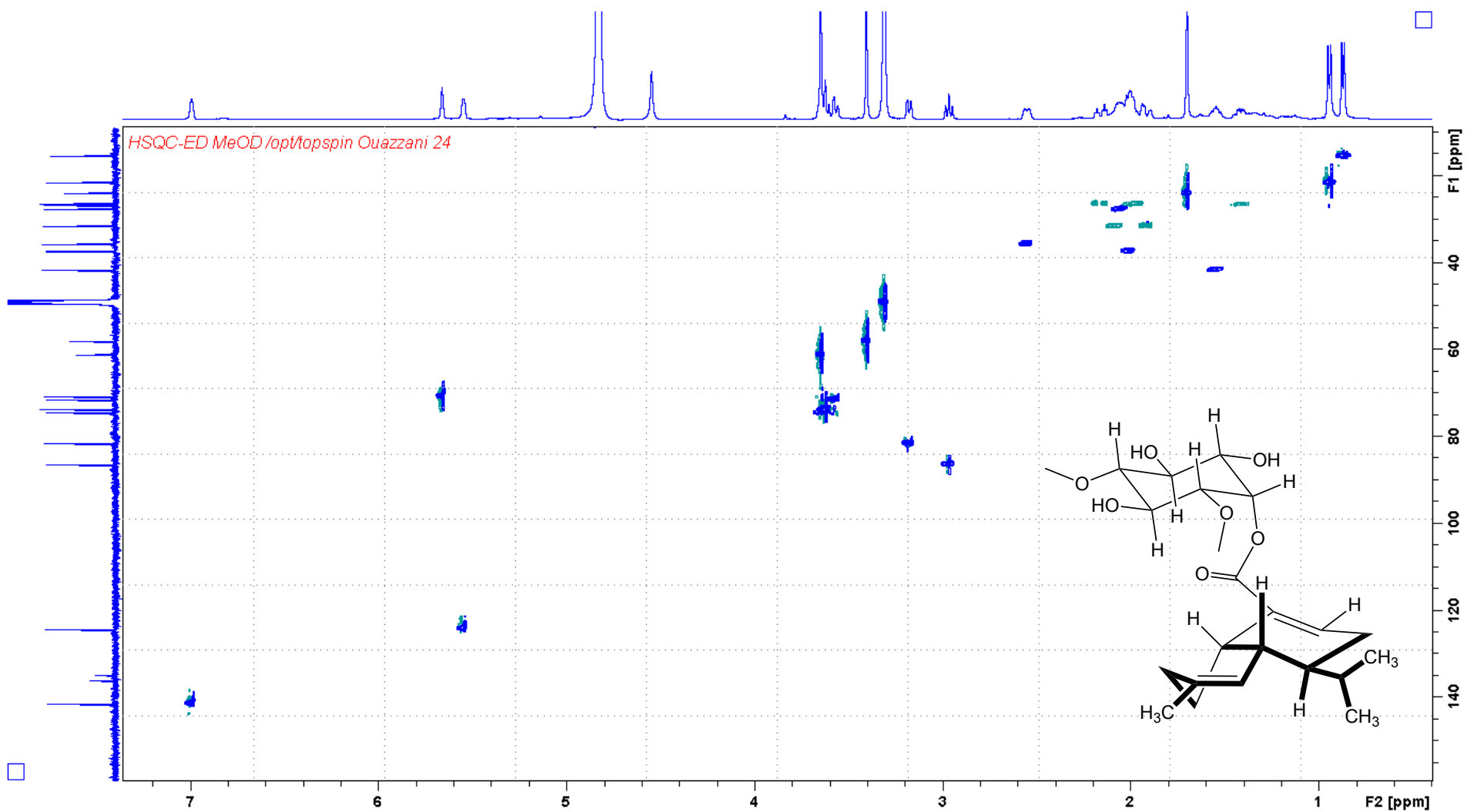
S33. ¹H NMR spectrum of sclerosporide (5) (CD₃OD, 500 MHz).



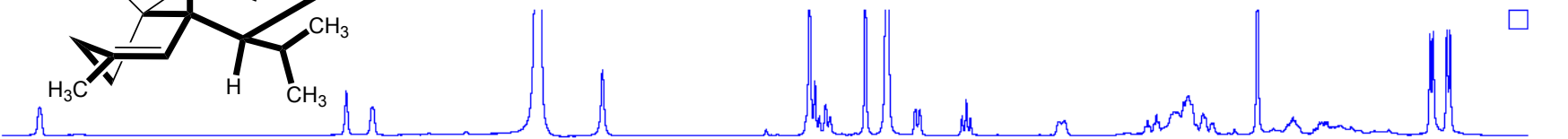
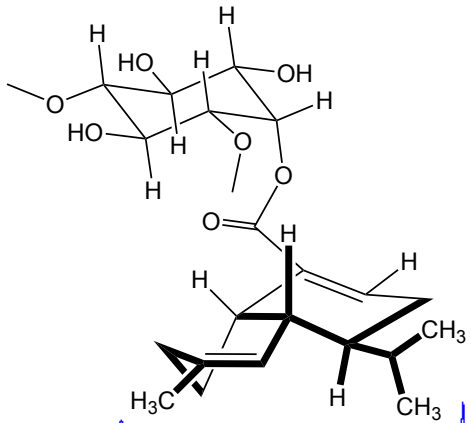
S34. ^{13}C NMR spectrum of sclerosporide (5) (CD_3OD , 125 MHz).



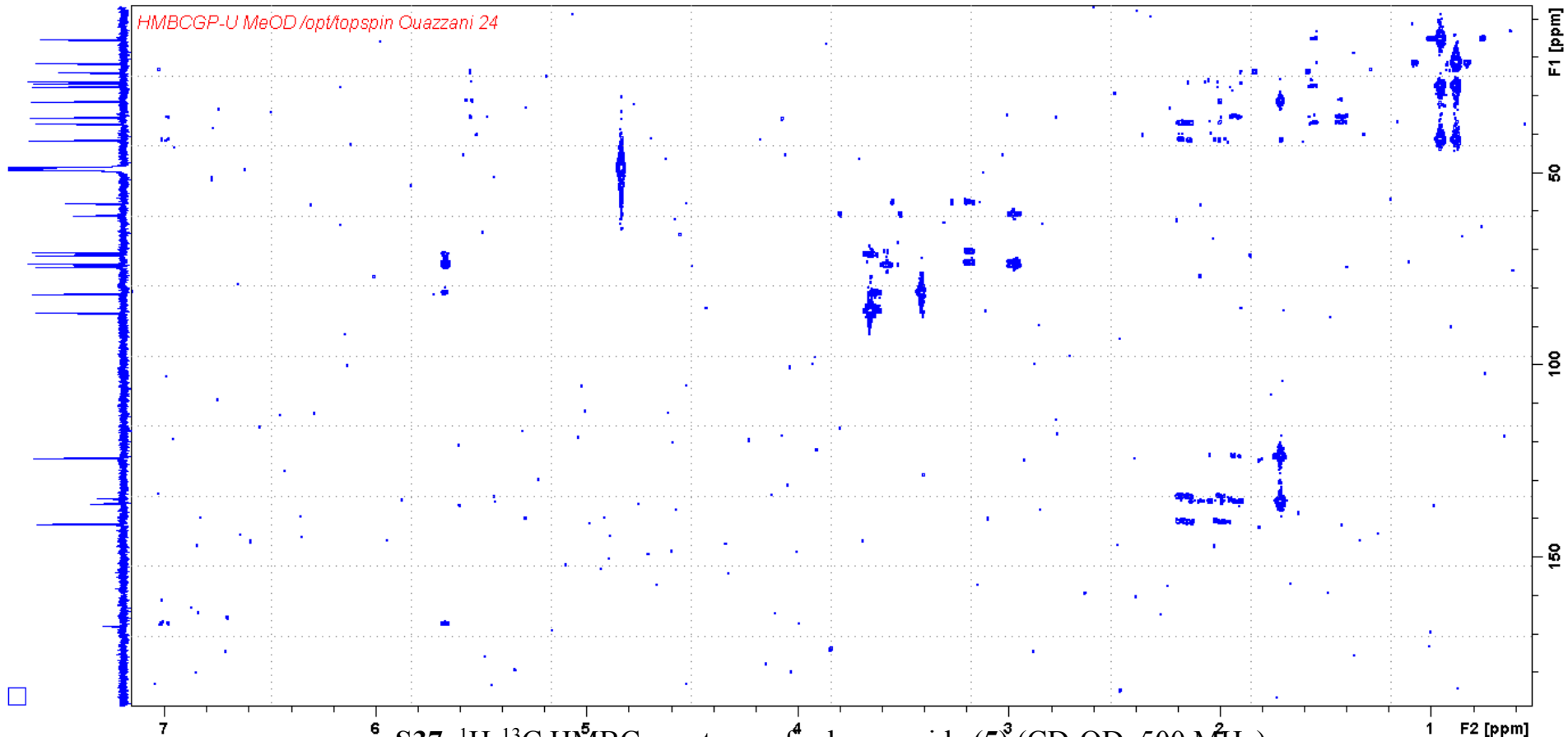
S35. ^1H - ^1H COSY spectrum of sclerosporide (**5**) (CD_3OD , 500 MHz).



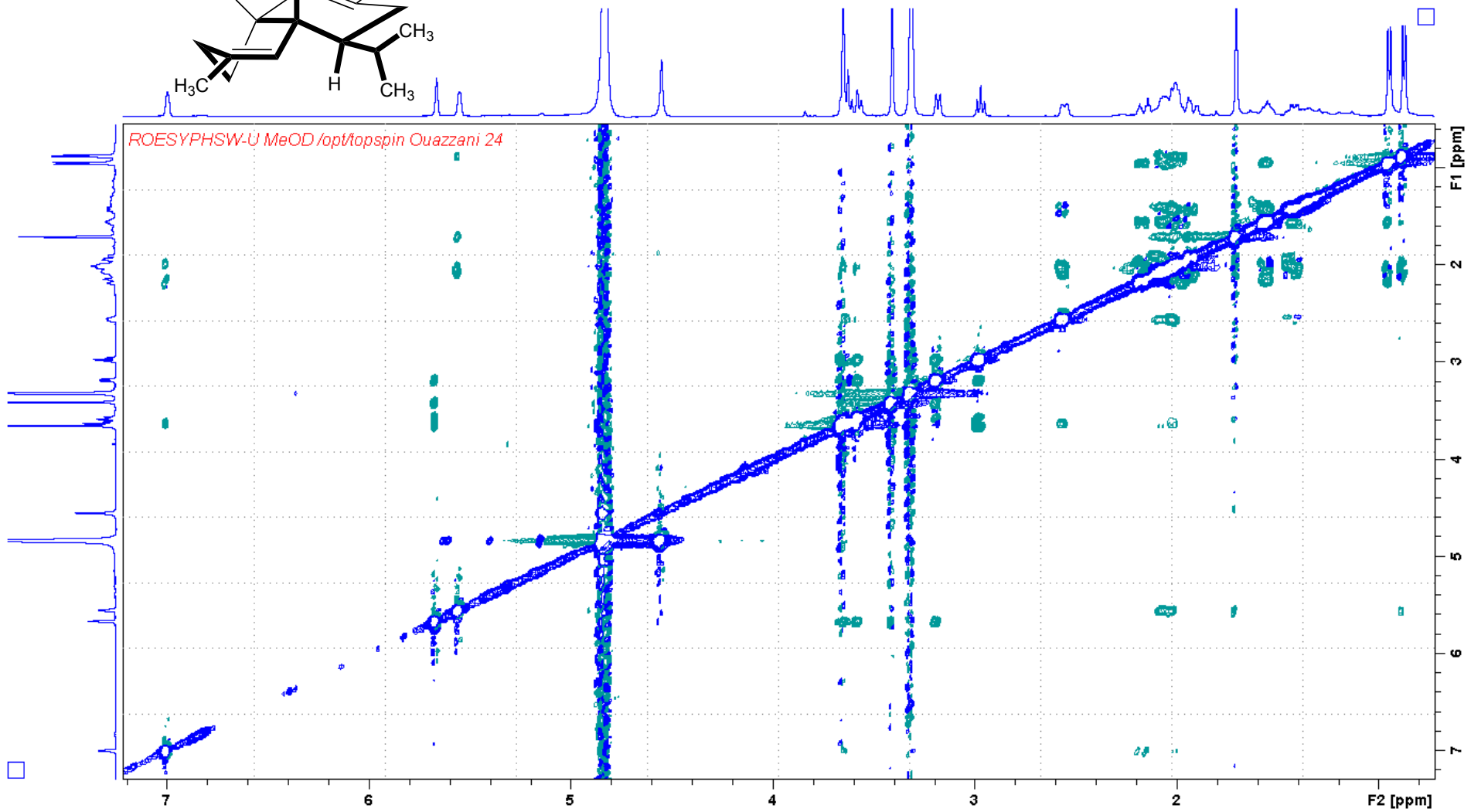
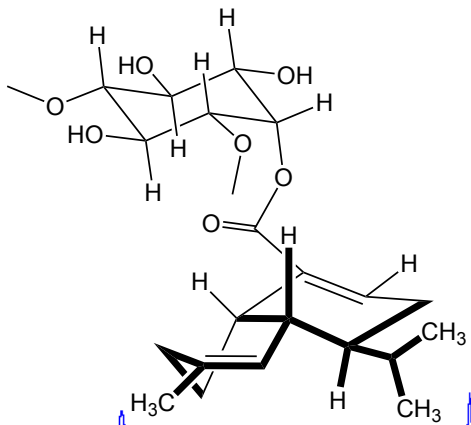
S36. ¹H-¹³C HSQC-ED spectrum of sclerosporide (**5**) (CD₃OD, 500 MHz).



HMBCGP-U MeOD /opt/topspin Ouazzani 24



S37. ^1H - ^{13}C HMBC spectrum of sclerosporide (**5**) (CD_3OD , 500 MHz).



S38. ^1H - ^1H ROESY spectrum of sclerosporide (**5**) (CD_3OD , 500 MHz).

Elemental Composition Report

Single Mass Analysis

Tolerance = 10.0 PPM / DBE: min = -1.5, max = 100.0

Element prediction: Off

Number of isotope peaks used for i-FIT = 9

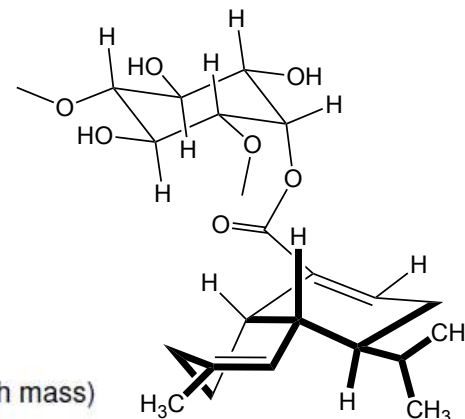
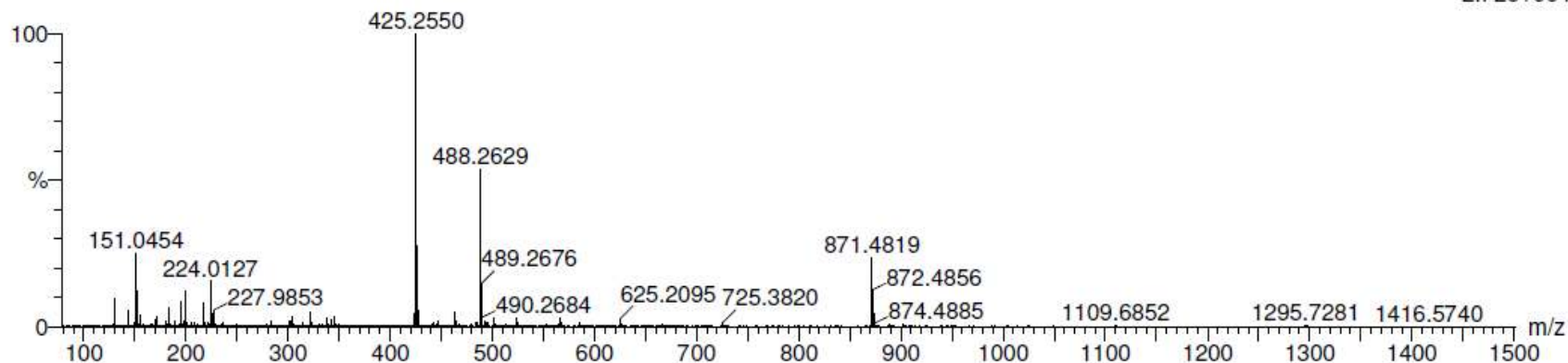
Monoisotopic Mass, Even Electron Ions

245 formula(e) evaluated with 2 results within limits (all results (up to 1000) for each mass)

Elements Used:

C: 0-70 H: 0-100 O: 0-50 Cl: 0-2

OUAZZANI_arcile116-4 21 (0.573) Cm (17:31)

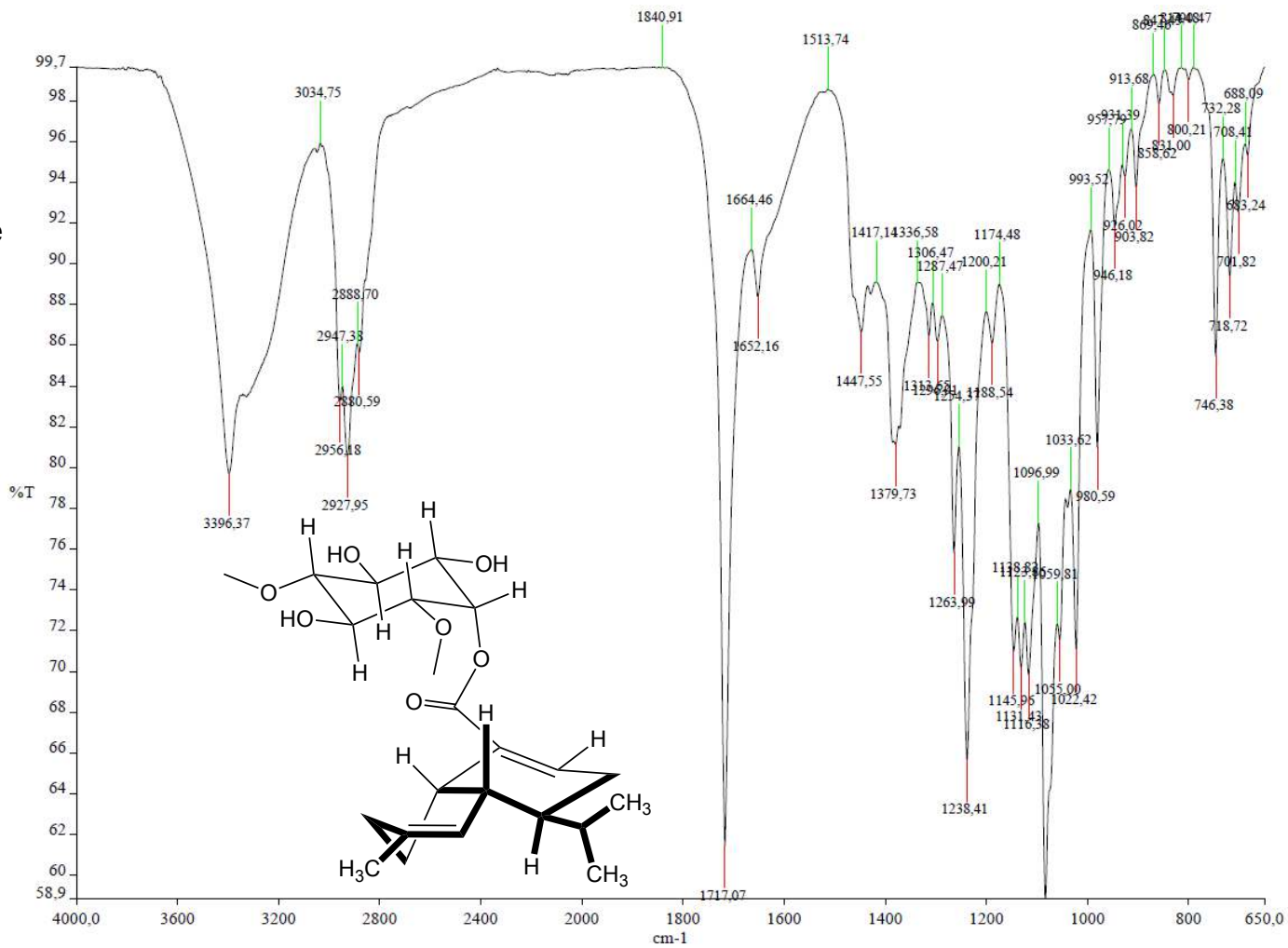
1: TOF MS ES+
2.72e+004

Minimum: -1.5
Maximum: 5.0 10.0 100.0

Mass	Calc. Mass	mDa	PPM	DBE	i-FIT	i-FIT (Norm)	Formula
425.2552	425.2539	1.3	3.1	5.5	1033.5	0.0	C23 H37 O7
	425.2589	-3.7	-8.7	0.5	1069.5	36.0	C22 H43 O3 Cl2

S39. HRESIMS of sclerosporide (5)

Sclerosporide



S40. IR spectrum of sclerosporide (5)

	δ_{exp} (3)	δ_{calcd} (3)	δ_{diff} (3)	δ_{exp} (4)	δ_{calcd} (4)	δ_{diff} (4)
H-1	1.38	1.45	0.07	1.31	1.44	0.13
H-1	1.56	1.47	0.09	1.56	1.58	0.02
H-2	2.09	2.12	0.03	2.09	1.91	0.18
H-2	2.47	2.55	0.08	2.51	2.80	0.29
H-4	2.17	2.29	0.12	2.09	2.12	0.03
H-6	1.02	0.79	0.23	0.93	0.93	0.00
H-6	2.16	1.99	0.17	2.39	2.12	0.27
H-7	1.77	1.72	0.05	1.69	1.56	0.13
H-7	1.93	1.87	0.06	1.98	1.87	0.11
H-8	3.56	3.77	0.21	3.22	3.09	0.13
H-10	1.91	1.67	0.24	2.33	2.46	0.13
H-11	1.38	1.32	0.06	2.03	2.13	0.10
H-11	1.66	1.69	0.03	1.06	0.92	0.14
H-12	1.53	1.48	0.05	1.67	2.04	0.37
H-12	1.73	1.55	0.18	1.42	1.35	0.07
H-13	3.53	3.46	0.07	3.16	3.14	0.02
Me-15	1.19	1.17	0.02	1.19	1.03	0.16
Me-16	1.17	1.17	0.00	1.26	1.26	0.00
Me-17	0.83	0.78	0.05	0.83	0.74	0.09
Me-18	0.94	0.98	0.04	0.99	1.03	0.04
H-19	4.48	4.68	0.20	4.48	4.60	0.12
H-19	4.20	4.27	0.07	4.21	4.29	0.08
H-20	2.60	2.52	0.08	2.65	2.63	0.02
H-20	2.81	2.70	0.11	2.85	2.92	0.07
Me-26	1.92	1.85	0.07	1.93	1.78	0.15
Me-27	2.19	2.19	0.00	2.20	2.15	0.05
MUE^a			0.09			0.11
RMSE^b			0.11			0.14

a MUE : mean unsigned error

b RMSE : root mean square error

S41. Comparison of ^1H NMR Data from Experimental Chemical Shifts (δ_{exp}) vs Calculated Chemical Shifts by DFT-NMR (δ_{calcd}) for compounds **3** and **4** (δ_{H} in ppm)

	$\delta_{\text{exp}} (3)$	$\delta_{\text{calcd}} (3)$	$\delta_{\text{diff}} (3)$	$\delta_{\text{exp}} (4)$	$\delta_{\text{calcd}} (4)$	$\delta_{\text{diff}} (4)$
C-1	24.70	27.50	2.80	23.50	25.25	1.75
C-2	33.30	35.24	1.94	33.00	33.58	0.58
C-3	150.80	157.43	6.63	150.70	157.12	6.42
C-4	56.10	56.57	0.47	57.20	58.25	1.05
C-5	38.50	42.73	4.23	38.70	42.82	4.12
C-6	30.80	31.50	0.70	30.60	31.97	1.37
C-7	25.80	24.52	1.28	25.60	27.93	2.33
C-8	75.50	79.89	4.39	83.10	87.30	4.20
C-9	37.50	40.23	2.73	35.80	41.93	6.13
C-10	45.00	46.96	1.96	35.20	37.07	1.87
C-11	39.60	41.68	2.08	37.40	38.84	1.44
C-12	19.80	19.12	0.68	22.90	23.49	0.59
C-13	83.20	84.92	1.72	85.50	86.19	0.69
C-14	74.80	79.38	4.58	73.40	75.33	1.93
C-15	25.80	24.72	1.08	25.30	23.43	1.87
C-16	25.80	25.85	0.05	25.70	26.89	1.19
C-17	21.60	18.41	3.19	23.50	22.09	1.41
C-18	22.70	19.96	2.74	24.10	23.04	1.06
C-19	110.40	106.16	4.24	110.00	106.21	3.79
C-20	22.70	25.03	2.33	22.70	25.37	2.67
C-21	104.10	106.38	2.28	104.50	106.30	1.80
C-22	168.40	164.03	4.37	167.70	163.49	4.21
C-23	109.20	104.78	4.42	108.60	104.95	3.65
C-24	156.80	160.74	3.94	156.80	161.14	4.34
C-25	168.20	162.81	5.39	168.20	162.95	5.25
MUE^a			2.68			2.51
RMSE^b			3.15			3.03

a MUE : mean unsigned error

b RMSE : root mean square error

S42. Comparison of ^{13}C NMR Data from Experimental Chemical Shifts (δ_{exp}) vs Calculated Chemical Shifts by DFT-NMR (δ_{calcd}) for compounds **3** and **4** (δ_{H} in ppm)

	δ_{exp} (5)	δ_{calcd} (5)	δ_{diff} (5)
H-1	2.55	2.46	0.09
H-2	1.42	1.41	0.01
H-2	2.00	2.08	0.08
H-3	2.08	2.20	0.12
H-3	1.91	1.85	0.06
H-5	5.55	5.73	0.18
H-6	2.01	2.13	0.12
H-7	1.55	1.65	0.10
H-8	2.16	2.05	0.11
H-8	2.16	2.16	0.00
H-9	6.99	7.56	0.57
H-11	2.05	2.15	0.10
Me-12	0.87	0.87	0.00
Me-13	0.95	0.95	0.00
Me-15	1.70	1.73	0.03
H-1'	5.66	5.02	0.64
H-2'	3.18	3.20	0.02
H-3'	3.62	3.98	0.36
H-4'	2.94	2.79	0.15
H-5'	3.64	3.67	0.03
H-6'	3.65	3.44	0.21
Me-7'	3.41	3.66	0.25
Me-8'	3.65	3.69	0.04
MUE^a			0.14
RMSE^b			0.22

a MUE : mean unsigned error
b RMSE : root mean square error

S43. Comparison of ^1H NMR Data from Experimental Chemical Shifts (δ_{exp}) vs Calculated Chemical Shifts by DFT-NMR (δ_{calcd}) for compound **5** (δ_{H} in ppm)

	δ_{exp} (5)	δ_{calcd} (5)	δ_{diff} (5)
C-1	35.80	37.75	1.95
C-2	26.80	28.00	1.20
C-3	31.70	31.80	0.10
C-4	136.20	140.66	4.46
C-5	124.30	124.84	0.54
C-6	37.40	39.29	1.89
C-7	41.80	42.74	0.94
C-8	26.50	28.01	1.51
C-9	141.50	152.23	10.73
C-10	134.50	135.42	0.92
C-11	27.70	29.87	2.17
C-12	15.50	12.31	3.19
C-13	21.70	21.05	0.65
C-14	168.10	173.48	5.38
C-15	24.00	24.55	0.55
C-1'	70.90	80.78	9.88
C-2'	81.70	81.69	0.01
C-3'	74.00	79.09	5.09
C-4'	86.50	87.32	0.82
C-5'	74.50	78.66	4.16
C-6'	71.60	77.12	5.52
C-7'	58.00	60.86	2.86
C-8'	61.20	60.67	0.53
MUE^a			2.83
RMSE^b			4.03

a MUE : mean unsigned error

b RMSE : root mean square error

S44. Comparison of ^{13}C NMR Data from Experimental Chemical Shifts (δ_{exp}) vs Calculated Chemical Shifts by DFT-NMR (δ_{calcd}) for compound **5** (δ_{H} in ppm)

Colletochlorin D 9: colorless oil; IR ν_{\max} 3173, 2969, 1614, 1421, 1278, 1100 cm^{-1} ; NMR data, Table 1 and supporting information; HRESIMS m/z 255.0783 $[\text{M}+\text{H}]^+$ (calculated from $\text{C}_{13}\text{H}_{16}\text{O}_3\text{Cl}$ 255.0788).

Colletorin A 6: amorphous solid; IR ν_{\max} 3440, 2922, 1630, 1482, 1371, 1223, 1060 cm^{-1} ; ^1H NMR (CDCl_3 ; 500 MHz) 12.69 (s; 1H; HO-2); 10.10 (bs; 1H; CHO-7); 6.23 (bs; 1H; HO-4); 6.19 (s; 1H; 5-H); 5.29 (t; 1H; 6.7 Hz; 9-H); 3.40 (d; 2H; 7.2Hz; 8H); 3.35 (dd; 1H; 10.4, 1.4 Hz; 14-H); 2.48 (s; 3H; 18- CH_3); 2.27-2.15 (m; 2H; 12-H); 1.80 (s; 3H; 11- CH_3); 1.60-1.45 (m; 2H; 13-H) 1.18 (s; 3H; 16- CH_3); 1.14 (s; 3H; 17- CH_3); ^{13}C NMR (CDCl_3 ; 125 MHz) δ 193.0 (CHO-7); 163.8 (C-2); 162.5 (C-4); 142.4 (C-6); 138.1 (C-10); 122.2 (C-9); 113.3 (C-1); 112.2 (C-3); 110.7 (C-5); 78.1 (C-14); 73.4 (C-15); 37.0 (C-12); 29.5 (C-13); 26.7 (CH_3 -16); 23.3 (CH_3 -17); 21.0 (C-8); 18.2 (CH_3 -18); 16.3 (CH_3 -11); HRESIMS m/z 323.1862 $[\text{M}+\text{H}]^+$ (calcd for $\text{C}_{18}\text{H}_{27}\text{O}_5$ 323.1858).

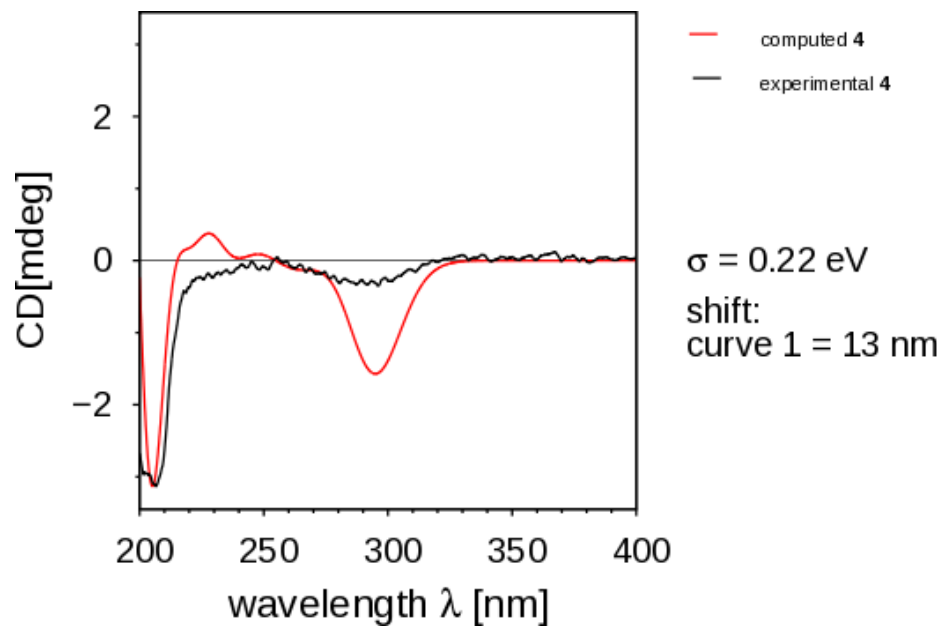
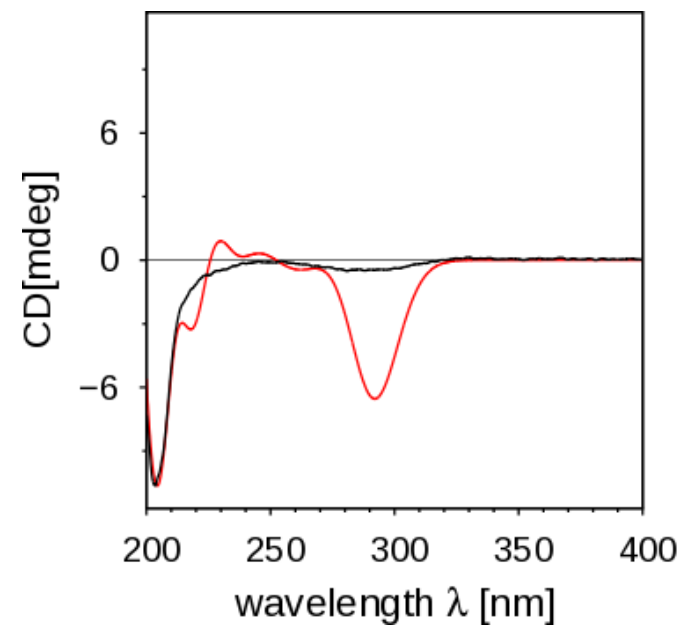
Colletochlorin A 7: amorphous solid; $[\alpha]_{\text{D}}^{25}$ +20.50 (c 0.4, MeOH); IR ν_{\max} 3325, 1627, 1374, 1243 cm^{-1} ; ^1H NMR (CDCl_3 ; 500 MHz) 12.69 (s; 1H; HO-2); 10.10 (bs; 1H; CHO-7); 6.23 (bs; 1H; HO-4); 5.25 (t; 1H; 7.1 Hz; 9-H); 3.40 (d; 2H; 7.2Hz; 8-H); 3.32 (dd; 1H; 10.4, 1.6Hz; 14-H); 2.60 (s; 3H; 18- CH_3); 2.23-2.08 (m; 2H; 12-H); 1.80 (s; 3H; 11- CH_3); 1.59-1.42 (m; 2H; 13-H); 1.18 (s; 3H; 16- CH_3); 1.14 (s; 3H; 17- CH_3); ^{13}C NMR (CDCl_3 ; 125 MHz) δ 193.3 (CHO-7); 162.4 (C-2); 156.5 (C-4); 137.9 (C-6); 136.7 (C-10); 121.4 (C-9); 114.1 (C-3); 113.8 (C-1); 113.4 (C-5); 78.6 (C-14); 73.0 (C-15); 37.0 (C-12); 29.6 (C-13); 26.3 (CH_3 -17); 23.3 (CH_3 -16); 22.0 (C-8); 16.3 (CH_3 -11); 14.5 (CH_3 -18); HRESIMS m/z 357.1478 $[\text{M}+\text{H}]^+$ (calcd for $\text{C}_{18}\text{H}_{26}\text{ClO}_5$ 357.1469).

Colletochlorin B 8: colorless oil; IR ν_{\max} 3227, 2342, 1634, 1371, 1266, 1129 cm^{-1} ; ^1H NMR (CDCl_3 ; 500 MHz) 12.69 (s; 1H; HO-2); 10.10 (bs; 1H; CHO-7); 6.23 (bs; 1H; HO-4); 5.21 (bt; 1H; 7.2 Hz; 9-H); 5.04 (bt; 1H; 6.5 Hz; 14-H); 3.40 (d; 2H; 7.2 Hz; 8-H); 2.60 (s; 3H; 18- CH_3); 2.04 (m; 2H; 13-H); 1.98 (m; 2H; 12-H); 1.80 (s; 3H; 11- CH_3); 1.64 (s; 3H; 16- CH_3); 1.57 (s; 3H; 17- CH_3); ^{13}C NMR (CDCl_3 ; 125 MHz) δ 193.3 (CHO-7); 162.4 (C-2); 156.5 (C-4); 137.9 (C-6); 137.3 (C-10); 131.8 (C-15); 124.1 (C-14); 120.6 (C-9); 114.5 (C-3); 113.8 (C-1); 113.5 (C-5); 39.9 (C-12); 26.7 (C-13); 26.5 (CH_3 -16); 22.0 (C-8); 17.8 (CH_3 -17); 16.3 (CH_3 -11); 14.7 (CH_3 -18); HRESIMS m/z 323.1404 $[\text{M}+\text{H}]^+$ (calcd for $\text{C}_{18}\text{H}_{24}\text{O}_3\text{Cl}$ 323.1414).

Higginsianin A: colorless crystal; $[\alpha]_{\text{D}}^{25}$ -64.5 (c 0.3, MeOH) ($[\alpha]_{\text{D}}^{25}$ -67.3, c 0.3, according to ref 14); IR ν_{\max} 3163, 2908, 1646, 1614, 1449, 1279, 1227, 1067 cm^{-1} ; NMR data, see Table 2 and supporting information; HRESIMS m/z 427.2852 $[\text{M}+\text{H}]^+$ (calcd for $\text{C}_{27}\text{H}_{39}\text{O}_4$, 427.2848).

Higginsianin B II: colorless crystal; $[\alpha]_{\text{D}}^{25}$ -71.2 (c 0.4, MeOH) ($[\alpha]_{\text{D}}^{25}$ -68.8 (c 0.25 according to ref 14); IR ν_{\max} 3211, 2931, 1643, 1573, 1433, 1383, 1203, 1060 cm^{-1} ; ^1H NMR (MeOD; 500 MHz) 5.17 (bt; 1H; 13-H); 4.50 (dd; 1H; 19-H); 4.24 (dd; 1H; 19-H); 3.65 (dd; 1H; 8-H); 2.84 (dd; 1H; 20-H); 2.67 (dd; 1H; 20-H); 2.45 (td; 1H; 2-H); 2.33 (td; 1H; 6-H); 2.23 (s; 3H; 27-H); 2.19 (m, 1H; 12-H); 2.19 (dd; 1H; 4-H); 2.11 (dd; 1H; 2-H); 2.02 (m; 1H; 7-H); 1.99 (m; 1H; 12-H); 1.96 (s; 3H; 26-H); 1.93 (dd; 1H; 10-H); 1.71 (s; 3H; 15-H); 1.67 (s; 3H; 16-H); 1.65 (m; 1H; 7-H); 1.63-1.35 (m; 2H; 1-H); 1.48 (td; 1H; 11-H); 1.31 (m; 1H; 11-H); 1.02 (s; 3H; 18-H); 1.00 (td; 1H; 6-H); 0.89 (s; 3H; 17-H); ^{13}C NMR (MeOD; 125 MHz) δ 168.3 (C-22); 168.2 (C-25); 156.9 (C-24); 150.6 (C-3); 131.6 (C-14); 127.1 (C-13); 110.0 (C-19); 108.8 (C-23); 104.3 (C-21); 73.6 (C-8); 56.7 (C-4); 41.4 (C-10); 41.2 (C-11); 40.4 (C-9); 39.0 (C-5); 33.0 (C-2); 29.9 (C-6); 27.1 (C-7); 25.9 (C-15); 24.1 (C-1); 23.6 (C-18); 22.8 (C-20); 22.8 (C-12); 19.7 (C-17); 17.8 (C-16); 17.3 (C-27); 10.4 (C-26); HRESIMS m/z 429.3011 $[\text{M}+\text{H}]^+$ (calcd for $\text{C}_{27}\text{H}_{41}\text{O}_4$, 429.3005).

S45. Experimental data for known compounds isolated in this study



S46. Superposed experimental ECD spectrum (black) with the ECD computed spectrum (red) for compounds **3** (left) and **4** (right).